e-ISSN : 2320-0847 p-ISSN : 2320-0936

AJER

American Journal of Engineering Research

Volume-2 Issue-6

AJER

American Journal of Engineering Research

American Journal of Engineering Resaerch

Editorial Board

CONTENTS

American Journal of Engineering Research (AJER)
e-ISSN : 2320-0847 p-ISSN : 2320-0936
Volume-02, Issue-06, pp-01-08
www.ajer.org

Research Paper Open Access

Adsorption of amitraz on the clay

Jale Gülen, Zehra Altın, Mahmure Özgür*
Yıldız Technical University, Chemical Metallurgical Engineering Faculty, 34210, Davutpasa Campus, Esenler – Istanbul
* Yıldız Technical University, Faculty of Scinece and Letters, 34210, Davutpasa Campus, Esenler – Istanbul

Corresponding author: Jale Gülen, Yıldız Technical University, Chemical Engineering Department, Davutpasa Campus, 34210 Esenler – Istanbul / TURKIYE Tel:+90 212383 4754

Abstract : Amitraz (AZ) that is used as acaridies was tried to extract with a clay. The experimental data were modelled as using Langmuir and Freundlich isotherms. The adsorption data fit well with Langmuir isotherm that indicated the AZ adsorption is homogeneous and monolayer. The monolayer adsorption capacity was found to be 35.02 mg/g at 20 ºC temperature. Effect of the phases contact time, the initial solution pH and the initial pesticide concentration were investigated from the point of adsorption equilibrium and yield. The adsorption kinetics were investigated by applying pseudo first order, pseudo second order and intra particle diffusion laws. Adsorption of AZ was found to be best fitted by the pseudo second order model. The intra particle diffusion also plays an important role in adsorption phenomenon.

Key words: Adsorption, amitraz, clay, pesticide

I. INTRODUCT ON

Pesticides have advantage from the point of controlling insects, disease and weeds in crops and postures and also disadvantage of causing serious problems in water quality. Once a pesticide is applied to crops, several processes may be observed. It may be taken up by plants and/or ingested by animals, insects, worms or microorganisms in the soil; it may downward in the soil and adhere to soil particles, or it may dissolve, it may volatilize; it may be broken down into less toxic compounds; it may be leached or moved out of the plants' root zone by rain or irrigation water; or it may be carried away by run off water or erosion (Amin and Jayson, 1996, Chen et al., 2004).

Pesticides are detected world wide in surface and ground water in agricultural areas, especially in North America and Europe (Pickon et al., 1998); http;//comwinchen...2013; Senseman et al., 1997).

Amitraz is the most used acaricide as commercial formulation. The molecular formula and weight of Amitraz is $C_{19}H_{23}N_3$ and 293.41 gram per mole. The chemical name of it is 1,5-Di (2,4-dimethylphenyl)-3-methyl-1,3,5-triazapenta-1,4-diene; Methyl-bis(2,4xylyliminomethyl) amine. It is a white to buff crystalline powder

Clays are the main components of the mineral fraction of soils. They are effective natural adsorbents due to their small particle sizes, lamellar structures and negatively charged surfaces, with make them good cation adsorbents with large reactive surface areas for ion exchange or electrostatic attraction (Tsai et al., 2003).

Anionic clays also called layered double hydroxides (LDH) or hydrotalcites (HT) are natural or synthetic materials containing magnesium (II) hydroxide by Al(III). The net positive charge is compensated with hydrated inorganic or organic anions in the interlayer (De Roy et al., 1992; Rives and Ulibarri, 1999). These anionic clays can be represented by the general firmula.:
$[M_{1-x}^{II} M_x^{III}(OH)_2]^{x+}[X^{m-}_{x/m}nH_2O]^{x-}$, abbreviated as $[M_{II}M_{III}\text{-}X]$ where M_{II}: Mg^{2+}, Mn^{2+}, Zn^{2+}..., $M_{III}=Al^{3+}$, Fe^{3+}, Cr^{3+}... and $X=CO_3^{2-}$, Cl^-, NO_3^-...

Anionic clay structure (Chibue and Jones, 1989); Meyn et al., 1990) results in their ability to be used as suitable materails for adsorption of anionic contaminants from water. They can be used for removal of inorganic anions (Nethravathi et al., 2011), phenolic compounds (Liotta et al., 2009), surfactants (Lin et al., 2009) or pesticides (Inacio et al., 2001, Gülen et al., 2012).

The aim of this study was to use clay for removal of amitraz. Several factors that effecting the adsorption ability of clay were also tested.

II. MATER ALS AND METHODS

II.1 Adsorbate Characterization

The amitraz (AZ) used in this study was supplied by Hektaş AŞ, in Turkey. Amitraz is a non-systemic acaricide and insecticide. Amitraz has been found to have an insect repellent effect, works as an insecticide and also as a pesticide synergist. It's effectiveness is traced back on alpha-adrenergic agonist activity, interaction with octopamine receptors of the central nervous system and inhibition of monoamine oxidases and prostaglandin synthesis. Therefore it leads to overexcitation and consequently paralysis and death in insects. Because amitraz is less harmful to mammals, amitraz is among many other purposes best known as insecticide against mite- or tick-infestation of dogs. Pestiside stock solution was prepared by dissolving 0.01 g amitraz in 100 ml distilled water. The chemical formula is given in Fig 1. Its characteristics are listed in Table 1 (http://en.wikipedia.org 2013).

II.2 Adsorbent Characterization

The clay belongs to Bartın area of Black Sea region of Turkey. The chemical characteristics are given in Table 2.

II.3 Adsorption Experiment

The adsorption experiments were carried out in batch system and the adsorbent amount was kept constant as 0.1 g in the experiments. Amitraz solutions with the amount of 20 ml each were prepared at several concentrations of 1, 2, 3, 4 and 5 mg/L in an erlenmeyer flask. The adsorption test was conducted by adding 0.1 g clay in each of the flasks. Initial solution pH was adjusted to desired pH. 0.1 M HCl and 0.1 M NaOH were used to adjust the AZ-Clay system to the desired pH. The flasks were then inserted in a thermostath shaker (Nüve ST402) set at 250 rpm with temperature of 20 ºC. At the end of the predetermined time intervals, the samples were centrifuged at 4000 rpm for 5 min. Changes in the concentration readings of the mixture were analyzed every 30 minutes using ATI UNICAM UV/VIS Spectrophotometer. The adsorption wavelength of the AZ was obtained at 245 nm from the first derivetive absorption spectra. The absorbance-concentration relationship was y = 0.5171x+0.024 (R^2=0.9884).

II.4 Equilibrium studies

For the adsorption experiments, a 5 ml stock solution was diluted to 40 ml with distilled water. An 3 ml aqueous solution was diluted to 20 ml again. The concentration of the pesticide solution was 2 mgL^{-1} (2 ppm). The amount of adsorption at equilibrium, q_e(mg/g) was calculated using the following equation:

$$q_e = \frac{(C_0 - C_e)V}{W}$$

where,
C_o (mg/L) and C_e (mg/L) are liquid phase pesticide concentrations at initially and at equilibrium, respectively.
V is the volume of the pesticide solution (L) and
W is the mass of adsorbent (g)

II.5 Kinetic studies

The amount of adsorption at time t, q_t (mg/g) was calculated by:

$$q_t = \frac{(C_0 - C_t)V}{W}$$

where,
C_o (mg/L) and C_t (mg/L) are pesticide concentrations (mg/L) at the beginning and at t time
V is the volume of the pesticide solution (L)
W is the mass of adsorbent (g).

II.6 Effect of initial solution pH

The pH value of the initial experimental solution was 5. The effect of pH on removal of amitraz was studied by varying the pH of the medium from 2.5 to 11 (pH values are 2.5, 3.5, 5, 7, 9, 11). The measurements were performed using WTW series inolab meter. An adsorbent (0.1 g) was added to each samples. After 3 hours, the adsorbance equilibrium values were measured by UV spectrometer. The experiments were performed at temperatures of 20 ºC.

II.7 Effect of initial pesticide concentration

Initial pesticide concentration is one of the important factors that affect adsorption kinetics. The effect of initial AZ concentration on clay was studied at different initial concentrations (5, 10, 15, 20 mgL^{-1}) at 20 ºC. The experiments were performed at fixed adsorbent dose (0.1 g), initial solution pH (pH=4) (due to the maximum adsorption yield) and phases contact time (3 h).

II.8 Adsorption isotherms

Experimental data were modelled using some isotherms such as Langmuir, Freundlich. The Langmuir equation (Kadirvelu et al., 2003; İmamoğlu and Tekir, 2008) is in the linear form,

$$\frac{C_e}{x/m} = \frac{1}{K.X_m} + \left(\frac{1}{X_m}\right)C_e$$

where x/m represents the amount of pesticide ions adsorbed at equilibrium, C_e is the equilibrium concentrations, X_m and K are Langmuir constants related to maximum adsorption capacity (mono layer capacity) and energy of adsorption, respectively (Machido et al., 2005).

The Langmuir isotherm can be defined as dimensionless constant separation factor R_L by

$$R_L = \frac{1}{1 + K.Co}$$

K= the Langmuir constant
C_o=the highest pesticide concentration (mg/L)
The values of R_L

$R_L>1$	The adsorption is unfavorable
$R_L=1$	The adsorption is linear
$0<R_L<1$	Adsorption is favorable
$R_L=0$	Adsorption is irreversible

The Freundlich equation (Kalavathy et al., 2005; Liang et al., 2006) is in the linearised form,

$$\log\frac{x}{m} = \log k + n.\log C_e$$

where x/m is the amount of pesticide ions adsorbed at equilibrium, C_e is the equilibrium concentrations, k and n are Freundlich constants concerning the multilayer adsorption capacity and adsorption intensity, respectively (Rao et al., 2006; Machido et al., 2005).

II.9 Adsorption dynamics

The study of adsorption dynamics describes the solute uptake rate and evidently this rate controls the residence time of adsorbate uptake at the solid-solution interface. The kinetics of amitraz adsorption on the clay were analyzed using pseudo first order (Lagergren, 1898), pseudo second order (Ho et al., 2000) and intra particle diffusion (Yue et al., 2007) kinetic models. The conformity between experimental data and the model predicted values was expressed by the correlation coefficients (R^2 values close to or equal to 1). A relatively high R^2 value indicates that the model successfully describes the kinetics of amitraz adsorption.

The pseudo first order equation (Lagergren, 1898) is generally expressed as follows:

$$\frac{dq_t}{dt} = k_1(q_e - q_t)$$

where
q_e and q_t are the adsorption capacity at equilibrium and at time t, respectively (mg/g)
k_1 is the rate constant of pseudo first order adsorption (l/min^{-1})
After integration and applying boundary conditions t=0 to t=t and $q_1=0$ to $q_t=q_e$, the integrated form of Eq becomes

$$\log(q_e - q_t) = \log(q_e) - \frac{k_1}{2.303}t$$

The values of log (q_e-q_0) were linearly correlated with t. The plot of log (q_e-q_0) vs t should give a linear relationship from which k_1 and q_e can be determined from the slope and intercept of the plot, respectively.

The pseudosecond order adsorption kinetic rate equation is expressed as (Ho et al., 2000)

$$\frac{dq_t}{dt} = k_2(q_e - q_1)^2$$

where

k_2 is the rate constant of pseudo second order adsorption (g/mg.min)

For the boundary conditions t=0 to t=t and q_1=0 to q_t=q_e, the integrated form of Eq becomes

$$\frac{1}{(q_e - q_t)} = \frac{1}{q_e} + kt$$

which is the integrated rate law for a pseudo second order reaction. Equation can be rearranged to obtain Eq which has a linear form.

$$\left(\frac{t}{q_t}\right) = \frac{1}{k_2 q_e^2} + \frac{1}{q_e}(t)$$

The intra particle diffusion model is expressed (Yue et al., 2007)

$$R = k_{id}(t)^2$$

A linearised form of the equation is followed by

log R=log k_{id} +alog(t)

where

R is the percent of pesticide adsorbed

t is the contact time (h)

a is the gradient of linear plots

k_{id} is the intra particle diffusion rate constant (h^{-1})

A depicts the adsorption mechanism, k_{id} may be taken as a rate factor, ie percent pesticide adsorbed per unit time.

III. RESULTS AND DISCUSSION

III.1 Effect of contact time

For the adsorption process, the experiments were carried out for different contact times with a fixed adsorbent dose of 0.1 g with the 2 mg/L concentration at 20 ºC. Fig 2 shows the relationships between equilibrium concentration and time at 20 ºC temperature and Fig 3 shows the adsorption capacity as a function of time. As it can be seen from Fig 2, the experiment became constant in 3 hours. q_t was determined from the formula given before. 58 % adsorption capacity was established in 1 hour of contact, 82 % of pesticide removal was achieved at the end of adsorption in 3 hours (Fig 3).

III.2 Effect of pH

The effect of pH is shown in Figure 4 in term of uptake % - pH.

Uptake % was determined from the formula given below.

$$Uptake\% = \frac{C_0 - C_e}{C_0} x100$$

C_0 = initial concentration (mg/L)

C_e = equilibrium concentration (mg/L)

The adsorption percent were 17 and 23 % at 2.5 pH value increased to 37.5 % at 3.5 pH value. The acidic region (2.5-5) gave approximately about 29 and 45 % absorbance. This high values can be affected by the acidic character of pesticide and anionic structure of clay. The uptake values were found as 14 % at pH 11 for 20 ºC.

III.3 Effect of pesticide concentration

The results of pesticide concentration effect are shown on Fig.5. The increase in the pesticide concentration over 20 ppm did not affect the adsorption capacity significantly.

III.4 Adsorption isotherms

The graphics and the constants of Langmuir and Freundlich isotherm models are given in Fig. 6, 7 and Table 3, respectively. The experimental values conform to the Langmuir equation with respect to the low correlation value of the Freundlich equation as seen in Table 3. The process is a monolayer process based on the Langmuir isotherm model. The amount of R_L was calculated to as 0.24. That shows us Langmuir adsorption was favorable.

III.5 Adsorption dynamics

The kinetic graphics are given in Fig. 8, 9 and 10. The pseudo fisrst order, second order and intra particle rate coefficients were calculated. The values of k_{id} were calculated from the slope of such plots and the R^2 values led to the conclusion that the intra particle dissusion is the rate limiting step. Higher values of k_{id} illustrate an enhancement in the rate of adsorption, whereas larger k_{id} values illustrate a better adsorption mechanism, which is related to an improved bonding between pesticide ions and the adsorbent particles (Table 4).

IV. CONCLUSIONS

The amitraz, a kind of acaricide was extracted with a clay adsorbent. Adsorption tests were carried out as a function of contact time, pH, pesticide concentration at fixed adsorbent dose. The adsorption completed in 3 hours. Removal of pesticide % was almost 40 % in the first hour and at the end of process the yield increased to 60 %. pH was effective for amitraz removal. The percentage of removal increased with the increasing concentration of pesticide in the solution. The fitness of the adsorption data onto Langmuir isotherm confirmed the monolayer adsorption due to the high correlation coefficient. The monolayer capacity was found as 35 mg/g. The results show us that pseudo second order kinetics was managed the process. Intra particle diffusion played an important role in the whole process. Given the facts that clay is ecofriendly and low cost, and it has a satisfying adsorption efficiency.

V. ACKNOWLEDGEMENTS

This study has been supported by the Research Fund of Yıldız Technical University (YTU BAPK 28-07-01-05).

REFERENCES

[1] Amin S, Jayson G G, 1996. Humic substance uptake by hydrotalcites and PILCs, Water Res., 30: 299, 077.

[2] Chen J P,. Pehkonen Simo O, Lau Chia-Chiun, 2004. Phorate and terbufos adsorption onto four tropical soils, Colloids and Surfaces A: Physicochem Eng. Aspects. 240; 55-61.

[3] Chibue M, Jones W, 1989. Intercalation of organic and inorganic anions into layered double hydroxides, J. Chem. Soc. Common., 921-927

[4] De Roy A., Fioani C., El Malki K., Bessa JP, 1992. in Occeli, M.L. Robson, H. E. (Eds.). Expanded Clays and other microporous solids, vol. II, Van Nostrand, Reinhold, NY.

[5] http://comwinchem.en.alibaba.com/product/224273334-203737015/Amitraz_acaricide_insecticide_33089_61_1.html accesed at 1/1/2013).

[6] http://en.wikipedia.org/wiki/Amitraz (accessed at 29.1.2013).

[7] Gülen J, Turak F, Ozgur M. 2012. Removal of amitrole by activated clay. International Journal of Modern Chemistry. 2(2): 47-56.

[8] Ho Y, McKay G, 2000. The kinetics of sorption of divalent metal ions onto sphagnum moss peat. Water Res. 34:, issue 3: 735-742.

[9] İmamoğlu M, Tekir O, 2008. Removal of copper (II) and lead (II) ions from aqueous solutions by adsorption on activated carbon from a new precursor hazelnut husks, Desalination 228: 108-113.

[10] Inacio J, Taviot-Gueho C, Forano C, Besse JP, 2001. Adsorption of MCPA pesticide by MgAl-layered double hydroxides, Appl. Clay Sci. 18: 255-264.

[11] Kadirvelu K, Kavipriya M, Karthika C, Radhika M, Vannilamani N and Pattabhi S, 2003. Utilization of various sgricultural wastes for activated carbon preparation and application for the removal of dyes and metal ions from aqueous solutions. Bioresouce Technol., 8: 129-132.

[12] Kalavathy MH, Karthikeyan T, Rajgopal S and Miranda L R, 2005. Kinetic and isotherm studies of Cu(II) adsorption onto H_3PO_4 activated rubber wood saw dust. J. Coll. Interface Sci. 292, issue 2: 354-362.

[13] Lagergren S. 1898. About the theory of so-called adsorption of soluble substances. Kungliga Svenska Vetensk Handl , 24: 1.

[14] Liang CS, Dang Z, Mao BH, Huang WL and Liu CQ, 2006. Equilibrium sorption of phenanthrene by soil humic acids. Chemosphere, 63, issue 11: 1961-1968.

[15] Lin S H, Teng, MY, Juang RS, Nov. 2009. Adsorption of surfactants from water onto raw and HCl activated clays in fixed beds, Desalination vol 249, issue 1: 116-122.

[16] Liotta, LF, Gruttadauria M, Carlo GD, Perrini G, Librando V. March 2009. Heterogeneous Catalytic Degredation of phenolic Substrates: Catalyst activity, Journal of Hazardous Materials, vol: 162, issue 2,3: 588-606

[17] Machido M, Yamazaki R, Aikawa M and Tatsumoto H, 2005. Role of minerals in carbonaceous adsorbents for removal of Pb(II) ions from aqueous solution. Sep. Purif. Technol., 46, issue 1-2: 88- 94,

[18] Meyn M, Beneke K, Lagaly G, 1990. Anion exchange reaction of layered double hydroxides.Inorg. Chem., 29: 5201-5207.

[19] Nethravathi C, Rajamathi JT, George P, Rajanathi M. Feb. 2011. Synthesis and anion exchange reactions of a new anionic clay, a magnesium hydroxide. Journal of Colloid Interface Science. 354, issue 2: 793-797.

[20] Pickon V, Charpak M, Hennion MC, 1998. Multiresidue analysis of pesticides using new laminar extraction disks and liquid chromatography and application to the french priority list, Journal of Chromatography A, 795: 83-92.

[21] Rao M M, Ramesh A, Rao G P C and Seshaiah K, 2006. Removal of copper and cadmium from the aqueous solutions by activated carbon derived from Ceiba pendantra hulls. J. Haz. Mat. 129 : 123-129

[22] Rives V, Ulibarri MA, 1999. Layered double hydroxide (LDH) intercalated with metal coordination compounds and oxometalates. Coord. Chem. Rev. 181: 61-120.

[23] Senseman SA, Naxy T L,. Daniel T C, Jan 1997. Monitoring ground water for pesticides at selected mixing loading sites in Arkansas, Environ. Sci. Technol. 31: issue 1, 283-288.

[24] Tsai W T, Lai C W, and Hsien K J, 2003. Effect of particle size of activated clay on the adsorption of paraquat fro maqueous solution, Journal of Colloid and interface Science, 263: 29-43.

[25] Yue Q.Y., Li Q, Gao B.Y. , Wang Y. 2007. Kinetics of adsorption of disperse dyes by polypicholorohydrin-dimethylamine cationic polymer/bentonite. Sep. Purif. Technol. 54, issue 3: 279-290.

Table 1. Chemical characteristics of Amitraz

Chemical name	[N-di-(2,4-ksiliminometil)metilamin]
Molecular formula	$C_{19}H_{23}N_3$
Molecular weight	293.4 g/mol
Melting point	86–87 ºC

Table 2. Chemical composition of clay

Compo.	B_2O_3	SO_4^{2-}	CaO	Na_2O	SiO_2	MgO	SrO	Al_2O_3	Fe_2O_3	Heatloss
Weight%	14	2	13.53	6.87	13.8	11.8	1.15	0.94	0.35	35.75

Table 3. Langmuir ve Freundlich isoterm constants at 20 ºC.

İsoterm tipi	Constants		R^2	Q_{max}(mg/g)
Freundlich isotherm	n = -1.2558	k = 3.9343	0.936	3.93
Langmuir isotherm	X_M = 0.029	K = -4.656	0.956	35.02

Table 4. Kinetic rate constants of adsorption dynamics

		R^2	q_e mg/g
k_1 (min^{-1})	**0.89**	**0.94**	**724.44**
k_2 ($g.mg^{-1}min^{-1}$)	**17.01**	**0,98**	**0.096**
$k_{\square d}$	**1.06**	**0.97**	

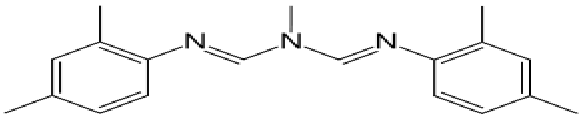

Fig.1 **Chemical structure of A**mitraz molecule

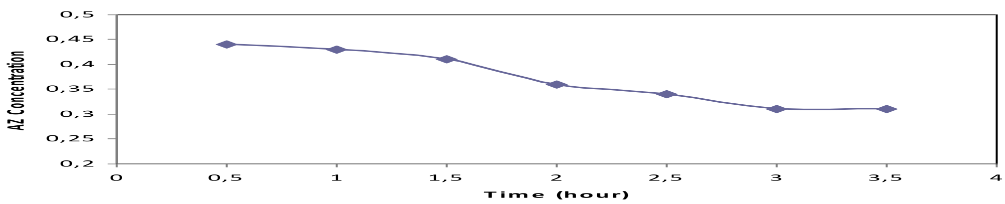

Fig 2. AZ Concentation vs time relationship T=20 ºC (clay dose= 0.1 g, C_{AZ}=2 mg/L, pH=5)

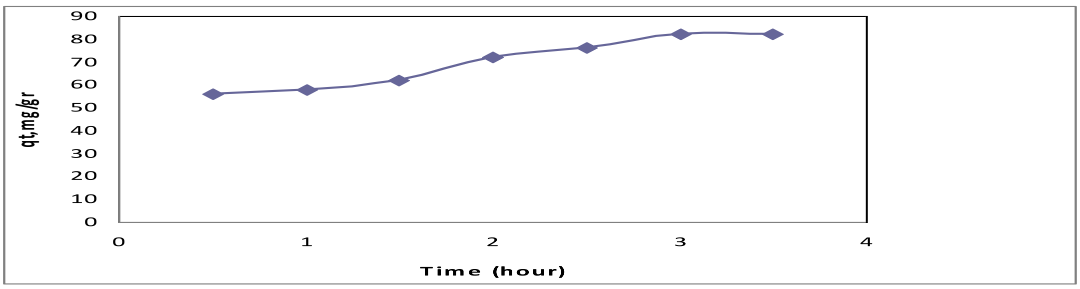

Fig 3. q_t(mg/g) vs time relationship (clay dose 0.1 g, C_{AZ}= 2mg/L, pH=5, T=20 °C)

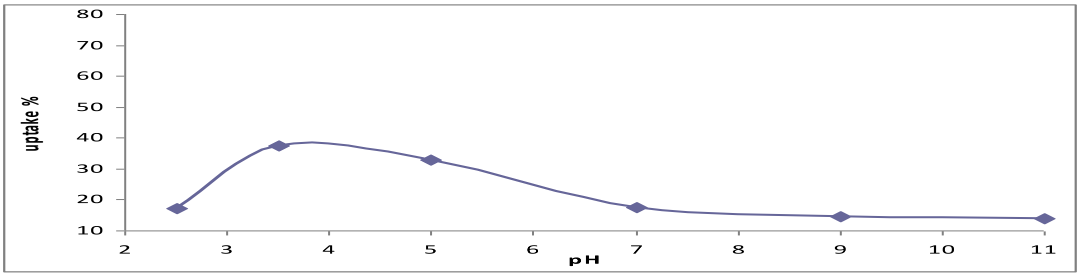

Fig 4. Effect of initial solution pH on adsorption of AZ on clay (C_{AZ}=2 mg/L, T=20 °C, clay dose=0.1 g, pH=4

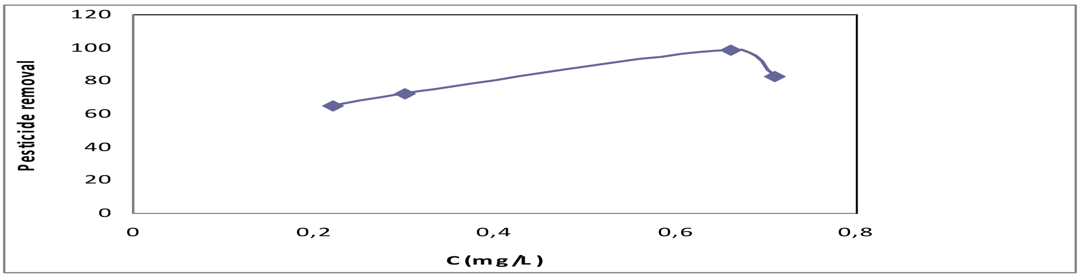

Fig 5. Effect of AZ concentration on the adsorption of amitraz by clay (phase contact time 3 hours, clay dose 0.1 g, pH=4, T=20 °C)

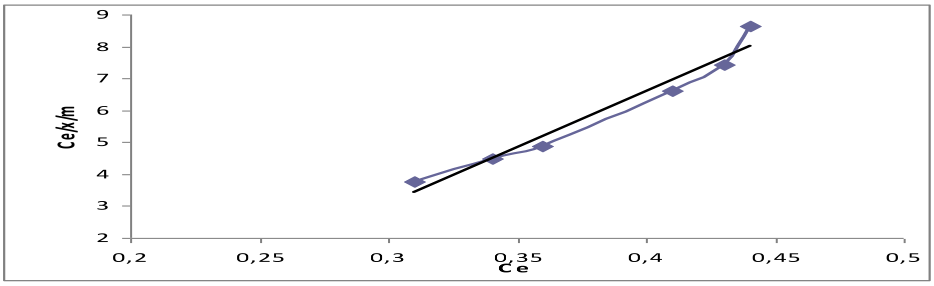

Fig 6.Linearized Langmuir isotherm

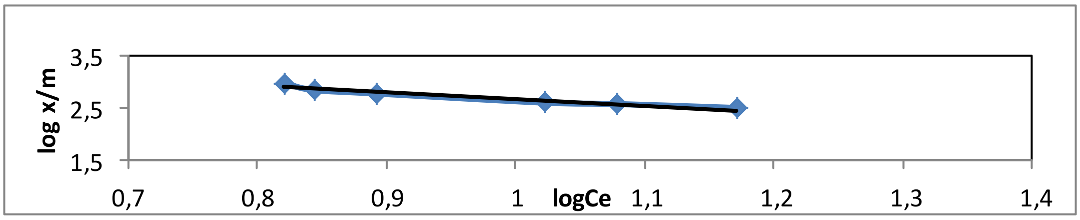

Fig 7. Linearized Freundlich isotherm

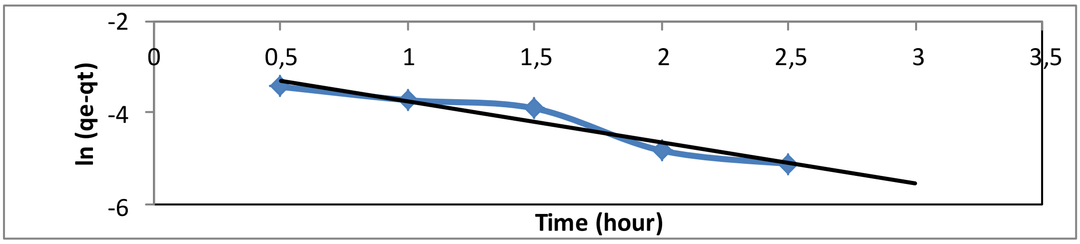

Fig.8. Pseudofirst order kinetics

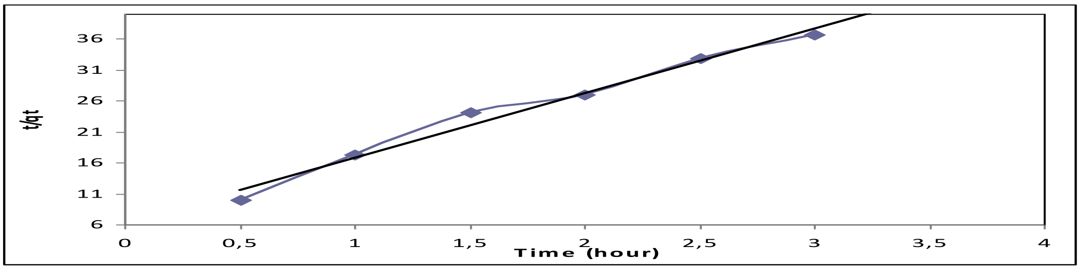

Fig 9. Pseudosecond order kinetics

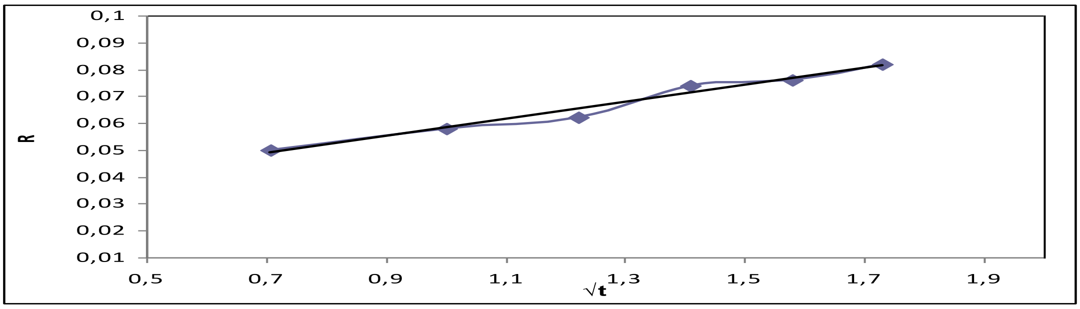

Fig 10. Intra particle kinetics

American Journal of Engineering Research (AJER)
e-ISSN : 2320-0847 p-ISSN : 2320-0936
Volume-02, Issue-06, pp-09-13
www.ajer.org

Research Paper Open Access

Framework Model for a Soil Suitability Decision Support System for Crop Production in Nigeria

AdekunleYinka[1],Bisong, Ekaba Ononse[2], Fagbemi, Oluwabanke[3], Obuke, Enifome[4], Alao, Jimi[5], and Maitanmi, Olusola[6]
[1,2,3,4,5,6] Computer Science, Computing Engineering Science, Babcock University, Nigeria

Abstract: - A typical problem is faced in Nigeria, where agricultural lands are largely underutilized and mostly suffering from degradation leading to an unmitigated food security problem. Currently, food production growth rate in Nigeria remains unable to feed its fast growing population. This is largely attributed to the farm management practices on agricultural lands employed in crop production. A step in the right direction is to provide a central repository of data and knowledge where decision support on the best crop production practices to provide optimum yield in quality and quantity is made available in a view easily interpreted by the chief implementers, which in this case are the local farmers. This can be accomplished in part by building a system to provide soil suitability decision support. In this paper, a framework for building a soil suitability decision support system (SSDSS) to tackle the problem of poor farming methods and low crop growth is presented. It documents a solution of coordinating the diverse nature of variables faced by the decision-maker in the crop production process into a software system that would support decision making activities and hide the user of the system from the technicalities and complexities of the underlying data.

Keywords: - *agricultural lands, crop production, soil suitability decision support system, decision support framework*

I. INTRODUCTION

Nigeria faces huge food security challenges. Nigeria has about 79 million hectares of arable land, of which 32 million hectares are cultivated. Smallholders, mostly subsistence producers account for 80% of all farm holdings. Both crop and livestock production remains below potentials. Inadequate access to and low uptake of high quality seeds, low fertilizer use and inefficient production systems has led to this shortfall. Despite a seven percent growth rate in agricultural production (2006 – 2008), Nigeria's food import bill has risen. The growing population is dependent on imported food staples, including rice, wheat and fish (Nwajiuba C., 2012).Nigerian agriculture contributes to global warming albeit to s small extent through bush burning and other poor land management practices. This matches the findings on the state of agriculture in sub-Saharan Africa, summarized in the international assessment of agricultural knowledge, science and technology (IAASTD, 2008 cf. Nwajiuba C., 2012).

The problems of agriculture in Nigeria begin with the soil. Most of the farmable land in Nigeria contains soil that is low to medium in productivity. According to the Food and Agriculture Organization of the United Nations (FAO, 2001), "with proper management, the soil can achieve medium to good productivity".

To obtain optimum results in crop production, certain strategies must be taken into consideration, which includes the extensive use of arable land and where necessary with the application of irrigation. According to the Global Land Assessment of degradation (Glasod) estimation, in Africa, of the 3.2 billion hectares available which are under pasture, 21 percent are degraded, while of the nearly 1.5 billion hectares in the crop lands, 38 percent are degraded in various degrees. The degradation of cropland appears to be most extensive in Africa affecting 55 percent of the crop area, compared with 51 percent in the Latin America and 38 percent in Asia. This all limits the extent of which we can make use of available arable land. Declining yields or increasing input requirements will be the consequence. Another strategy of making intensive use of the available arable land is to irrigate it where necessary. The potential for increasing the overall irrigated area in the developing countries is at 110 million hectares. This could provide an additional 300-400 million tons of grain, enough to provide a basic diet for more than 1.5 billion people (FAO Food Security Assessment Document WFS/tech/7, Rome 1996, p.16. cf. Sakariyawo O. S., Bugaje S. M., Kuta D. D., Magashi A. I., Ubale A. S., 2000).

The constraints earlier highlighted leave us with the option of intensive method of Agriculture, which is knowledge based. The role of the crop research cannot be overemphasized namely: agronomy; plant breeding: plant physiology and biochemistry; plant protection; biotechnology etc. According to Ben Miflin (Journal of Experimental Botany, Vol.51, No.342 MP special issue, pp1-8, January 2000), the vast majority of the increase in the crop yields that took place in the last century has been powered by changes in the genetical potential of the crop and the way in which it has been managed (Sakariyawo O. S., Bugaje S. M., Kuta D. D., Magashi A. I., Ubale A. S., 2000).

The application of Soil Suitability Decision Support System (SSDSS) in the Nigerian Agricultural sector/ domain combines data, knowledge and mathematical models from crop production research to enhance the decision-making capabilities of farmers in their bid to optimize the quality and quantity of cultivated crops.

II. THE STUDY AREA, RESEARCH SIGNIFICANCE AND OBJECTIVES

Soil types in Nigeria are influenced by and follow very broadly, the climatic and vegetational zones of the country. This is expected because the degree of available moisture in the soil is an important factor in soil reactions and fertility and productivity. The soils of the humid tropical forests are quite different from those of the drier forests and the savanna zone, which in turn are different from the savanna zone (Oyenuga, 1967). The major soil types in Nigeria, according to FAO soil taxonomy legends are fluvisols, regosols, gleysols, acrisols, ferrasols, alisols, lixisols, cambisols, luvisols, nitosols, arenosols and vertisols. These soil types vary in their potential for agricultural use (Aregheore, E. M., 2005).

The irrational use of agricultural lands as well as the adoption of archaic methods has resulted in the sector producing less than its expected capacity and in the process contributes to the current food security challenges. Zhi-Qiang, W., &Zhi-Chao, C., 2010 states that more advanced methods and technologies are needed to manage all the information from different sources, and interruptedly analyze all the information to get better strategies for crop production. A SSDSS can, obviously, meet the needs. But up to now, there is no such decision support system available in the field.

The paper aimed at developing a SSDSS framework to cater for the best practices needs of farmers to produce optimal results during the crop production process. The facets to be operated upon by the decision maker are, cropping systems, fertilizer and their right uses, tillage practices, seed & seedlings, soil and water conservation, irrigation and drainage, weed and weed control, pest and diseases, crop improvement, harvesting and processing of field crops and storage of field crops, to determine the suitability of a particular soil type to produce optimum yield in quality and quantity for a particular crop specie in a particular location within the country.

The decision support to be catered for includes:

- The analysis and characterization of the samples for physical and chemical properties; in the case of soils and quality characteristics in respect of water.
- The recommendation of types of fertilizers, application rates, application methods and optimum time of application for each crop in the state.
- The recommendation of land management practices to be adopted by each state, to maintain soil fertility.
- The recommendation of water management practices based on baseline values on surface and groundwater generated during the study.
- The recommendation of disease and pest control practices to be adopted by each crop in a particular soil location.
- The recommendation of seed varieties to be cultivated in a particular soil location.
- The recommendation of weed and weed control practices to be adopted by each crop in a particular soil location.
- The recommendation of crop improvement techniques to be adopted in a particular soil location.
- The recommendation of harvesting and processing techniques to be adopted in a particular soil location.The recommendation of the climatic condition in a particular soil location as it affects a particular crop.

III. SSDSS FRAMEWORK

With the development of the Internet, Web-based Decision Support Systems (DSS) have become a new trend in DSS research. Compared to traditional DSS, there are two changes brought by the Web-based DSS. First, the underlying architecture for Web-based DSS has moved from main frames, to client–server systems, to Web- and network technology-based distributed systems. Consequently, large amounts of data and related decision support tools from multidisciplinary sources, which may be located in a distributed computing environment, have the possibility to be integrated together to support decision-making. Second, differing from traditional DSS, such as data-driven DSS focusing on access to and manipulation of a timeseries of data, model-driven DSS focusing on access to and manipulation of a domain-related model, and knowledge-driven DSS focusing on high-level knowledge extraction and data mining, Web-based DSS provide the ability to build a hybrid DSS (Zhang, S. & Goddard, S., 2005).

The framework for the SSDSS is shown in Figure 1 below.

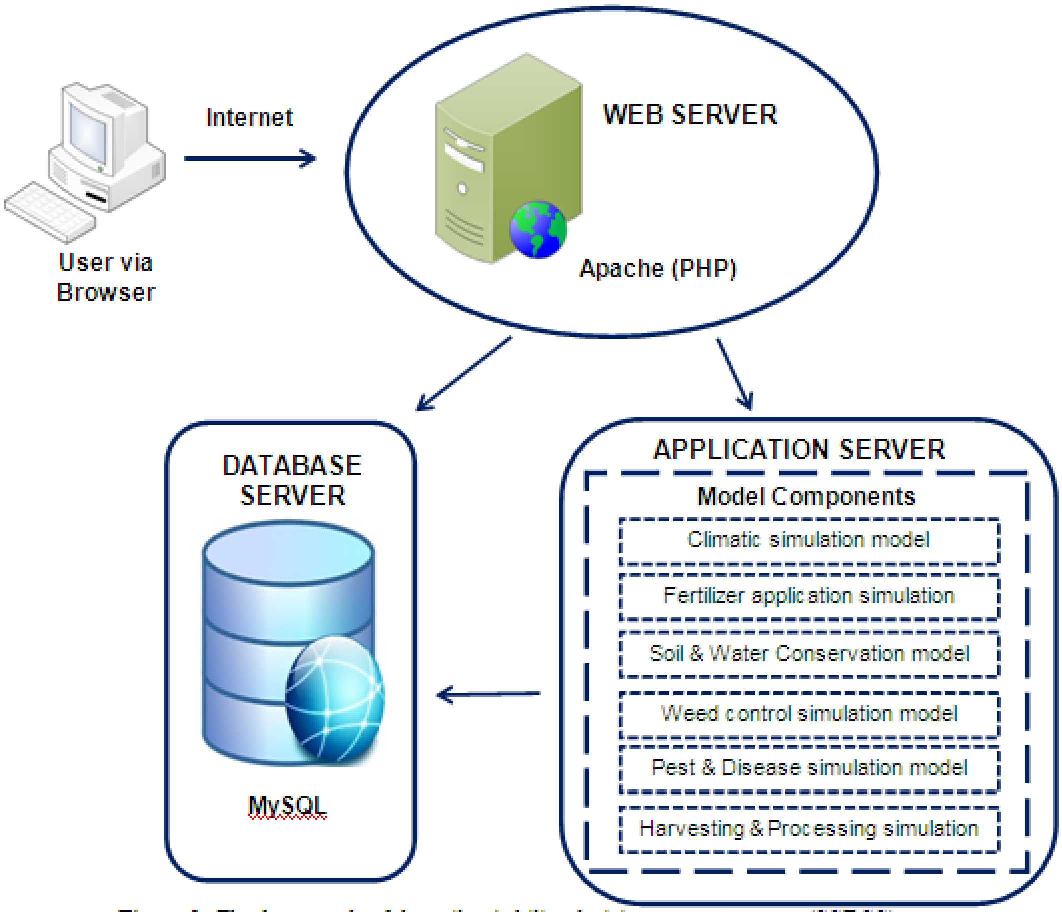

Figure 1: The framework of the soil suitability decision support system (SSDSS)

There are three fundamental components of the SSDSS as it corresponds to the components of a DSS as shown in Druzdzel and Flynn, 2002.

- Database management system (DBMS). It serves as a data bank for the DSS. It stores large quantities of data and provides logical data structures (as opposed to the physical data structures) with which the users interact. It separates the users from the physical aspects of the database structure and processing.
- Model-base management system (MBMS). It provides independence between specific models that are used in the DSS from the applications that use them. The purpose of the MBMS is to transform data from the DBMS into information that is useful in decision making. Since many problems that the user of a DSS will cope with may be unstructured, the MBMS can assist the user in model building.
- Dialog generation and management system (DGMS). As their users will mainly be farmers who are not computer-trained, the DSS is equipped with intuitive and easy-to-use interfaces. These interfaces aid in model building, but also in interaction with the model, such as gaining insight and recommendations from it. It is the user interface accessed from the browser.

IV. DEVELOPMENT OF THE SSDSS

IV.1 Development of data warehouse for soil suitability decision variables

The SSDSS data warehouse includes data to provide decision support for each crop in a particular soil type (i.e. fluvisols, regosols, gleysols, acrisols, ferrasols, alisols, lixisols, cambisols, luvisols, nitosols, arenosols and vertisols), the databases contained are:

- database for cropping systems,

- database for fertilizer and their right uses,
- database for tillage practices,
- database for seed & seedlings,
- database for soil and water conservation,
- database for irrigation and drainage,
- database for weed and weed control,
- database for pest and diseases,
- database for crop improvement,
- database for harvesting and processing of field crops,
- database for storage of field crops, and
- database for physical and chemical properties of soil types,

The database was developed using MySQL to input, store, manage, query and index data to provide soil suitability decision support. MySQL is picked as the DBMS of choice because it supports a rich set of data types capable of representing nearly every conceivable data format with powerful security models. Web frameworks help the programmer to embrace best practices, simultaneously decreasing errors and eliminating redundant code. A number of them are PHPMyAdmin, MySQL Administrator, MySQL Workbench 5.3 CE, etc.

IV.2 Development of soil suitability decision models

By examining the variety of decisions to be made and the variables that surround them, many problems faced by the user of the DSS will be unstructured. Data from the DSS can be used in model building to generate information useful for decision making. Some of the models that can be generated include:

- ✓ Climatic simulation model,
- ✓ Fertilizer application simulation model,
- ✓ Soil & water conservation simulation model,
- ✓ Weed control simulation model,
- ✓ Pest & disease simulation model,
- ✓ Harvesting & processing simulation model, and
- ✓ Storage simulation model

IV.3 Development of the View and Controller

PHP Hypertext Pre-Processor is employed as the preferred language for server-side development to coordinate the request – response cycle from the web browser to the server for processing. It is well suited for the creation of dynamic user interfaces (views) in conjunction with client side technologies such as HTML, CSS, JavaScript and AJAX thatinteract with the database as well as generated simulation models. It is ideal for a web based software development.

The architectural design pattern employed here is the MVC (Model-View-Controller) design pattern, which dividesthesystem into three interoperable albeit loosely coupled components. The model represents the data warehouse/ simulation models for crop production recommendation and prediction. It notifies the view when it changes and lets the controller access the system functionality encapsulated by the model. The View on the other hand gets data/ information from the model and specifies how it should be presented to the user of the system. It updates data representation each time the model changes. The controller is responsible for the application behavior as it dispatches user requests and selects views for presentation.

AJAX calls are employed to facilitate a seamless transfer of user request from the browser to the server; this is done by asynchronously passing information to the serverthereby enhancing the overall user experience while using the system.

V. CONCLUSION

In Nigeria, we have a rich pool of agricultural data available yet little or no knowledge gleaned from it. A famous aphorism goes that “we are drowning in data, but starving for knowledge!!” as is the case in the Nigerian agricultural sector. Various researches and scientific explorations have been conducted over the years by government agencies, non-governmental organizations (NGOs) and university scholars that have produced ground-breaking results, with huge potentials to take the agricultural sector in Nigeria to the next level. Unfortunately we find this knowledge being swept under the carpet in the archival shelves as the proverbial candle lighted and put under a bushel and not readily available to the common populace especially for the chief implementers, which in this case are the farmers. Those that are available are either too technical for common consumption or have a narrow spread, hence not accessible to all stakeholders across the country. As this information is not readily made available, it has become quite common for crop farmers to use substandard approaches which have resulted in low productivity in terms of quality and quantity. We also find many farmers holding on to archaic ideas/ methods, therefore not being able to achieve maximum productivity in crop production. A SSDSS solves this problem.The future of this work is to add intelligence to decision making by computing inferential rules and metrics to provide decisions based on data read from our design model. Consequently it becomes possible to tell the soil type that would provide maximum yield in quantity and quality for a particular crop based on computations on the chemical and physical properties of the soil types matched with computations on the chemical properties of the crop, to find the optimal result. This example and other matrices can and should involve computational analysis to increase decision support.

REFERENCES

[1] Aregheore, E. M., Country Pasture/Forage Resource Profiles. Nigeria. http://www.fao.org/ag/AGP/AGPC/doc/Counprof/nigeria/nigeria.htm#2b, 2005.

[2] Druzdzel M. J., Flynn R. R., Decision Support Systems. Decision Systems Laboratory School of Information Sciences and Intelligent Systems Program University of Pittsburgh. To appear in Encyclopedia of Library and Information Science, Second Edition, Allen Kent (ed.), New York: Marcel Dekker, Inc., 2002.

[3] Nwajiuba C., Nigeria's Agriculture and Food Security Challenges. http://www.ng.boell.org/downloads/Agriculture_-_Green_Deal_Nigeria_study.pdf, 2012.

[4] Sakariyawo O. S., Bugaje S. M., Kuta D. D., Magashi A. I., Ubale A. S., Food Security in Nigeria: The importance of Crop Research. Paper presented at the conference of young agricultural specialists: "Food security in Nigeria", which took place between 22nd July - 5th August at the People's Friendship University of Russia, Moscow. The conference was organized by SELHOZ (A Nigerian NGO, based in Russia). http://www.nigeriaworld.com/feature/article/food_security.html, 2000.

[5] Zhang S., Goddard S., A software architecture and framework for Web-based distributed Decision Support Systems. Elsevier. Decision Support Systems 43 (2007) 1133– 1150, 2005.

[6] Zhi-Qiang W., Zhi-Chao C., A Web-based Agricultural Decision Support System on Crop Growth Monitoring and Food Security Strategies. ISBN 978-952-5726-10-7. Proceedings of the Third International Symposium on Computer Science and Computational Technology (ISCSCT '10). Jiaozuo, P. R. China, 14-15, August 2010, pp. 487-491, 2010.

American Journal of Engineering Research (AJER)
e-ISSN: 2320-0847 p-ISSN : 2320-0936
Volume-2, Issue-06, pp-14-18
www.ajer.org

Research Paper Open Access

Developing a Matrix Based Sales Configurator for Modular Product

Antti Huuskonen[1], Esa Hietikko[2]
[1](*Savonia University of Applied Sciences, Finland)*
[2](*Savonia University of Applied Sciences, Finland)*

Abstract: - For several years, the structuring approaches for modular product families have been developed in industry. The modularization leads often to the use of configurator, which is a computer application used to manage the relations of modules, connections and rules between different customer segments. Configurator brings benefits to the whole delivery process, by removing the information gaps from which are needed in the product order. Matrix based sales configurator can make order delivery process to go through faster, and especially help to keep the product knowledge of modules and modular structures of complex products in order as well as to make the updating of them easier by its illustrative user interface. MS Excel was used in the first developed version of the sales configurator prototype and it was found to be good platform for testing configurability in machine industry companies, because of its prevalence. Second development version, the server-client sales configurator expanded the possibilities of the application and improved user safety compared to the MS Excel version of the sales configurator and matrix rule table. The research project described in this paper was started because there was demand for a flexible sales configurator in local heavy machine industry. The paper describes the project where new prototype of sales configurator application was developed in just over a year in cooperation with case company from machine industry.

Keywords :- *Variant products, Configuration knowledge, Product structuring, Modularization, Product development process.*

I. INTRODUCTION

For several years, the structuring approaches for modular product families have been developed in industry. The target of modular structure is to achieve a comprehensive selection of products to fulfill the needs of different customer segments. The modularization makes also the production more simple and standardized. This increases the efficiency of product management and fastens the order-delivery process. To be efficient also the modularized product structure must have similarities with the production. As well this must be an essential part of the product development process starting from the beginning.[1], [2]

The modularization leads often to the use of configurator, which is a computer application used to manage the relations of modules, connections and rules between different customer segments.[3] In many cases matrices have been used to represent product structures and selection criteria of modules and configuration knowledge.[1] Starting to use sales configurator in order-delivery process should be considered after modularization, in order to maintain interchangeability of modules in the product.[4] Benefits of using configurator are i.e. providing delivery time and price instantly, detection of the inconsistencies and dependencies between different options, reduced complexity of specifications and reduced time used for making the specification. Configurator can be used also in co-designing products with customers, where it helps in communication.[5]

Configurator brings benefits to the whole delivery process, by removing the information gaps which are needed in the product order. This is done by forcing the customer to answer to every critical question already when the order specification is made. By using configurator, non-standard products can be identified in the first phase of the sales process and customer can be guided to choose more standard features.[6] The configuration process will typically include at least the clarification of customer's requirements and the selected components, alongside forming the price, as well as the technical specification. In addition, the configuration process detects the functionality of the configured product.[7] These issues gave aims and restrictions for the research group.

The target of this research was to develop and test a prototype configurator application based on an idea of using the V-matrix representation of configuration rules. After developing and testing the first version of the prototype configurator application, aim was to develop a prototype of client-server version of the sales configurator application.

In order to use configurator efficiently in a company, many times companies' processes needs to be taken into consideration and under development.[7] Because of this it was decided that these aspects will be noticed already in configurator development phase and research and development needs to be done in cooperation with the end users in machine industry. This paper describes how this project was done. Aim was to develop a matrix-based configurator rule table in Excel and to develop a database based client-server configurator application's working prototype for the use of sales departments in machine industry.

II. THE RESEARCH PROCESS

In order to succeed in a difficult new application development project, a case study approach was adopted. Application prototypes were developed as an action type of re-search. Project researchers implemented the project in cooperation with one case company from machine industry. One member of the research team was located in the company, which made continuous collaboration possible with the key processes in the company, considering configurator stakeholders. The empirical research and literature study process of this project can be seen as a systematic combining process. [8]

III. CONFIGURATION RULES AND MATRIXES

The relations between product family modules are guided by rules that in most commercial configurators are in form of "if-then-else" statements. In complicated situations the management of the rule base may become very hard or even impossible. The other option to define the rule base is to use a matrix representation. In it the rule base is easier to update and maintain. The matrix can also be used to visualize the module relations in one view and they represent the configuration knowledge as simple as possible. Matrix also provides the generic product structures for the modular systems.[1]

The mostly used matrix applications are K- and V-matrixes (Fig. 1). In K-matrix the properties and modules are on the different sides of the matrix while in V-matrix the rows and columns are copies of each other. K-matrix is more simple but also more difficult to use.[9] In V-matrix it is possible to set a relation of every module and property to any other modules and properties. The matrix view is clear and no programming skills are needed to manage the rules in it. Matrix structures done in this study was made and tested first in Microsoft Excel, which is an excellent tool to compare and test different matrix applications. It is well known and widely used. These reasons affected when the first phase of the research and development project was started and platform was chosen. It's suitability for this job was also already proved in Nummela's research done about the same subject.[1]

IV. V-MATRIX RULE TABLE

The developed application prototype is based on V-matrix. This is because it was essential to be able to have correlations between sales features of modules. This makes it possible to exclude those features that are not compatible with the selections already made, when using the configurator in a sales situation. While the configuration approaches there is no possibility to make incorrect selections.

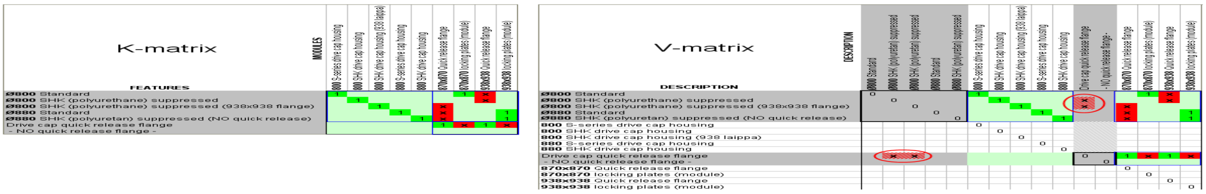

Figure 1. K- and V-matrixes.

In the V-matrix it is possible to make the selections in random order, other than in many commercial configurators using if-then-else rules. This helps in the situation where it is more important for a customer to start from some specific feature of the product con-figured, and not necessarily go through step by step. A configurator which uses if-then-else rules, the configuration order is forced to go only step by step on one path. Because rules are presented in the V-matrix graphically, it is easier to upkeep, comparing to configurator using if-then-else rules, which needs coding skills from its user. Graphic user interface in V-matrix also shows visually how the change relates to other modules and features.

When using a matrix based configurator it is also possible to use numerical relations between modules and properties. For example, if user wants to select some specific module or feature which demands two pieces of another module, this type of numerical relation is used. Or if the relation number is 0 then selecting a module with numerical relation would exclude the related module or property. These rules can be made by the person who upkeeps the rule table simply by adding the number where appropriate.

In Fig. 2 there is an example of the use of the V-matrix. On the upper left corner there is a column identifier showing the item numbers of modules. Category shows the number of property combo box in user interface. The X-marks shows the restrictions of features. For example selecting the feature 1 from first line would exclude the features 5 and 6 from the combo box 2. Correspondingly selection of the feature 2 would exclude the features 3 and 4. Features 1 and 2 cannot be selected simultaneously because they belong in the same category. If you select for example features 1, 3 and 7, you will get the structure modules 1,2,4,8, and 9.

V. SALES CONFIGURATOR IN MS EXCEL

The first prototype of the configurator application prototype developed through the re-search project presented in this paper, was performed by using an MS Excel spreadsheet and VBA-programming. Result was a V-matrix-based configurator rule table and sales configurator prototype working in MS Excel.

The first developed prototype in Excel can be used as a sales configurator that finally produces the bill of material (BOM-structure) of the configured product and guides the sales person when choosing the features for the customer order. With the guidance pro-vided by the rule table, inappropriate module relations can be avoided. Application also gives the price and weight information based on the selected modules. The BOM item numbers are similar to the item numbers in PDM-system, so the BOM can be directly transferred into it for further processing.

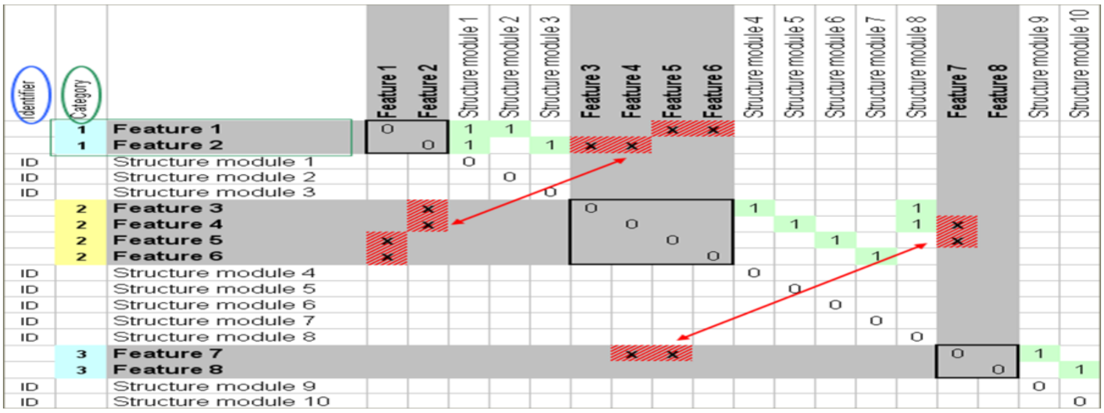

Figure 2. Example of the use of V-matrix.

As a benefit for different departments in a machine industry company, it was seen that V-matrix presentation gave a common language for different departments and most importantly, it made possible to see all modules and possible combinations available for the machine in one sheet. This brings benefits for example for the design department and situations where module changes are discussed with sales, because the dependencies of the modules and technical features can be seen immediately.

Excel does, however, have some disadvantages that make its use difficult in real production situations. One of the worst is that the spreadsheet is just one file. It would be very difficult to control its use and updating. When modifications and updates are made to the spreadsheet which consist all configuration data, it needs high level of attention because it can be possible that the change is done to wrong field or for wrong item by mistake. Depending on the amount of dependencies of features, one mistake can lead to numerous wrong non-functional modules and products, or leave out choices what should have been possible to make.

VI. SERVER-CLIENT SALES CONFIGURATOR

The second phase was started alongside with the rule table development in Excel. In this phase researchers started to develop database-based client-server configurator application's working prototype for the use of sales departments. This was also done in cooperation with the case company and end users of the configurator. Aim of the configurator application development in the second phase, was to design it to work in larger scale with more configurable machines and data, and with use of sales persons anywhere in the world, as well as make it possible to communicate with other systems used in the factories. Architecture for the second phase prototype can be seen in Fig. 3.

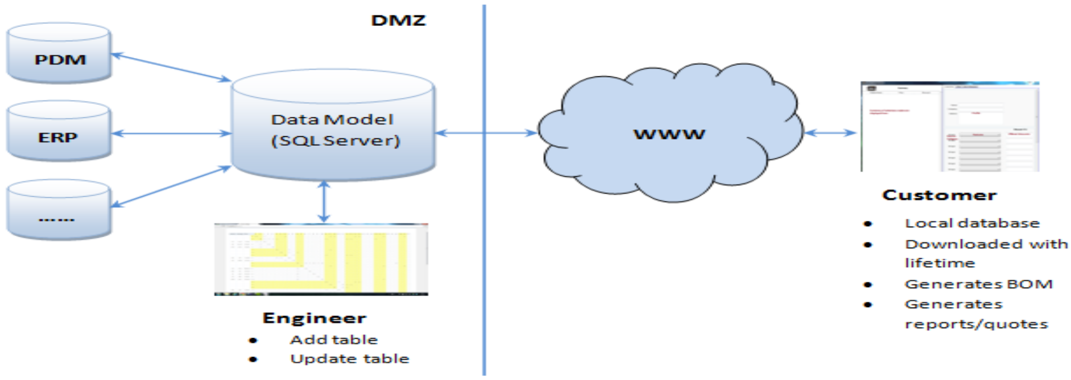

Figure 3. Sales configurator architecture.

In the sales-client application prototype, the V-matrix serves as the admin tool to visualize the relationships between the tables in the database in a compatibility matrix. Changes can be made to the database from this matrix view, which is developed as a web page using the MVC (Model-View-Controller) model approach.

As safety in use was one important aspect in the research and development of the configurator prototype, many features of the second version of the application were auto-mated, so that use of it would be easier and safer. For example additional features and modules can be created by clicking on the provided links on the V-matrix web page. Colors are used to distinguish between the features and the modules i.e. yellow color for the features, white color for the modules.

Changes made to the number of modules belonging to a particular row of features by typing the desired numerical value or changes made to the compatibilities by typing “x” in the appropriate cell on the matrix table, can all be saved into the database by clicking on the “Submit” button at the foot of the page. Before saving the data, application shows the user all data to be changed and asks approval for it. These functions are important benefits when second prototype is compared to first version of the configurator prototype.

The sales configurator is a client’s user interface consisting of combo boxes which contains features. Configurations can be set by selecting different features from the available combo boxes. The combo boxes in this user interface are all generated at runtime i.e. it is generic, and works even if the database is modified. The sales configurator was developed using WPF (Windows Presentation Form), with C# as the coding language.

To help sales persons working in different countries, the client’s sales configurator can be downloaded from a secured address, with the right username and password. The software can then be installed on a personal computer running Windows XP, Vista or 7. When the program is started for the first time, the sales configurator software downloads the database via a provided web service address and populates the combo box items with features from this database. At other times after the first launch, it checks for any update and if it finds one, it makes a request to update its local database. If the request is granted, it will update the local database with the most recent data. And if otherwise request is denied, it will continue using the current local database until its specified lifetime ends. Lifetime prevents sales using outdated product data in new orders, which might lead to difficulties in the production.

VII. CONCLUSIONS

Because of the flexibility of Excel based configurator, it is easy to use with any modular product families. It is a cheap way to find out how configurable the products are. Matrix based rule table and Excel configurator is a light way to test configurability of the modular products in the machine companies, because expensive investments are not needed and the first step towards configurator and configurable products is very easy to take.

However, the modular product structure must be first well defined for all product families which are configured with the application. Also the investigation of product sales features has to be done before the configurator development may begin. The maintenance and update of big matrix rule base is not easy task. It demands deep knowledge of product structure and the functional properties of modules.

When the products come more complex and the number of configured product families grows, a database solution is the safest way to handle all product related data. It makes it easier and safer to have everything up to date, as well as it is updated immediately to configurator when changes occur. And when the configurator is used by multiple sales persons in the same time, the server-client sales configurator makes it easy to force everyone to use the same most up to date data. Also the security aspects are better, because the configuration files have many times secret company specific information and connectivity to other company systems are easier to implement than in the first version of the sales configurator prototype in Excel, which needed filter applications for transfer-ring the data.

When developing a configurator application it is important to take into account the demands of continuous update and maintenance of configuration knowledge. This is because the product structure is under continuous development and the configurator that does not correspond to the product is useless.

As from the research project view point, dividing the development project in two phases, using different software for finding the best solution and doing the development work from scratch with the end user companies, was found very efficient in terms of finding as many problems as fast as possible. This way the companies can have faster an application what they really want, which works and they can use efficiently..

VIII. ACKNOWLEDGEMENTS

This research has been supported by the European Structural Funds programme for Eastern Finland through the research project LEKA. The paper is based on the research work made by the team that consisted of the authors of this paper as well as Petri Leivo, Teuvo Heikkinen, Lauri Alonen, Mikko Pääkkönen, Mohamed Mursal and Paul Ashaolu.

REFERENCES

[1]. Nummela, J., Integrated Configuration Knowledge Management by Configuration Matrices – A Framework for Representing Configuration Knowledge, Thesis for the degree of Doctor of Technology, Tampere University of Technology, Publication 589, 2006

[2]. Sarinko, K., Asiakaskohtaisesti muunneltavien tuotteiden massaräätälöinti, konfigurointi ja modulointi, Thesis work, Helsingin teknillinen korkeakoulu, Konetekniikan osasto, [online document] [latest access 5.9.2012] Can be found on: http://www.soberit.hut.fi/pdmg/papers/Sari99Mas.pdf, 1999.

[3]. Jahnukainen, J. Lahti, M. Virtanen, T. Loginet: Toimittajayhteistyö tilausohjautuvissa toimitusketjuissa, Metalliteollisuuden kustannus Oy, 1997

[4]. Huuskonen, A., Configuration of a Modular Product, Bachelors thesis, Savonia University of Applied Sciences, 2008

[5]. Ristov, P., Ristova, A., T., WEB-BASED PRODUCT CONFIGURATION FOR MASS CUSTOMI-ZATION-Towards developing mass customization strategy, Thesis work, Tekniska Högskolan, Jönköping, 2011

[6]. Jahnukainen, J., Lahti, M., Luhtala, M., Logipro: Tilausohjautuvien toimitusketjujen kehittäminen, Metalliteollisuuden kustannus Oy, 1996

[7]. Tiihonen, J., Soininen, T, Product Configurators - Information System Support for Configurable Products. Otaniemi, 1997

[8]. Dubois A. & Gadde L., Systematic combining: an abductive approach to case research, Journal of Business Research, Vol. 55, Iss. 7, pp. 553-660, 2000

[9]. Bongulielmi, L., Henseler, P., Puls, Ch. and Meier, M. THE K- & V-MATRIX-METHOD IN COMPARISON WITH MATRIX-BASED METHODS SUPPORTING MODULAR PRODUCT FAMILY ARCHITECTURES. Federal Institute of Technology, Institute for Mechanical Systems Switzerland, [online document] [latest access 4.9.2012] Can be found on: http://www.coma.imes.ethz.ch/pdf/PaperNordDesign02.pdf

American Journal of Engineering Research (AJER)
e-ISSN : 2320-0847 p-ISSN : 2320-0936
Volume-02, Issue-06, pp-19-24
www.ajer.org

Research Paper Open Access

Developing Rainfall Intensity–Duration–Frequency Models for Calabar City, South-South, Nigeria.

AKPAN, S. U. and OKORO, B. C.
Department of Civil Engineering, Federal University of Technology, PMB 1526, Owerri, Imo State, Nigeria.

Abstract: - Rainfall Intensity – Duration – Frequency (IDF) models for Calabar city are presented based on 10 years (2000 - 2009) rainfall data. The statistical method of least squares was used and the models developed are categorized into two sets. The first set of models represents an inverse relationship between rainfall intensities and duration for specified frequencies which are called "INTENSITY – DURATION MODELS" and frequencies of 1, 1.1, 1.2, 1.4, 1.6, 1.8, 2.2, 2.8, 3.7, 5.5, and 11 years are used; and very high and positive regression coefficient ranging from 0.9372 to 0.9930 and goodness of fit 0.8788 to 0.9851 were recorded. The second set of models represents rainfall intensities and frequencies for specified duration which are called "INTENSITY – FREQUENCY MODELS", and durations of 15, 30, 45, 60, 90, 120, 180, 300 and 420 minutes were used, and very high and positive regression coefficients ranging from 0.7908 to 0.9890 and goodness of fit 0.6263 to 0.9863 were obtained. The range of frequencies and durations used are based on assessment of the data obtained, which included all critical rainfalls of high intensities. A total of 20 models were developed; this includes 11 Intensity – Duration models and 9 Intensity – Frequency models. Their coefficient of correlation is estimated to show the degree of correctness. The two sets of models obtained from this research, will serve as an important tool for the prediction of the occurrence of any given rainfall amount in Calabar city as well as for use in the design of structures that control storm runoff and flooding in Calabar and cities of similar rainfall characteristics.

Keywords:- Correlation Coefficient, Least Squares, Rainfall Intensity, Intensity- Duration Model, Intensity-Frequency Model

I. INTRODUCTION

Models can be expressed mathematically to represent a system or sets of data; Models are also seen as mathematical representations of sets of relationships between variables or parameters (Nwaogazie, 2006; Nwadike, 2008). In this study, we shall be looking at Mathematical models as representing a set of variables which establishes relationships between these variables.

A major challenge any hydrologist or engineer will encounter in the planning and design of water resources structure is that of unavailability or limited required long-term rainfall data. The development of rainfall models requires long-term rainfall records with durations. Only a few meteorological stations in a developing country like Nigeria can boast of consistent 30 years rainfall data; some of these stations are in Lagos, Calabar, Benin, Port Harcourt, Kano, Owerri and Onitsha, with missing data in-between and some without the duration of the rainfall events. The remaining stations nation-wide have very short records of rainfall data (Nwaogazie and Duru, 2002).

Every design of a water resources structure needs an engineer to carry out a careful analysis on the existing rainfall data. In the analysis involving such rainfall event, randomness is present. Design of water resources structures become difficult to handle when the problem of inconsistency and unavailability of required long-term rainfall data exist. The engineer has to then adopt frequency analysis through which future probabilities are determined from the past rainfall events.

The design of hydraulic structures such as drainage structures is a problem when there are no measured values of rainfall history of such an environment. The quantity of water the drains should collect is assumed rather than calculated. Sometimes this assumption of rainfall quantity can cause temporary floods in such areas.

Hence, the need for the development of rainfall models for Calabar city, a major town and capital of Cross River State, Nigeria.

II. METHODOLOGY

2.1 Study Area and Data Collection

Calabar City lies within the South-South region of Nigeria. It is located at $4^0 57' 0''$ North and $8^0 19' 0''$ East of Nigeria. Calabar city falls under the mangrove region where rainfall is very high .The available rainfall data obtained from the region covered the period between the year 2000 and 2009 which includes the amounts and duration of rainfalls.

2.2 Model Development

The analysis of the Calabar ten (10) years rainfall involved sorting of the rainfall amounts against durations of 15, 30, 45, 60, 90, 120, 180, 300 and 420 minutes and converting the rainfall amounts to intensity value in millimeter per hour (mm/hr). The resulting rainfall intensity was assigned the rank of 1.The probabilities of the rainfall events were obtained using the Weibull's formula shown in equation (1) indicating a return period of one year longer than the period of record for the largest value (Chow, 1952). Tables 1 and 2 showed the rankings of the various rainfall durations and their calculated intensities.

$$P(X_m) = \frac{m}{n+1} \qquad (1)$$

Where,

$P(X_m)$ = Probability of exceedence of variate X_m

m = Rank of descending values, with largest equal to 1,

n = Number of years of record

Return periods (frequencies) of the rainfall events were calculated as the reciprocals of their corresponding probabilities as also shown in Table 1 and 2.

Table 1: Rainfall ranking and probability of event

S/NO.	15MINS INTENSITY (mm/hr)	30MINS INTENSITY (mm/hr)	45MINS INTENSITY (mm/hr)	60MINS INTENSITY (mm/hr)	90MINS INTENSITY (mm/hr)	RANKING	FREQUENCY
1	147	75.42857143	118.8	62.06896552	57.22105263	1	11
2	124.6153846	61.93548387	85.06666667	58.78125	39.68571429	2	5.5
3	107.4	60.54545455	51.84	52.24615385	39.53333333	3	3.7
4	100.8	53.4	38.26666667	46.8	34.75862069	4	2.8
5	99.81818182	43.09090909	33.75	35.79661017	33.38823529	5	2.2
6	91.2	40.32	32.26666667	35.54716981	33.20454545	6	1.8
7	78.5	36.24	31.59183673	28.125	32.21917808	7	1.6
8	74.76923077	33.6	30.57142857	24.70588235	29.92307692	8	1.4
9	49.89473684	33.08571429	27.06666667	22.4	26.85714286	9	1.2
10	48.6	31.15384615	25.22727273	22.19047619	25.44303797	10	1.1
11	46	30.18181818	22.95	20.94545455	21.97894737	11	1.0

Table 2: Rainfall ranking and probability of event in Calabar City

S/NO.	120MINS INTENSITY (mm/hr)	180MINS INTENSITY (mm/hr)	300MINS INTENSITY (mm/hr)	420 INTENSITY (mm/hr)	RANKING	FREQUENCY
1	112.324493	38.06896552	20.32807571	19.71818182	1	11
2	44.41935484	28.6	20.32807571	14.26666667	2	5.5
3	40.89473684	25.77777778	19.66956522	14.18734177	3	3.7
4	26.953125	24.32727273	19.66	13.91646192	4	2.8
5	26.03478261	24	19.464	11.6	5	2.2
6	24.04918033	23.78313253	19.10460251	10.77889447	6	1.8
7	23.73214286	20.78350515	18.775	10.4	7	1.6
8	21.73109244	20.0106383	17.57777778	9.383886256	8	1.4
9	21.19672131	19.60869565	16.53488372	8.8	9	1.2
10	20.86725664	19.05	14.67391304	8.313253012	10	1.1
11	20	18.29268293	14.55652174	8.171428571	11	1.0

The mathematical equation employed in developing a relationship between rainfall intensity and duration for a given recurrence period is given as equation (2)

$$i = \frac{A}{t+B} \qquad (2)$$

Where,

i = rainfall intensity in mm/hr
t = duration in minutes
A and B= regional constants

Equation (2) can be represented in a linear form as:

$$y = a_1 x + a_0 \qquad (3)$$

Where

$y = \frac{1}{i}$, $a_1 = \frac{1}{A}$ and $a_0 = \frac{B}{A}$.

The solution of Equation (3) was achieved with the aid of a computer program.
Table 3 showed all the intensity duration models developed, for frequencies of 1, 1.1, 1.2, 1.4, 1.6, 1.8, 2.2, 2.8, 3.7, 5.5, 11 years. The rainfall intensity duration curves are linear in nature as shown in Figure 1

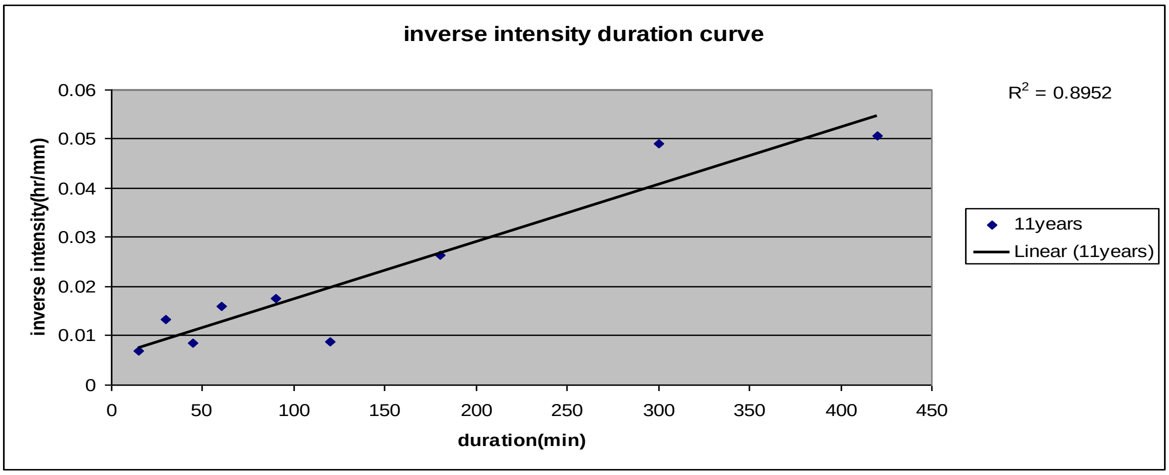

Figure 1: Rainfall intensity duration curve for 11 years frequency

Table 3:Summary of all intensity duration models developed

s/no	Frequency	Intensity duration model $i = \frac{A}{t+B}$	Checks
1.	11	$i = \frac{8576.33}{t+47.8216}$	CC = 0.9489 GF = 0.8952
2.	5.5	$i = \frac{6915.6293}{t+55.8645}$	CC = 0.9907 GF = 0.9851
3.	3.7	$i = \frac{7110.3527}{t+76.7918}$	CC = 0.9930 GF = 0.9815
4.	2.8	$i = \frac{7494.0048}{t+114.6583}$	CC = 0.9751 GF = 0.9505
5.	2.2	$i = \frac{6620.7627}{t+108.9115}$	CC = 0.9601 GF = 0.9218
6.	1.8	$i = \frac{6620.7627}{t+108.9115}$	CC = 0.9520 GF = 0.9061
7.	1.6	$i = \frac{6189.2678}{t+120.0718}$	CC = 0.9454 GF = 0.8933
8.	1.4	$i = \frac{5605.0670}{t+114.8478}$	CC = 0.9372 GF = 0.8788
9.	1.2	$i = \frac{5451.9682}{t+127.5761}$	CC = 0.9361 GF = 0.8782
10.	1.1	$i = \frac{5006.2578}{t+118.9487}$	CC = 0.9508 GF = 0.9041
11.	1.0	$i = \frac{5080.0101}{t+135.1283}$	CC = 0.9433 GF = 0.8896

± Rainfall intensity is given in mm/hr

- Regression parameter: GF = Goodness of fit and
  CC = Coefficient of Correlation

Another model employed to fit rainfall intensity values is the Power model. Its form is presented as equation (4)

$$i = aR^b \qquad (4)$$

Where
i = Rainfall intensity (mm/hr)
R = Return period or frequency (yrs)
a and b are regional constants

Equation 4 can be represented by

$$y = a_1 x + a_0 \qquad (5)$$

Where,

$$y = \log i$$

a_1 = b and $a_0 = \log a$

Equations can be used to fit rainfall data. Using the statistical method of least squares in regression, the constants *a* and *b* can be evaluated.
The solution of Equation (5) was also achieved with the aid of a computer program.

Table 4 shows all the intensity return period models developed, for durations of 15, 30, 45, 60, 90, 120, 180, 300, 420 minutes. The rainfall intensity return period curves are linear in nature as shown in Figure 2.

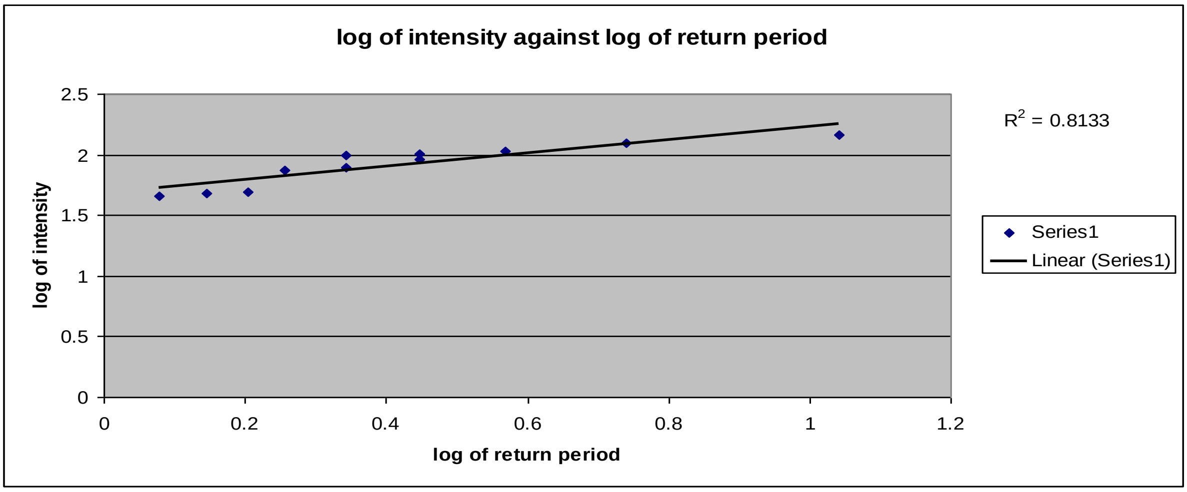

Figure 2: Rainfall intensity return period curve for 15 min duration

Table 4: Summary of all intensity return period models developed

s/no	Durations	Intensity return period models ($i = aR^b$)	Checks
1.	15	$i = 48.5176R^{0.5476}$	CC = 0.9890 GF = 0.8133
2.	30	$i = 27.68R^{0.4624}$	CC = 0.9435 GF = 0.9863
3.	45	$i = 18.3527R^{0.7844}$	CC = 0.9772 GF = 0.9549
4.	60	$i = 19.61R^{0.5845}$	CC = 0.9202 GF = 0.845
5.	90	$i = 22.7196R^{0.3857}$	CC = 0.9732 GF = 0.9459
6.	120	$i = 14.2659R^{0.7583}$	CC = 0.9567 GF = 0.9087
7.	180	$i = 17.005R^{0.3269}$	CC = 0.9851 GF = 0.9687
8.	300	$i = 15.6747R^{0.1503}$	CC = 0.7908 GF = 0.6263
9.	420	$i = 7.6542R^{0.4086}$	CC = 0.9555 GF = 0.9123

± Rainfall intensity is given in mm/hr

- Regression parameter: GF = Goodness of fit and
  CC = Coefficient of Correlation

III. DISCUSSION OF RESULTS

The first set of the models involved finding solution to Equation (3) using available rainfall intensity-duration data for specified frequencies of 1, 1.1, 1,2, 1.4, 1.6, 1.8, 2.2, 2.8, 3.7, 5.5 and 11 years. A total of eleven (11) rainfall models were developed with very high and positive values of goodness of fit, ranging from 0.8788 to 0.9851 and coefficients of correlation of 0.9372 to 0.9930. The plots of intensities against duration for the eleven (11) models provided a good basis for the predicted results.

The second set of the rainfall calibration involved solving Equation (5) using as input data, rainfall intensities and frequencies for specified durations of 15, 30, 45, 60, 90, 120, 180, 300, and 420 minutes. A total of nine (9) rainfall models were developed with positive values of goodness of fit of 0.6263 to 0.9863, and coefficient of correlation of 0.7908 to 0.9890, indicating a good correlation. Also the plots of the models provided a good basis for the predicted results. The following observations are characteristic of Calabar city rainfall pattern:

- The high intensity storms correspond to short durations, a common feature of tropical thunderstorms.
- The curves are linear in nature (see Figures 1 and 2)

These observations are in agreement with other literatures (Thunderstorm Rainfall, 1947; World Meteorological Organization, 1969, Viesma et al., 1977; Nwaogazie and Duru, 2002; Linsley and Franzini, 1979). In drainage design and construction, it is a common knowledge that the cost of drainage increases as the size of the gutter design capacity is increased. On account of the above, urban drainage design calculations as adopted in this research work were based on average rainfall intensity that has a return period of 10years. This is in keeping with the recommendations made in the Highway design manual, Part – 1 (FMW&H, 2006). This work has succeeded in presenting Calabar City as well as towns with similar climatic conditions in South-South region of Nigeria with set of well defined models that can serve very well in water works and hydraulic structures design.

IV. CONCLUSION

The rainfall intensity-frequency relationship is one of the most commonly used tools in Water Resources Engineering, either for planning, designing and operation of water resources projects, or for various engineering projects against floods. It is therefore, important in the determination of rainfall intensity for any desired period as a guide in the design of water related structures. The availability of Rainfall Intensity-Frequency Regimes will really make the design of some hydraulic structures easy for civil and water resources engineers, as well as other environmentalists carrying out works relating to rainfall around the study area.

For calabar city, the study simply developed models from past available records of rainfall events which gave high and positive coefficients of correlation using the regression data fitting approach. It provided the desired basic rainfall information required for the design of drains for Calabar city.

REFERENCES

[1] **Chow, V. T. (1952).** "Engineering Analysis of Hydrological data with special Application to rainfall intensities" Uni. Of Illinois Eng. Expt. Station, Bull 414 July.

[2] **FMW&H (2006).** Federal Republic of Nigeria Highway Design Manual, Part – 1, Federal Ministry of Works.

[3] **Hadadin, N.A. (2005). "**Rainfall intensity–duration–frequency relationship in the Mujib basin in Jordan", *Journal* of Applied Science, 8 (10) (2005), pp. 1777–1784.

[4] **Leton, T. G. (2005). "**Elements of Civil Engineering Hydraulics", 1st Edition, Published by Reynold Grifts Publishing Co: Lagos; Nigeria.

[5] **Linsley, R. K** and **Franzini J. B.(1979). "**Water Resources Engineering", 3rd Edition, McGraw-Hill, New York.

[6] **Linsley, R. K. ; Kohler M. A,** and **Paulhus J. L. H. (1982). "**Hydrology for Engineers", McGraw-Hill Book Co., New York.

[7] **Nwadike, C. N. (2008).** "Developing Rainfall Models for Enugu City", M.Eng. Thesis, Dept., of Civil Engineering , Federal University of Technology, Owerri(FUTO), Imo State, Nigeria.

[8] **Nwaogazie, I. L. (2006). "**Probability and Statistics for Science and Engineering Practice". 2nd edition, Prints Konzults Lagos.

[9] **Nwaogazie, I. L.** and **Duru, E. O. (2002). "**Developing Rainfall – Intensity – Duration – Frequency Models for Port Harcourt City", Nig. Society of Engineers Technical Transaction, Vol. 37, No. 2, pp 19 – 32.

[10] **Nwoke, H. U.** and **Okoro, B. C. (2012). "**Rainfall Intensity- Frequency Regime For Warri, South – South Nigeria". Journal of New Clues In Sciences 2(2012)42 – 49.

[11] **Thunderstorm Rainfall (1947). "**Hydrometerological Rept. No.5", U. S. Weather Bureau in cooperation with Corps of Engineering, pp 234 – 259.

[12] **Viessman, W.; John W. K.; Lewis, G. L.** and **Harbaugh, T. E. (1977). "**Introduction to Hydrology", 2nd edition, IEP – Dun – Donnely, Harper & Row Publishers, New York.

American Journal of Engineering Research (AJER)
e-ISSN : 2320-0847 p-ISSN : 2320-0936
Volume-02, Issue-06, pp-25-33
www.ajer.org

Research Paper Open Access

Prediction of Extrusion Pressure And Product Deflection Of Using Artificial Neural Network

D.T. GUNDU[1], K.K. IKPAMBESE[2], AND A. ASHWE[3]
[1,2,3](Department of Mechanical Engineering, University of Agriculture Makurdi-Nigeria).

Abstract: - *In this paper artificial neural network was used as a modeling tool for simulation and prediction of extrusion pressure and product deflection of extrudes of lead alloys. An extensive experimental program was undertaken to extrude a lead (Pb) alloy on ELE Compact-1500 compression machine. The neural model of extrusion pressure and product deflection was developed based on groups of experiments carried out as samples, Eight (8) die bearing parameters (die bearing length, radius of curvature, slip angle, die angle, die ratio ram displacement, pocket depth and die diameter) were used as inputs into the network architecture of 8 $[4\text{-}3]_2$* ***2*** *in predicting the extrusion pressure and product deflection. After series of network architectures were trained using different training algorithms such as Levenberg-Marquardt, Bayesian Regulation, Resilient Backpropagation using MATLAB 7.9.0 (R20096, the LM8 $[4\text{-}3]_2$* ***2*** *was selected as the most appropriate model. Prediction of the neural model exhibited reasonable correlation with the experimental extrusion pressure and product deflection. The predicted extrusion pressure and product deflection gave reasonable errors and higher correlation coefficients indicating that the model is robust for predicting extrusion pressure and product deflection.*

Keywords: - *Artificial neural network, Extrusion pressure, die bearing, modeling, product deflection,*

I. INTRODUCTION

Extrusion is a plastic deformation process in which a block of metal called the billet is compressed through the die opening of a smaller cross-sectional area than that of the billet [1]. According to [2] extrusion is one of the forming techniques used in materials processing. The term is usually applied to both the process, and the product obtained when a cylindrical work piece or billet is pushed through a shaped die, thereby reducing its section. The resulting section can be used in long lengths or cut into shorter parts for use in structures, vehicles or as components. Also, extrusions are used as starting or feed stock for drawn rod, cold extruded and forged products. While the majority of presses used for extrusion worldwide are covered by the description above, some presses accommodate rectangular shaped billets for production of extrusions with wide sizes. Other presses are designed to push the die into the billet or indirect extrusion. The versatility of the process in terms of both alloys available and shapes possible makes extrusion most valued assets for solution to design requirements [3].

The design of extrusion dies depends on the experience of die designers. After production of the die, it is tested and modified severally until it works properly. Die design is therefore by trial and error and this is expensive. However, the die has been recognized as the heart of the extrusion process as product quality and productivity depends highly on its performance. A major challenge has been to maintain uniform flow throughout the cross-section to avoid twisted, bent or out-of-tolerance extrusion [4]; [5]. Traditionally, flow control has been achieved using different bearing configurations from shear to slip dies, dies with relieved bearings, dies with pocket bearings e.t.c. Each of these achieves improvements in product quality or reduction in extrusion pressure at the expense of the other.

One of the greatest challenges in the design of an actual extrusion operation is to obtain realistic manufacturing process parameters to plan t execution. Conventional finite element analysis and other numerical methods been applied to extrusion processes. However, these do not consider the manufacturing constraints in their modeling and hence, the process parameters obtained through such analysis were more theoretical and not realistic enough. Also, due to the inherent time consuming nature of such methods, quick and rapid problem solving as desired by industries have not been achievable. Also, these mathematical models when presented with new set of data, do not yield desired results [1].

Artificial neural network (ANN) as a modeling and simulation tool has been widely employed in engineering processes and systems. This is as a result of its capability to capture all input parameters that can be related to the output (s). Bajimaya et al [1] used neural network model to predict the manufacturing process parameters such as pressure, temperature and velocity, the results obtained were in agreement with the experimental values. Neural network modeling and optimization of semi-solid extrusion for aluminium matrix composite was also investigated by [6]. Satisfactory results were achieved with the deforming force of semi-solid extrusion being reduced significantly, indicating the feasibility of the proposed method according to derived data from experiment. Interest in artificial neural network (ANN) modeling in other field of engineering has also increased rapidly. For instance, predictions of friction and wear properties of composite and metallic alloys were carried out by [7] and [8]. Several other investigators like [9]; [10]; and [11] have found corrosion rates of different materials in different media effectively using artificial neural network.

The present study has been conducted to establish an appropriate artificial neural network model for predicting the extrusion pressure and product deflection of Lead Alloy extrudes. The neural model of the prediction of extrusion pressure and product deflection was used for the approximation between the technological parameter inputs such as die bearing length, radius of curvature, slip angle, die angle, ram displacement, pocket depth, extrusion diameter and die ratio against extrusion pressure and product deflection as outputs. Validity of the proposed model was also assessed using standard statistical parameters.

II. MATERIALS AND METHODS

2.1 Preparation of extrude billets

The lead alloy having appropriate composition 67% Pb, 26.5 %Sn and 6.5% Bi was obtained from automobile battery grids and terminals. The melts were cast in galvanized steel moulds of 26 mm diameter and later machined into test billets of dimension 24.4 mm by 25.4.

2.2 Extrusion procedure

The extrusion billets, machined to diameter of 25.4mm by 26mm were directly extruded on manual ELE Compact-1500 hydraulic press shown in Fig.1. Split dies were used to facilitate easy separation of extrudes after each extrusion. Load readings were taken at 1 mm of ram travel, and the maximum load noted for each extrusion. Average values of extrusion loads were obtained for each extrusion at the steady stage of the process, and by dividing the corresponding loads by the cross-sectional area of the billets, values of extrusion pressure were obtained. The extrusion dies were machined to extrude solid circular sections to reduction ratios of 0.21, 0.3, 0.4 0.48 and 0.62 (corresponding to extrude diameter of 11.5 mm, 16.0 mm, 17.01 mm, 20.0 mm and 22.4 mm. The dies for determining the effect of the die angles on extrusion parameters were produced.

Fig. 1: Extrusion setup on ELE Compact-1500 hydraulic machine

2.3 Experimental

2.3.1 Extrude curvature and deflection.

Extrudes were carefully separated from the dies and were held on a lathe machine using a three- jaw chuck. By rotating the chuck slowly the axial deflection of the extrudes were measured at a distance of 25 mm from the face of the chuck using a vertical height gauge with sensitivity of 0.001 mm [12]

2.4 Neural network modeling

The development of the neural network for prediction of extrusion pressure and product deflection was based on the experimental data. The experiment was carefully planned to provide the input/ouput quantities for neural networks training, validation, testing and simulation as explained in the methodology. The following steps were considered in modeling the extrusion pressure and product deflection of lead alloy extrudes [13]; (i) data generator (ii) definition of ranges (iii) data pre-processing, (iv) selection of neural network architecture (v) selection of training algorithms (iv) training the neural network, and (vii) testing or predicting.

2.4.1 Input data and output data

The input data or parameters captured in the artificial neural networks model are discussed and presented in **TABLE 1**, while the output data or parameters captured in the artificial neural networks model are also discussed and presented in **TABLE 2.**

Input data S_{T1}-ST_{10} was used for training the network while S_{P1}-S_{P5} for testing the prediction capabilities of the artificial neural network. The data for the neural network modeling was obtained from ten (10) groups of experimental data collected as samples and the working together of the influence of these eight (8) inputs parameters on extrusion pressure and product deflection are shown in Fig 2.

Table 1: Set of input parameters used for training and testing.

		Test	Data	set		
Parameters	**Training data set ST_1-ST_{10}**	**S_{P1}**	**S_{P2}**	**S_{P3}**	**S_{P4}**	**S_{P5}**
Die bearing length (mm)	1-18	1	2	5	8	10
Radius of curvature (mm)	200-460	269	301	355	434	355
Slip angle (deg)	20-80	40.8	43.75	46	53.75	60
Die angle (deg)	50-180	60	75	90	105	120
Die ratio	0.26-20	0.62	0.62	0.62	0.62	0.62
Ram displacement (mm)	5-20	8	10	12	14	16
Pocket depth (mm)	1-10	2	3	4	5	6
Die diameter (mm)	10.5-30.6	11.5	16	17.6	20	22.4

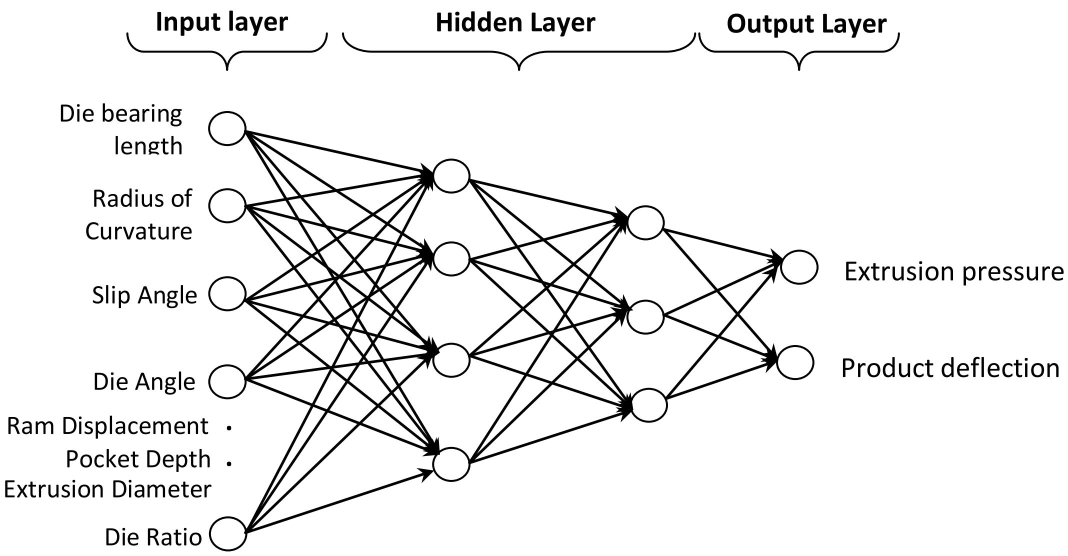

Fig.2: Neural network architecture used

Table 2: The experimental extrusion pressure and product deflection

Output parameter	S_{E1}	S_{E2}	S_{E3}	S_{E4}	S_{E5}
Extrusion pressure (MPa)	82.39	86.83	94.72	122.36	132.40
Product deflection (mm)	0.28	0.26	0.24	0.23	0.21

2.4.3 Data pre-processing

Pre-processing of the inputs and output parameters was carried out before the neural network training. The experimental data involving the inputs and outputs were measured in different units, the data of different types have great difference. Such difference will decrease the convergence speed and accuracy within the network. Therefore before network training, the input and output data set measured in different units need to be normalized into the dimensionless units to remove the arbitrary effect of similarity between the different data [14].

The eight (8) input parameters (excluding die ratio) were scaled within the range of 0-1 using the relation given in equation (2) [14]:

$$I_{Skal} = 1 + \frac{(I_{Curr} - I_{Max})}{(I_{Max} - I_{Min})} \qquad (1)$$

Where; I_{Curr} –is current input value, I_{Max} - the maximum input value and I_{Min}-the minimum input value.

The output parameter extrusion pressure was normalized within the range from 0-1 using the relation in equation (3) [13]:

$$y_n = \frac{y - 0.95 y_{min}}{1.05 y_{max} - 0.95 y_{min}} \qquad (2)$$

Where y_n the normalized value of y. y is the experimental data, y_{max} and y_{min} are the max and min value of y respectively.

2.4.4 Network training

The best neural network's architecture and learning algorithm are unknown in advance; a trial and error approach was used to find the best network's architecture for matching input/output relationship. The following networks architectures were investigated); one layered network 8 $[1]_1$ **2,** 8 $[5]_1$ **2,** two layered network 8 $[4\text{-}3]_2$ **2,** 10 $[4\text{-}3]_2$ **2,** three layered network 8 $[4\text{-}3\text{-}2]_3$ **2,** 10 $[4\text{-}3\text{-}]_3$ **2** in a MATLAB 7.9.0 (R20096)

These networks architecture were trained using the Levenberg- Marquard (LM), Bayesian Regulation (BR), and Resilient Backpropagation (RB). The sigmoid function given in equation (4) was used between the input and the hidden layers:

$$f(x) = \frac{1}{1+e^{-x}} \qquad (3)$$

and linear function f(x) =x was used between the hidden and output layer, where x is the value of weight used.

III. RESULTS AND DISCUSSION

The summary of the results of the tested ANN architecture is presented in **TABLE 3**. The neural model LM 8 $[4\text{-}3]_2$ **2,** was chosen because its exhibited higher correlation coefficient for both training and testing compared with the other architectures and algorithms. Training performance indicated values of correlation coefficient R=1.00 at epoch 12 for training, R=1.00 for testing with validation checks was 6 at epoch 18 while the overall correlation coefficient (R) for training, testing, and validation was 0.90458.

Table 3: Summary of the results of tested ANN architecture.

Architecture	Training	Testing
LM 8 $[1]_1$ **2**	0.701	0.641
BR 8 $[5]_1$ **2**	0.997	1.000
LM 8 $[4\text{-}3]_2$ **2**	**1.000**	**1.000**
BR 10 $[[3\text{-}2]_2$ **2**	0.840	0.572
LM 10 $[4\text{-}3\text{-}2]_3$ **2**	0.731	1.000
RB 10 $[5\text{-}4\text{-}3]_3$ **2**	0.812	0.761

The correlation coefficient (R) was used to examine the strength of linear relationship between predicted and experimental values using the relation in equation (4) [16]:

$$R = \frac{\sum_{i=1}^{N}(E_i - \bar{E})(P_i - \bar{P})}{\sqrt{\sum_{i=1}^{N}(E_i - \bar{E})^2 \sum_{i=1}^{N}(P_i - \bar{P})^2}} \qquad (4)$$

Where E is the sample of the experimental value, p is the sample of predicted value by an ANN model $\bar{E}$ and $\bar{P}$ are the mean value of E and P respectively, N is the number of sample. This established neural model was used to predict extrusion pressure and product deflections.

Table 4 shows the values of the predicted extrusion pressure and experimental (real) extrusion pressure with their respective mean square errors and correlation coefficients. It was observed that the neural network prediction of extrusion pressure was in consonance with the experimental (real) extrusion pressure with minimal network errors of -0.1380, 0.0105, 0.00113, 0.0000349, 0.0000092, and higher correlation coefficient of 1.0000, 1.0000, 0.9956, 1.0000 respectively.

The values of the correlation coefficients were better compared with the values of 0.99997, 0.99999, 0.99997 and 0.99998 by [14]. The slight disparity in some of the predicted and experimental could be attributed ro errors in tha data arising from poor experimental design, fault in equipment or miscalculation.

TABLE 5 shows the predicted and experimental values product deflection with their corresponding networks errors and correlation coefficients (R). It was also observed that the neural network prediction of the product deflection of the lead alloy extrudes showed good agreement with the experimental values. The minimal network errors of 0.05976, 0.32981, -0.00012899, -0.000005 -0.00000095 and higher correlation coefficient R=1 for all the predicted and experimental values were observed.

Table 4: Predicted and experimental (real) extrusion pressure

Predicted (MPa)	Experimental (MPa)	Mean square error (MSE)	Correlation coefficient (R)
84.17	82.89	-0.13072	1.0000
93.1	86.83	0.010595	1.0000
95.02	94.72	0.001127	0.9956
122.75	122.36	0.000349	1.0000
132.40	132.40	0.000009	1.0000

The quality of the prediction of the extrusion pressure and product deflection of the lead alloy extrudes was evaluated taking into cognizance the following points (i) the quality of prediction of extrusion pressure against die bearing length (ii) extrusion pressure against die diameter (iii) product deflection against die bearing length (iv) product deflection against die diameter (v) response 3-D stem graph of extrusion pressure against die bearing with die diameter for predicted and the experimental values of extrusion pressure (vi) response 3-D stem graph of product deflection against die bearing length with die diameter for the predicted and experimental values.

Table 5: Predicted and experimental (real) product deflection

Predicted (MPa)	Experimental (MPa)	Mean square error (MSE)	Correlation coefficient (R)
0.28	0.28	0.05976	-1.0000
0.23	0.26	0.32981	1.0000
0.24	0.24	0.001127	1.0000
0.23	0.23	-0.000005	1.0000
0.21	0.21	-0.00000095	1.0000

Fig. 3 shows comparison between the experimental and predicted extrusion pressure against the die bearing length. The graph showed that both the predicted and experimental values of the extrusion pressure increased exponentially with increased die bearing length. The results generally agree with the findings of a related study by [17], and also confirm earlier findings by [18]. Fig. 4 shows the extrusion pressure against die diameter. It was also observed that both the predicted and experimental extrusion pressure increased with die diameter.

The influence of die bearing length on the product deflection of predicted and experimental values is shown graphically in Fig. 5. Deflection for the predicted and experimental values decreased as the die bearing length increased which shows that die bearing length has significant influence on the product deflection and lower product deflection were obtained with dies of larger bearing length. As shown on the graph, product deflections tends towards zero for the predicted and experimental values as die bearing lengths become large. Fig. 6 shows the plot of product deflection against die diameter. It was observed that the predicted and product deflection decreased as the die diameter increased.

The capability of neural network modeling of predicted and experimental extrusion pressure against die bearing length with die diameter was further illustrated by 3-D stem graphs as shown in Figs. 7 and 8. It was observed that both the predicted and experimental extrusion pressures increased with increased in die bearing length and die diameter. This indicates that the neural model has perform well as reported by other researchers, [16], and [11].

Figs. 9 and 10 also show the 3-D stem plot of ANN for the predicted and experimental product deflection against die bearing length with die diameter. It was equally observed that product deflection decreased as the extrusion diameter and bearing length increased thus, proving the capabilities of the model.

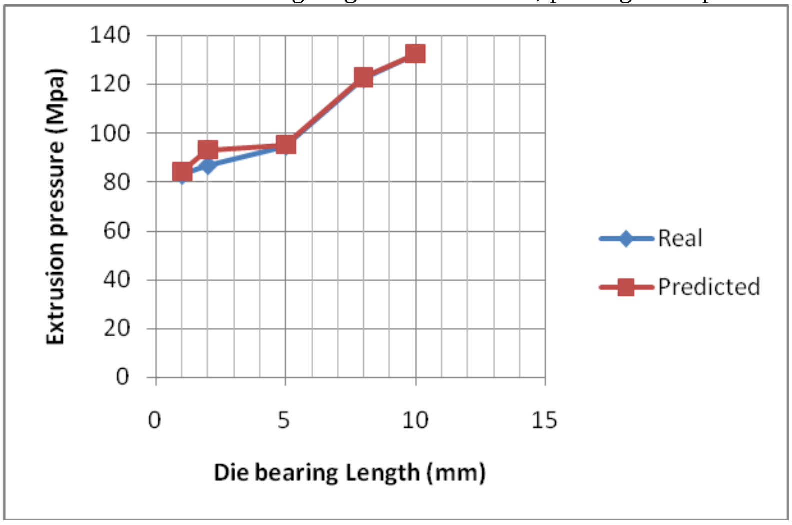

Fig. :3 Plot of predicted and experimental extrusion against die bearing length.

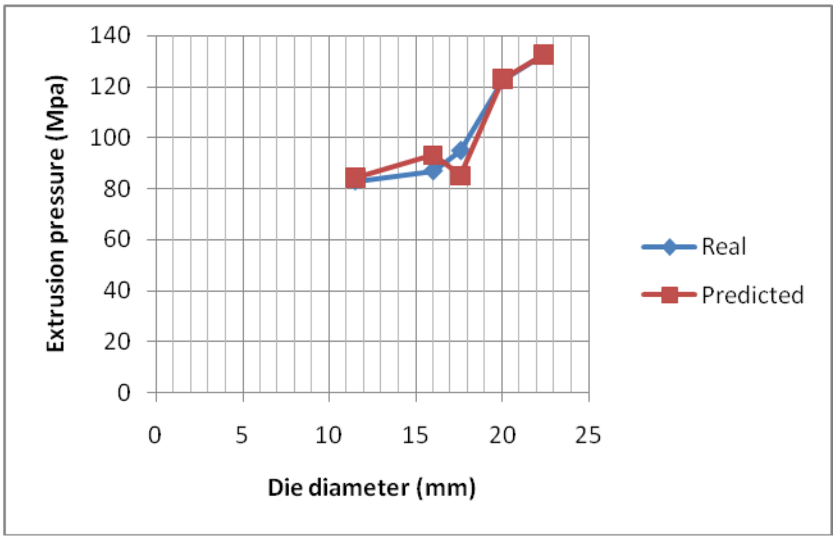

Fig. 4: Plot of predicted and experimental extrusion pressure against die diameter.

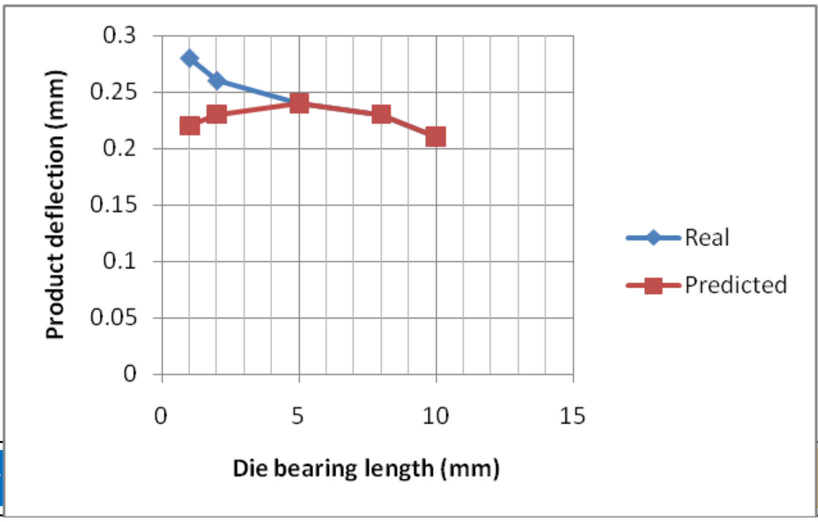

Fig. 5: Plot of predicted and experimental product deflection against die bearing length.

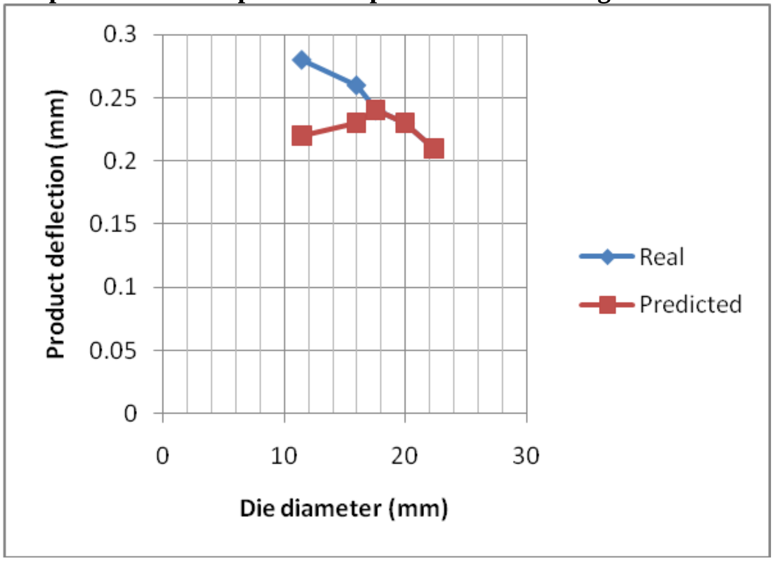

Fig. 6: Plot of predicted and experimental product deflection against die diameter.

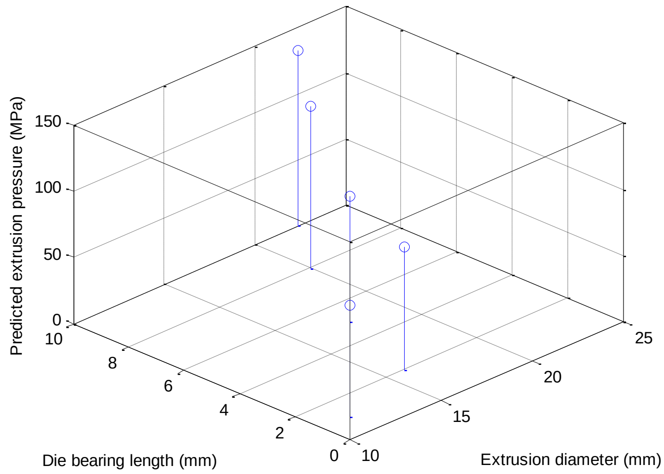

Fig. 7: 3-D stem plot of predicted extrusion pressure against die bearing length and diameter.

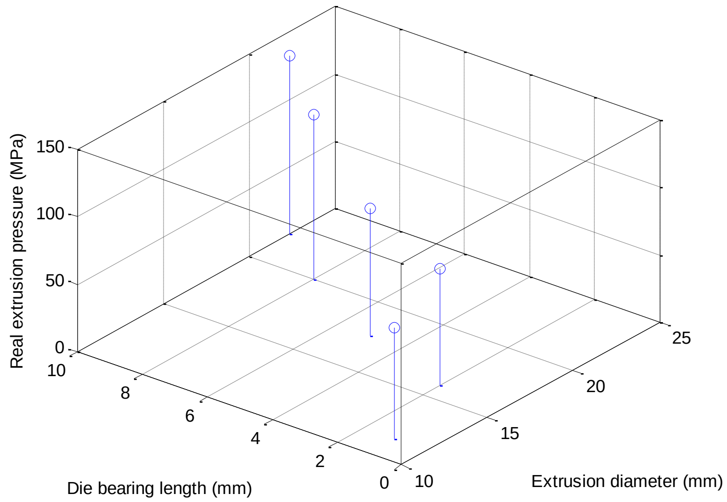

Fig. 8: 3-D stem plot of experimental extrusion pressure against die bearing length and diameter

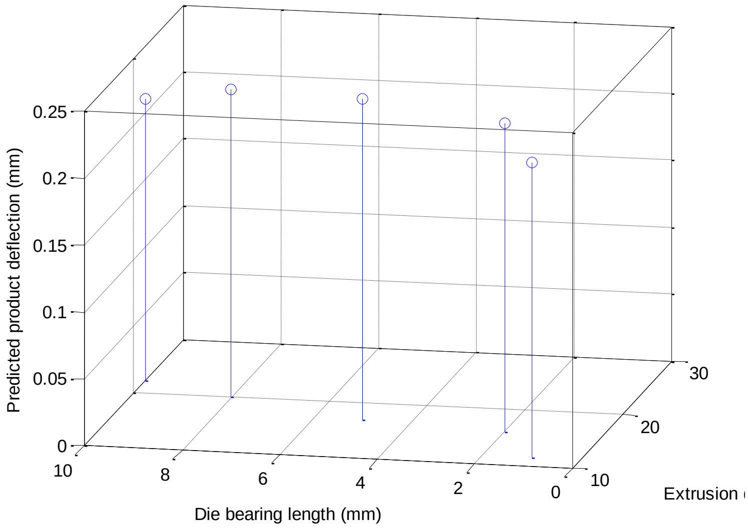

Fig. 9: 3-D stem plot of predicted product deflection against die bearing length and diameter

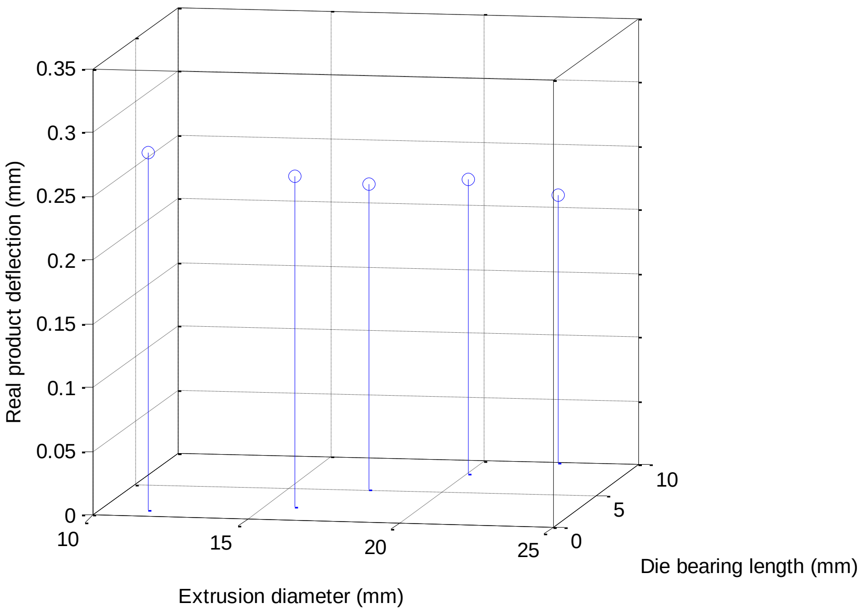

Fig. 10: 3-D stem plot of experimental product deflection against die bearing length and diameter

IV. CONCLUSION

The prediction of extrusion pressure and product deflection using artificial neural network provided an excellent matching with the experimental values. The ANN based model can be used with a high degree of accuracy and reliability, this was possible because reasonable number of variables were used during training of the neural model architecture LM 8 $[4\text{-}3]_2$ **2**.

REFERENCES

[1] S.M. Bajimaya, S.C. Park, G.N. Wang, , *Predicting extrusion process parameters using artificial neural networks. Int. J. Mech. Sys. Sci & Eng. 1(3)*, 2007, 161-165.

[2] J. Charkrabarty, Theory of plasticity (Int. Ed, McGraw-Hill, Inc., Singapore, 1987)

[3] J. Caloska, J. Lazarev, A. Nospal, and H. Stojkovki , *Exit velocity profile at the extrusion process of aluminum square pipe, South-eastern Europe FLUENT Users Group Meeting, Thessalonica, Greece, 2002*, 6.

[4] A.P. Roger, and V.I Johannes, *The evolution and changing role of die correction in the production of extrusions fielding, Light Metal Age 63(2)*, 2005, 6-21

[5] S.J.J, Carmai, S. Pitakthapanaphong, A. Sechjarern, *3-D finite element analysis of metalflow in hot aluminium extrusion of T-shaped profile with various offset pockets. J Achievements in Mat. And Manufac. Eng., 31(2), 2008,* 463-468.

[6] H.J. Li, L.H. Qi, H.M. Han, and L.J Guo, *Neural network modeling and optimization of semi-solid extrusion for aluminum matrix composites. Journal of Materials processing Technology, 151 ,2004,* 126-132.

[7] K. Velten, R. Reinicke, and K. Friedrich,*Wear volume prediction with artificial neural networks. Tribology International, 33, 2000,* 734

[8] Z. Zhang, K. Friedrich, K. Velten, *Prediction on tribological properties of short fibre Composites using artificial neural networks. Wear, 252, 2002*, 348.

[9] S. Pintos, N.V. Queipoa, O.R. Troconis, A. Rincon, M. Morcillo, *Artificial neural network modeling of atmospheric corrosion in the MICAT project, Corrosion science, 42, 2000*, 35.

[10] R.A. Cottis, O. Qing, G. S.J. Gartland, I.A. Helliwell, and, M. Turega, *Neural network methods for corrosion data reduction, Materials and Design, 20, 1999,* 169.

[11] D. K. Elaine, S.C.P. Ramón, A. Luiz. de Lacerda, C. S. Yuri, P. de. S Gabriel, L. José, *Artificial neural network corrosion modeling for metals in an equatorial climate. Corrosion Science, 51, 2009*, 2266.

[12] D.T Gundu, *Investigations and numerical modeling of material flow in forward extrusion using pocket die bearings, doctoral diss., University of Agriculture,* Makurdi – Nigeria, 2010.

[13] K.K. Ikpambese, L.T. Tuleun, and P. Ager, *Artificial neural network prediction of compressibility and oil absorbtion of gasket produced from palm kernel fibres. Journal of Engineering research,17 (3), 2012*, 46-70.

[14] Lv, W.Q. Quan, Y.P. Mao, Y.W. Zhang, and J. Zhou, *Prediction of flow stress in a wide temperature for as-cast Ti-6Al-2Zr-1Mo-1V alloy by artificial neural network, Materials and Design, 50, 2013,* 51-61.

[15] Dragan, A., *Neural network prediction of brake friction materials wear, Wear, 268, 2010,* 117-125.

[16] N. Haghadadi, A. Zarei-Hanzaki, A.R. Khalesian, and H.R. Abedi, *Artificial neural modeling to predict the hot deformation behavior of an A356 aluminium alloy. Materials and Design, 49, 2013,* 386-391.

[17] J. Lof, J. Huetink, K.E. Nilsen, FEM simulations of the material flow in the die bearing area of the aluminium extrusion process, Proc. 7th International Extrusion Technology Seminar, Wauconda, Illinoise, 2000, 211-222.

[18] P. Tiernan, B. Draganescu, M.T. Hillery, *Modeling of extrusion force using the surface response method. Int. J. Manuf. Tech., 27, 2005,* 48-52.

American Journal of Engineering Research (AJER)
e-ISSN : 2320-0847 p-ISSN : 2320-0936
Volume-02, Issue-06, pp-34-41
www.ajer.org

Research Paper Open Access

Groundwater Quality Assessment for Domestic and Irrigation Purposes in Yola, Adamawa State Northeastern Nigeria

[1]Hong, Aliyu Haliru, [2]Law Puong Ling, [2]Onni, Suhaiza Suleiman, [1]Mboh, A.B.S.

[1]Department of Agricultural and Environmental Engineering, Modibbo Adama University, Yola
[2]Department of Civil Engineering University of Malaysia, Sarawak

***Abstract:* -** To assess groundwater quality for domestic and irrigation purposes in Yola Adamawa State during the peak of dry season, groundwater samples were collected for analysis from fifteen boreholes and five hands dug wells that cover twenty wards of the City. The area investigated falls within longitude 12^{o} 26' E and Latitude 9^{o} 16' N. The groundwater samples collected were analyzed using Atomic Absorption Spectrophotometer (AAS), multi – analyte photometer and flame photometer while interpretation of the results was done by Comparison with the World Health Organization (WHO) and the Nigerian Standard for Drinking Water Quality (NSDWQ) guidelines for portable water. The pH values ranged from acidic to slightly alkaline 5.5 – 7.4, turbidity recorded 0 – 40NTU with four samples above the limit of 5NTU.

TDS and EC recorded values ranged between 17 – 1200mg/l, 129 - 1600μs/cm with two samples each above stipulated limit. The concentrations of the cat ions (Ca, Mg, Na, and K) are all found below the guideline of WHO and NSDWQ. Sulphate and bicarbonate recorded value range of 2 – 94.1mg/l and 11 – 630mg/l, which are also below the value of 100mg/l and 1000mg/l set by NSDWQ and WHO standards; however the recorded value of nitrate exceeded the specified limit of 50mg/l in seven water samples. Five water samples are classified as hard water based on the limit of 150mg/l and 500mg/l total hardness classification by the limit under consideration. The concentrations of heavy metals cadmium, lead, chromium, copper, manganese and iron were all found to exceed the WHO and NSDWQ standards. Iron concentration exceeded 0.3mg/l in seventeen water sample, manganese concentration exceeded 0.2mg/l and 0.05mg/l in twelve water samples, lead exceeded the limit of 0.01mg/l in seven water samples, also, chromium and cadmium exceeded limits of 0.05mg/l and 0.003mg/l in four and six water samples, copper exceeded set limit in only one sample while Nickel concentration exceeds in two water samples; others are beyond detection level. In all, concentration of heavy metals in groundwater is in the order Mn >Fe > Pb > Cd > Cr > Cu > Ni. The implication of the elevated levels of heavy metals in some samples of groundwater is a serious cause for concern to public health. Most of the groundwater samples are good and can be used for irrigation with adequate soil management.

***Keywords:* -** *Groundwater, heavy metal, physicochemical parameters, water quality.*

I. INTRODUCTION

Groundwater is globally important for human consumption and changes in quality with subsequent contamination can definitely, affect human health. Water is essential natural resources for the sustainability of life on earth. Humans may survive for several weeks without food, but barely few days without water because constant supply of water is needed to replenish the fluid lost through normal physiological activities, such as respiration, perspiration, urination, (Chinedu *et al*., 2011).

Due to rapid growth in population, urbanization, industrialization and the extensive use of chemical fertilizers for urban and peri- urban Agriculture are some of the factors that have direct effects on the quantity and quality of groundwater resources especially in arid and semi – arid region of northern Nigeria. Globally, the quantity and quality of groundwater reserves is diminishing on daily basis. Therefore, any study that can aid in identifying new sources of threats to groundwater is desirous not only around the study area but everywhere

(Abdullahi *et al*., 2010a). There is no life without water, therefore it is essential to safeguard the future of our water resources by studying past and present both quantitatively and qualitatively.

Water pollution is defined as contamination of water or alteration of the physical, chemical or biological properties of natural water. Water is said to be polluted when it changes its quality or composition either naturally or as a result of human activities, thus becoming unsuitable for domestic, agricultural, industrial, recreational uses and for the survival of wildlife. A water pollutant can be defined as an agent affecting aesthetic, physical, chemical and biological quality and wholesomeness of water.

Anthropogenic practices like mining and disposal of untreated waste effluents from slaughter houses, mechanical workshops, and hospitals containing toxic heavy metals are some of the causes of groundwater pollution because these heavy metals finally infiltrate into the soil and could reach the groundwater table and hence the water become polluted (Laar *et al*., 2011).

Groundwater pollution has become a major subject of public concern the world over. Musa, *et al* (2004) in their study of lead concentration in well and borehole water in Zaria, found out that the lead concentration ranged from 0.000786 to 0.0595mg/l with 91% of the samples above the 0.01mg/l WHO drinking water guideline level. Adekunle *et al*;(2007) in their study on the assessment of groundwater quality in a typical rural settlement in the southwest Nigeria, noted elevated level of nitrate, cadmium and lead which was a course for serious concern. Abdullahi *et al* (2010b) in their investigation of groundwater quality around Gubrunde and environs, northeastern Nigeria found out that samples had nitrate that ranged from 53mg/l to 106mg/l which exceeded WHO standard of 50mg/l which has the tendency of causing asphyxia to infant less than three months old. Longe E.O and Balogun M.R,(2010), in their study on Groundwater quality assessment near a municipal land fill in Lagos found out that concentration of nitrate in leachate is 62.8mg/l, while in groundwater levels ranged between 20.4mg/l and 60.5mg/l exceeding the WHO stipulated tolerance level of 10mg/l, Chromium ranged between 0.02mg/l to 0.71mg/l which is above the highest permissible level allowed by Nigerian Standard for Drinking Water Quality and the WHO permissible limits (NSDWQ,2007; WHO, 2004). Saleem *et al* (2012) in their study of physico – chemical quality of groundwater quality in Gulbarga City in South India concluded that groundwater was very hard and saline and the presence of high chlorides and nitrates concentrations indicated potential influence of sewage pollution owing to poor drainage and solid waste disposal system in the City. Fluoride values were high in few samples and concluded that the water is not fit for drinking purpose.

Tmava *et al*; (2013) in their study on the assessment of Groundwater in the mining areas in Stan Terg, Kosovo discovered that Zinc, manganese, lead and iron were the dominant element in groundwater and they are of the order Zn>Mn>Pb>Fe>Cu>Ni.

Inadequate solid waste management is a major environmental problem in Yola metropolis; the contributing factors ranged from technical problem to financial and institutional constraints. The challenge of indiscriminate refuse disposal (solid waste) is enormous and has become very serious problem. Unfortunately, most of the refuse is permanently disposed at groundwater recharge points, open space or burrow pits, pit latrines, septic tanks for human wastes. Liquid wastes are admitted through the major drainage networks and finally emptied into river with the negative impact on groundwater, surface water and the environment and hence the need to assess the groundwater quality in other to avert contamination risk that it may pose to public health.

II. MATERIALS ANDMETHODS

2.1 Study Area

Adamawa state is located in northeastern part of Nigeria with a population of 3,737,223 people and land mass of 36,917km^2. Yola (jimeta) the Adamawa state capital is located between longitude 12^o 26' E and Latitude 9^o 16' N (http://www.en.wikipedia.org/wiki/jimeta) along the banks of River Benue (Adebayo, 1999). The state is in the Sahel region of Nigeria generally Semiarid with low rainfall, low humidity and high temperature. The area experiences two distinct wet and dry seasons, the wet season starts from April to October while the dry season starts from November to April. Mean daily temperature fluctuates with season from 25^o C to 40^{o}C and the mean annual rainfall received is between (250 – 1000mm). The climate is characterized by high evapotranspiration especially during dry season (Adebayo, 1999). Yola the state capital being an urban centre has an estimated population of about 200,000 people. There is high water demand for domestic as well as industrial and agricultural purposes. Jimeta metropolis consist of the following areas/wards; Karewa, Federal Secretariat, GMMC, FCE Yola, Police Barracks, Maskare, Malamre A, Malamre B, Karewa Extension, Legislative Quarters, Nassarawo, Luggere, Demsawo, Damilu, Jambutu, Old GRA, Bye – pass, Nepa ward, Old Abattoir, and Anguwan Tana.

2.2 Groundwater Sampling

Representative samples of groundwater was collected from 15 boreholes and 5 hands dug wells from 20 locations in march, 2013 based on distribution of bore holes and wells that represent groundwater and permission from owners prior to sampling. The water was collected in 1 litre plastic containers and prior to collection as part of quality control measures all the bottles were washed with non – ionic detergent and rinsed with de – ionized water prior to usage. The sampling bottles were rinsed three times with both borehole and well waters at the point of collection. Each bottle was labeled according to sampling location to avoid mixing error and was carefully preserved at 4^oC and transported directly the laboratory for analysis.

2.3 Sample Preparation and analysis

After each sample was collected, standard methods and procedures was adopted (APHA, 1992) to conduct the analysis. An in- situ measurement was made for conductivity, pH, TDS and temperature using Sension Platinum Series portable pH and conductivity meter (HACH made). Turbidity was determined using a standardized Hanna H198703 Turbidimeter. The samples were poured into the measuring bottle and the surface or the bottle was wiped with silicon oil. The bottle was then inserted into the turbidimeter and the reading was obtained. Total hardness was obtained by calculation. The water samples for anion analysis were filtered using a hand operated vacuum pump equipped with a 0.45µm cellulose acetate filter membrane. Chloride determination was undertaken using the argentometric titration. Bicarbonate (HCO_3^-) was carried out using acid titration, with methyl orange as indicator. Nitrate (NO_3^-), Sulphate (SO_4^{2-}) were determined using V2000 multi – analyte photometer, Na and K were carried out with a CORNING FLAMEPHOTOMETER 410 after calibrating it with analyte standard while the remaining Trace and heavy metals were carried out with a Varian model AA240FS Fast Sequential Atomic Absorption Spectrometer.

III. RESULTS AND DISCUSSION

3.1 Groundwater Quality:

The results of boreholes and wells which represent groundwater quality is presented in tables 1, 3, 4 and 5. The physicochemical quality parameters are in table 1, while the descriptive statistics of the same parameters is in (Table 3). The trace and Heavy metals concentrations and their descriptive statistics are presented in tables 3 and 4. The TDS value in groundwater ranged between 17mg/l to 1200mg/l, while in borehole water is in the range of 17mg/l to 220mg/l, the values in well water is between 240mg/l to 1100mg/l (Table 1). The TDS values in the borehole water are all below the maximum permitted level of 500mg/l set by the World Health Organization (WHO) and the Nigerian Standard for Drinking Water Quality (NSDWQ), while values in the wells WW3 and WW4 located in the Old Abattoir and Anguwan Tana exceeded the set limit. This could be inferred that open exposure of such wells without surface cover are subject to contamination from solid and liquid contaminants and hence responsible for the high TDS values. High value of TDS influences the taste, hardness, and corrosiveness property of water (Saleem *et al*; 2012, Subhadra Devi *et al*; 2003). Temperature recorded the minimum of 29.1^oC and the maximum of 33^oC with a mean value of 30.8^oC and standard deviation of 1.287(Table 3).

The groundwater samples are generally acidic to slightly alkaline with a minimum of 5.50 and a maximum of 7.40 and a mean of 6.60 which is below the World Health Organization (WHO) and the Nigerian Standard for Drinking Water Quality (NSDWQ) guidelines for portable water. Past studies had equally revealed the acidic nature in northeastern and western part of Nigeria (Adullahi et al; 2010a, b, Musa *et al*; 2004, Longe and Kehinde 2005; Longe and Enekwechi, 2007; Yusuf, 2007, Chinedu, *et al*; 2011). The pH of boreholes and well water were within the normal range of (6.0 – 9.0) acceptable for normal consumption except at BH5, BH10 and BH11with pH 5.50, 5.53 and5.5, the samples are from Police Barracks, Legislative Quarters and Nasarawo areas. Consumption of such acidic water could have adverse effect on the digestive and lymphatic system of humans. Turbidity values groundwater ranged from (0 - 40NTU) with the mean of 6.47NTU and standard deviation of 11.190(Table 3). From the Nigerian Standard for Drinking Water (NSDWQ), acceptable standard is 5TNU; this indicates that all groundwater taken from boreholes are within the acceptable limits while groundwater from wells labeled as WW1(12NTU),WW2 (14NTU),WW3(30NTU) and WW4(40NTU) had values above limit of 5NTU.

The electrical conductivity (EC) of groundwater ranged from 129µs/cm to 1600µs/cm and a mean of 667.86µs/cm and a standard deviation of 393.419 (Table 3), which consists of samples from sixteen boreholes and four hands dug wells. The lowest EC value was recorded in borehole BH2 (129µs/cm) and the highest in BH16 (1000µs/cm), the wells, recorded (678µs/cm) in WW1 as the lowest, while WW4 recorded a value of (1600µs/cm) as the highest value. The EC value in WW3 and WW4 from Old Abattoir and Anguwan Tana exceeded the maximum permitted value of 1000µs/cm by NSDWQ and WHO guideline for portable water. The electrical conductivity in water samples is an indication of dissolved ions. Thus the higher the EC, the higher the levels of dissolved ions in the sample.

Calcium and Magnesium had concentration of 1.30mg/l and 1.9mg/l as minimum and 190mg/l, 115mg/l as maximum with mean and standard deviation of 80.36mg/l, 40.08mg/l and 50.169 and 37.964 respectively. Also Sodium had a concentration of 9mg/l, 56mg/l as minimum and maximum with standard deviation of 16.222. Potassium recorded a mean value of 3.472mg/l and a maximum and minimum value of 6mg/l and 0.08mg/l all the values are within the maximum permitted limit set out by WHO(2004) and the Nigerian Standard for Drinking Water Quality (NSDWQ) guideline for portable water.

Fluoride concentrations in boreholes and well water samples were recorded as 0.014mg/l as minimum and 0.3mg/l as maximum with mean and standard deviation of 0.106mg/l and 0.098mg/l. This value is also below the save guideline of WHO and NSDWQ of 1.5mg/l. This means therefore that the boreholes and hand dug wells groundwater is safe for drinking. Chloride also had a recorded concentration of 4mg/l, 28mg/l, 13.10mg/l and 1.330 as minimum, maximum and standard deviation. Fluoride value also fall within safe and permissible limit of 1.5mg/l and thus the groundwater is safe for drinking and domestic purposes.

The concentrations of dissolved oxygen in wells and boreholes water samples were in the range of 3.1mg/l to 8.90mg/l with a mean value and standard deviation of 6.234mg/l and 0.562. The highest value of dissolved oxygen was in borehole water sample labeled as BH12 (8.90mg/l) and the lowest is in BH15 (3.7mg/l). In the wells, WW1 had dissolved oxygen value of 6.6mg/l and WW2 had 4.9mg/l. The lowest dissolved oxygen values in well water was in WW3 (3.2mg/l) and WW4 (3.1mg/l). Threshold for dissolved oxygen (DO) is 5.0mg/l for drinking water and should be more 5mg/l for agricultural purposes. The results revealed that borehole water and well water quality with respect to DO are good for drinking purposes, except that the low level of oxygen in WW3 and WW4 is not suitable for agricultural and fisheries project but high enough not to cause anaerobic conditions in drinking water. Very low DO may result in anaerobic conditions that cause bad odors.

The concentration of nitrate (NO_3^-) in groundwater generally is 8.85mg/l, 66.0mg/l and34.992mg/l as the minimum, maximum, and 23.088 as standard deviation. This minimum value of nitrate was recorded in borehole BH1while the maximum was in WW4 well water. In all, boreholes BH7,BH11 and well water WW1,WW2,WW3 and WW4 had nitrate concentration that exceeded the maximum permitted level of 50mg/l as defined by WHO (2004) and the Nigerian Standard for Drinking Water Quality (NSDWQ) guideline for portable water. All the 19 groundwater samples out of 20 had nitrate values above the stipulated tolerance level of 10mg/l for portable water. The high level of nitrate in groundwater used for human consumption is a serious source of concern to public health. Problems associated with high nitrate concentration in groundwater have become increasingly prevalent in the recent years. Natural levels of nitrate in groundwater may have been enhanced by anthropogenic, municipal, industrial and agricultural wastewaters from waste disposal sites. High nitrate concentrations have detrimental effect on infants less than six month of age. Nitrate reduces nitrite which can oxidize haemoglobin to methaemoglobin, thereby inhibiting the transport and availability of oxygen around the body or simply causes Cyanosis and asphyxia (blue – baby syndrome) (WHO, 1985, Alsabahi *et al*; 2009; Adullahi *et al*; 2010, Longe and Balogun; 2010).

The observed level of sulphate (SO_4^{2-}) in groundwater samples were 0.04mg/l minimum, 94.1mg/l maximum, while the mean of 34.99mg/l and standard deviation of 27.90 was observed. All the values observed for well and borehole are within the maximum permitted level stipulated by WHO and NSDWQ. The bicarbonate (HCO_3^-) observed water quality parameter indicated that the maximum of 630mg/l and minimum of 11.0 mg/l and a mean of 176.71mg/l with standard deviation of 184.35 were observed and all are below the limit of 1000mg/l by the World Health Organization Standard. The bicarbonate concentration tested in boreholes and wells can be said to be free and safe for use as house hold level.

Total Hardness (TH), the value of total hardness of groundwater samples measured as the sum of calcium and magnesium concentration express in terms of mg/l of calcium carbonate had a minimum value of 115mg/l and maximum of 630mg/l. Calcium and magnesium form an insoluble residue with soap. The degree of hardness is commonly based on the classification listed in Table 5 (Sawyer and McCarty, 1967).

Based on the classification above, 13 groundwater samples labeled as BH1, BH4, BH5,BH6,BH8, BH9,BH10,BH11,BH12,BH14,BH15,BH16 and WW4 are soft water because their values are below 75mg/l, BH13 and BH2 are within the class of moderately hard water. The concentrations of water samples WW3, with value of 200mg/l fall within the class of hard water, while samples, WW2, WW1, BH3 and BH7 are classified as very hard water. In all, 65% of the water samples are classified as soft water, 10% as moderately soft, 5% as hard water and 20% as very hard water, most of the groundwater samples are found to be below the Nigerian Standard for Drinking Water Quality (NSDWQ) guideline for portable drinking water except samples from Old Abattoir (WW3), Damilu (WW2), Demsawo (WW1), Malamre A (BH7) and GMMC (BH3) that are classified as hard to very hard. Hardness in groundwater is often cause by calcium and magnesium present in soils or rock that dissolves in the water to cause hardness. Hardness in groundwater is normally considered as an aesthetic water quality factor, it does not pose a health risk but higher concentration in water however creates consumer problems that ranged from wastage of soap and interferes with every cleaning task from laundry to household washing.

3.2 Heavy Metals in Groundwater Samples:

Measured values of heavy metals in boreholes and wells water samples and their descriptive statistics are presented in Table 4 and 5. The values of copper in all boreholes and wells water are all below the WHO standard of 2mg/l, while BH7 recorded 1.3mg/l above the NSDWQ permissible level of copper in the water sample (1mg/l). Cadmium concentration exceeded the WHO and NSDWQ in all wells and some boreholes in six locations. Elevated level of lead concentrations was also recorded in BH12 (0.1mg/l), BH13 (0.4mg/l), BH15 (0.6mg/l), WW3 (0.6mg/l) and WW4 (0.5mg/l) which is above 0.01mg/l set standard, others samples are beyond detection level. Chromium concentrations are detected in only 2 boreholes and 2 wells but also above the recommended standard World Health Organization (WHO) and NSDWQ value of 0.05mg/l (figure 1); others fell beyond the limit of detection. Heavy metal such as lead, cadmium, and copper in groundwater have been reported at excessive levels in groundwater due to land fill operations (Lee *et al*; 1986; Ogundiran and Afolabi, 2008, Longe and Balogun, 2010) These elevated level of copper, cadmium and chromium in groundwater has the potential of causing gastrointestinal disorder, while cadmium is toxic to the kidney, chromium remains on the top list of causing cancer and cancer related disorder.

Manganese concentrations are also found in appreciable quantity in all the tested groundwater samples except from 2 locations that are beyond detection limit. Most of the obtained values are above stipulated level of 0.2mg/l by NSDWQ and 0.05mg/l by the World Health Organization(WHO) standard. Nickel was also found in trace quantities in few of the samples, while most of the samples are beyond detection level.

The World Health Organization WHO and NSDWQ permissible level of iron (0.3mg/l) had been exceeded in all samples from boreholes and wells. The value of iron ranged from 0.6mg/l to 2.10mg/l with a mean of 1.11mg/l and standard deviation of 0.437. High iron level noticed in wells and boreholes is a characteristic of groundwater due to anthropogenic activities and local geology. Excessive dissolved iron and manganese concentrations result in taste and precipitation problems. In general, the concentration of heavy metals in groundwater is in the order Mn > Fe > Pb >Cd >Cr >Cu >Ni.

IV. SUITABILITY OF GROUNDWATER FOR IRRIGATION PURPOSES

The suitability of tested groundwater samples for irrigation purposes was assessed on the basis of TDS, Salinity or EC and Sodium adsorption ratio values.

4.1 Total Dissolved Solid (TDS):

Any increase in the amount of dissolved solids in irrigation water affects the efficiency, growth and yield of plants. Long time irrigation under average conditions, the total dissolved solid in irrigation water should not exceed 2000mg/l, higher salt content of irrigation water leads to salinization problems which result in high osmotic pressure in soils and water absorption via roots system becomes difficult. Classification of water according to TDS values (Wilcox, 1955) is given in Table 6.

The highest TDS value recorded in examined groundwater samples is 1200mg/l, while the lowest is 17mg/l, based on the categorization, most of the water samples are in the class of best quality water and is good for irrigation except WW3 and WW4 that fall into the class of water involving hazard.

4.2 Based on salinity hazard:

Groundwater samples can be classified into four categories (Table 7) Salinity hazard allowed the classification of groundwater into four categories C1 class with EC (100 -250µs/cm) as excellent water, C2 class with EC (250 - 750µs/cm) as good water, C3 class with EC (750 – 2250µs/cm) as doubtful water and C3 class with EC (> 2250µs/cm) as unsuitable water. Based on these, the groundwater's have 4 samples as excellent water, 11 samples as good water and 5 samples as doubtful water. The groundwater can adequately be used for irrigation with management practice.

V. CONCLUSION

The results of analysis and evaluation of groundwater from twenty locations in Yola metropolitan capital of Adamawa state for domestic and irrigation purpose revealed that the groundwater quality have been impacted by trace and heavy metals. The levels of nitrate, copper, cadmium, chromium, manganese and iron in some water samples in boreholes and wells are above the World Health Organization (WHO) and the Nigerian Standard for Drinking Water Quality (NSDWQ) guideline for portable water. Such elevated levels of nitrate, copper, Cadmium, Chromium manganese and iron in groundwater used for drinking is a serious cause for concern. The negative impact of these heavy metals which ranges from causing blue baby syndrome in infants less than three months, gastrointestinal disorder, cancer, kidney damage and neurological disorder may come up with time if remedial measures are not taken in good time. Some of the ground water samples can safely be used for drinking and irrigation purposes as their parameters are within the stipulated standards. It is recommended

that groundwater quality assessment be carry out in both wet and dry season to better understand the dynamic changes in water quality that may occur with time.
Source: Laboratory analytical data, 2012

Samples	TDS (mg/l)	Temp °C	pH	TUB (NTU)	EC (µs/cm)	Ca (mg/l)	Mg (mg/l)	Na (mg/l)	K (mg/l)	O_2 (mg/l)	Cl (mg/l)	F (mg/l)	NO_3^- (mg/l)	SO_4^{2-} (mg/l)	HCO_3^- (mg/l)	TH (mg/l)
BHI	35.0	31.2	6.0	0	230	29.0	6.9	12.0	5.4	6.5	9.0	0.10	8.85	13.0	30.0	30.0
BH2	22.0	31.0	7.4	0	129	103.0	25.8	16.0	3.9	6.3	6.0	0.16	11.0	9.0	85.0	85.0
BH3	70.0	30.0	7.2	0	235	190.0	115	14.0	5.0	5.6	9.0	0.24	26.5	10.0	403.0	403.0
BH4	18.0	30.1	6.5	0	234	83.0	19.7	13.0	0.08	6.6	10.0	0.01	17.7	0.60	67.0	67.0
BH5	110.0	33.0	5.5	0	390	47.0	114	12.0	3.0	7.8	20.0	0.03	17.6	4.0	64.0	64.0
BH6	17.0	32.5	6.0	0	470	162.0	39.4	9.0	5.0	8.4	17.0	0.20	46.6	4.0	62.0	62.0
BH7	40.0	29.1	7.0	0	490	1.30	1.9	9.0	2.1	7.5	20.0	0.26	62.5	9.4	400.0	400.0
BH8	19.0	33.0	6.7	0	420	81.0	19.7	17.0	0.08	6.5	10.0	0.01	17.6	0.04	66.0	66.0
BH9	190.0	30.7	7.1	0	430	140.0	34	23.0	6.0	7.7	10.0	0.01	35.3	11.0	147.0	147.0
BH10	100.0	32.4	5.53	0	450	36.0	8.75	18.0	6.0	4.5	10.0	0.02	53.0	3.0	45.0	45.0
BH11	90.0	30.1	5.5	0	407	38.0	19.5	17.0	5.0	7.6	10.0	0.03	62.0	4.0	48.0	48.0
BH12	26.0	32.1	6.7	0	689	39.0	9.48	15.0	5.5	8.9	11.0	0.01	13.2	2.0	16.0	16.0
WW1	390.0	29.6	6.6	12.0	678	50.0	100	12.0	0.7	6.6	22.0	0.03	62.0	52.5	630.0	630.0
WW2	240.0	29.8	6.5	14.0	670	48.0	102	32.0	0.8	4.9	22.0	0.04	60.0	53.0	540.0	540.0
BH13	220.0	32.1	7.3	0	700	102.0	24.7	34.0	3.8	5.6	5.0	0.15	11.0	8.0	85.0	85.0
BH14	221.0	30.1	7.0	0	802	101.0	23.6	36.0	3.0	8.9	4.0	0.20	11.0	6.0	60.0	60.0
BH15	220.0	29.5	7.0	0	900	100.0	22.8	50.0	3.1	3.7	6.0	0.10	10.0	5.0	62.0	62.0
BH16	90.0	30.1	6.5	0	1000	90.0	22	51.0	3.0	4.8	5.0	0.30	12.0	4.0	60.0	60.0
WW3	1200	30.3	6.3	30.0	1500	56.0	15.6	54.0	3.4	3.2	28.0	0.01	65.0	81.3	200.0	200.0
WW4	1100	29.1	7.0	40.0	1600	1.30	1.9	56.0	2.1	3.1	28.0	0.02	66.0	94.1	11.0	11.0
NSDQW	500	-	6.5-8.5	5.0	1000	-	0.20	200	50	5	250	1.5	50.0	100	-	150
WHO	500	-	6.5-8.5	-	-	75	50	50	55	-	250	-	50	250	1000	500

Table 2: CLASSIFICATION OF GROUNDWATER HARDNESS (Sawyer and McCarty, 1967)

Hardness range (mg/l of $CaCO_3$)	Water classification
0 - 75	Soft
75 - 150	moderately hard
150 - 300	Hard
>300	Very hard

Table 3: Groundwater Physico–Chemical Quality Parameters Descriptive Statistics

Parameters	Minimum	Maximum	Mean	Standard Deviation
TDS	17.00	1200.00	267.52	333.53
Temp	29.10	33.00	30.89	1.28
pH	5.500	7.400	6.60	0 .59
Turb	0.00	40.00	6.47	11.19
EC	129	1600	667.81	393.41
Ca^{2+}	1.30	190.00	80.36	50.16
Mg^{2+}	1.90	115.00	40.08	37.96
Na^+	9.00	56.00	26.47	16.22
K^+	0.08	6.00	3.47	1.91
Fr	0.014	0.30	0.106	0.09
Cl^-	4.00	28.00	13.10	1.33
O_2	3.10	8.900	6.23	0.56
NO_3^-	8.85	66.00	34.99	23.08
SO_4^{2-}	0.04	94.10	22.28	27.90
HCO_3^-	11.00	630.00	176.71	184.35
TH	115.00	630.00	176.71	184.35

N=20. All the values are in mg/l except EC, in µs/cm, Turbidity in NTU and Temperature in °C

Table 4: HEAVY METAL CONCENTRATIONS IN GROUNDWATERSAMPLES

Samples Standards	Cu (mg/l)	Cd (mg/l)	Pb (mg/l)	Cr (mg/l)	Mn (mg/l)	Ni (mg/l)	Fe (mg/l)
BH1	0.50	ND	ND	ND	0.02	ND	ND
BH2	0.04	ND	ND	ND	0.30	ND	1.20
BH3	ND	ND	ND	ND	0.05	ND	ND
BH4	0.40	ND	ND	ND	ND	ND	0.80
BH5	0.05	ND	ND	ND	0.06	ND	0.90
BH6	0.20	ND	ND	ND	0.20	0.001	0.70
BH7	1.30	ND	ND	ND	0.80	ND	0.90
BH8	0.03	ND	ND	ND	ND	ND	0.80
BH9	0.04	ND	ND	ND	0.50	ND	ND
BH10	0.03	0.002	ND	ND	3.00	ND	0.60
BH11	ND	0.001	ND	ND	2.00	ND	0.90
BH12	0.01	0.50	0.10	ND	0.30	0.30	1.20
BH13	0.03	0.60	0.40	0.40	0.30	ND	1.10
BH14	0.02	0.02	ND	ND	0.30	ND	1.00
BH15	0.02	0.01	0.60	0.30	0.30	0.20	1.00
BH16	0.01	0.10	ND	ND	0.20	0.001	1.10
WW1	0.04	0.40	0.02	ND	0.04	0.001	2.10
WW2	0.04	0.01	0.30	ND	0.06	0.002	2.10
WW3	0.06	0.40	0.60	0.20	0.06	0.02	1.40
WW4	0.30	0.30	0.50	0.10	0.08	0.03	1.60

ND: Not Detected
Source: Laboratory analytical data, 2012

Table 5: Descrptive Statistics Of Heavy Metal Concentrations In Groundwater Samples

Parameters (mg/l)	Minimum	Maximum	Mean	Standard Deviation
Cu	0.01	1.30	0.232	0.316
Cd	0.001	0.60	0.245	0.230
Pb	0.020	0.60	0.390	0.230
Cr	0.10	0.40	0.280	0.129
Mn	0.022	3.0	0.608	0.780
Ni	0.001	0.30	0.095	0.115
Fe	0.60	2.10	1.11	0.437

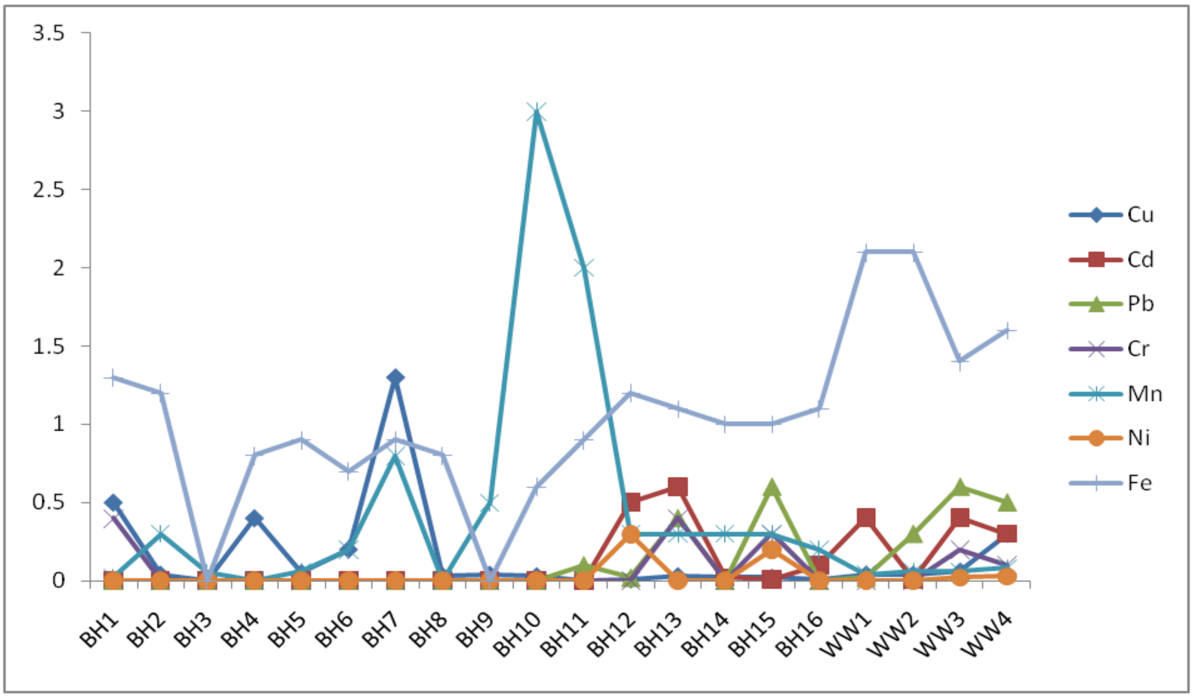

Figure 1: **A graph of Cu, Cd, Pb, Cr, Mn, Ni and Fe from the studied groundwater samples**

REFERENCES

[1] Abdullahi, A.S., Funtua, I.I., Dewu, B.L.M and Alagbe, S. A (2010). Study of the suitability of Groundwater for Household and Irrigation Purposes in Parts of Adamawa State, NortheasternNigeria. Int. Arch. Of Applied Science and Tech. Vol. 2 P 48 – 56.

[2] Abdullahi, A.S., Funtua, I.I., Alagbe, S.A., Zabroski, P., and Dewu, B.B.M (2010). Investigation of Groundwater quality for Domestic and Irrigation Purposes around Gubrunde and Environs, Northeastern Nigeria. Journal of American Science, 6(12).

[3] Adebayo, AA, Tukur, A. L (1999). Adamawa State in Maps. Paraclete publishers Yola. APHA, (1992). Standard Methods for Examination of Water and Wastewater. 18th Edition. AmericanPublic Health Association.

[4] Adekunle, I.M., M. T. Adetunji, A. M. Gbadebo and O.B Banjoko, (2007). Assessment of groundwater Quality in a typical rural settlement in Southwest, Nigeria. Int. J. Environ. Res. Public Health, 4(4):307 – 318.

[5] Alsabahi, E., S. Abdulrahim, W. Y. Zuhairi, F. Al – Nozaily and F. Alshaebi, (2009). The characteristics of leachate and groundwater Pollution at municipal solid waste landfill of Ibb City, Yemen. Am. J. Environ. Sci.,5(3): 256 -266.

[6] Chinedu, S .N., Nwinyi, O.C, Oluwadamisi, A.Y, Eze, V.N (2011). Assessment of water quality in Canaanland, Ota, Southwest Nigeria. Agric. Bio. J. N. Am 2(4): 577 – 583.

[7] Lee, G.F., R.A. Jones and C. Ray, (1986) Sanitary landfill leachate recycle. Biocycle, 27: 36 – 38.

[8] Longe, E.O. and M.O Kehinde, (2005). Investigation of potential groundwater impacts at an unlined Waste disposal site in Agege, Lagos, Nigeria. Proceeding of 3rd International Conference, Faculty of Engineering, University of Lagos, May 23 – 26, pp: 21 – 29.

[9] Longe, E.O. and Enekwechi, (2007). Investigation on potential groundwater impacts and influence of Local hydrogeology on natural attenuation of leachate at a municipal landfill. Int. J. Environ. Sci. Tech., 4(1): 133 – 140.

[10] Longe E.O. and Balogun M.R.,(2010). Groundwater Quality Assessment near a Municipal Landfill, Lagos, Nigeria. Res. J. Appl. Sci. Eng. Technol, 2(1): 39 – 44.

[11] Laar, C, Bam, EKP, Osae, S, Anim, A, Osei, J,Bimi, L, Nyarko, E, Ganyaglo, SY, Gibrilla, A, Adomako, (2011). Effect of anthropogenic activities on an ecologically important wetland in Ghana. J. Bio. And Env. Sci. 1(6): 9 – 21.

[12] Musa, H. Vakasai, I.A and Musa, A.H. (2004). Determination of lead concentration in well and borehole Water in Nigeria, Chemclass Journal, 14 – 18.

[13] NSDWQ, (2007). Nigerian Standard for Drinking Water Quality. Nigerian Industrial Standard NIS 554 Standard Organization of Nigeria, pp: 30.

[14] Ogundiran, O.O and T. A. Afolabi, (2008). Assessment of the physicochemical parameters and heavy

[15] Metals toxicity of leachate from municipal solid waste open dumpsite. Int. J. Environ. Sci. Tech., 5(2): 243 – 250.

[16] Subhadra Devi G, Barbaddha SB, Hazel D, Dolly C (2003). Physico – chemical characteristics of Drinking water at Velsao Gao. J. Environ. Monit. 13: 203 – 209.

[17] Sawyer, C. N., and Mc Carty, P.L (1967). Chemistry for Sanitary Engineers, and classification of Naturally soft and naturally hard waters to sources and hardness of their water supplies, J. Hyg. 1967.

[18] Saleem, A. Dandigi, M. N and Kumar K.V (2012). Correlation- regression model for physic – chemical Quality of groundwater in the South India city of Gulbarga.

[19] Tmava, A. Avdullahi, S, Fejza, I (2013). Assessment of heavy metal study on groundwater in the mining Area in Stan Terg, Kosovo. J. Bio. And Env. Sci. 2(3): 53 – 60.

[20] US Salinity Lab Staff (1954). Diagnosis and improvement of saline and alkaline soils USDA, USA.

[21] Wilcox, L.V. Classification and Use of irrigation Waters, U.S.A. Salinity lab. Circulation. No. 969 (1955).

[22] WHO, (1985). Health hazards from nitrate in drinking water. WHO Regional Office for Europe.

[23] WHO, (2004). Guideline for Drinking Water Quality. 3rd Edition Vol. 1 Recommendation, Geneva, 515.

[24] Wikipedia (http://www. en.wikipedia.org/wiki/jimeta). Downloaded on the 23rd march 2013.

[25] Yusuf, K.A (2007). Evaluation of groundwater quality characteristics in Lagos City. J. Applied Sci., 7(13): 1780 – 1784.

American Journal of Engineering Research (AJER)
e-ISSN : 2320-0847 p-ISSN : 2320-0936
Volume-02, Issue-06, pp-42-48
www.ajer.org
Research Paper Open Access

Environmental Degradation: Challenge to Food Security, local context global perspective, A case study of a village in Bangladesh

Shahid Mallick
Anthropologist and Director TREE-Training Research Education for Empowerment, Savar-Dhaka, Bangladesh

***Abstract:* -** Water, land and lights are three important and integral parts of food production. Pollute land, water and inadequate light/energy have sequential negative affects on total food and yield production. Bangladesh called the land of water as many as 310 rivers crisscross all over the country and source of surface water use. However, these natural resource base has been neglected in policy as a result many rivers in the country are about to dead and some are biologically dead because of anthropologic cause. Further, irrigation water used from this river and direct disposal of industrial chemicals and other waste polluted the land and reduces productivity and seems to ominous link to food insecurity. The present paper focuses and try to explore land and water pollution and its relationship with food security. The findings and outcomes of this paper is a research in a riverside village in Bangladesh and the methodology used for this study are focus group discussion (FGD), individual interview, observations, secondary information and review of literature.

***Keywords:* -** *food security, environmental degradation, Industrialization, land, pollution, water*

I. INTRODUCTION:

Bangladesh having a small land area total 14845 million hectares of land and cultivable land area is only 8.44 million hectares (Ministry of agriculture 2013) while the total population is 150.5 million (population census 2011). To feed these huge population always been a challenge for the country. However, because of the productivity of the lands, crop diversity and unique natural resources that is huge surface water base i.e. A network of rivers in Bangladesh are an opportunity for the country. Again all these are in threatened due to irrational behaviors of human and policy inadequacy of the country. In question of food security, land and water issue come first, further without land and water there is no questions about food production hence 1) physical availability of food 2) economic and physical access to food 3) food utilization and 4) food stability (FAO, EU 2013) which called food security. But without production there is no questions about availability, stability or distribution. Therefore once the productions are disturbing whole food security systems affected and thus challenge for food security at a local or national level.

The origin of agriculture, human settlement and civilization are linked with the water course and fertile land mass. Water, land and agricultural productions are in close linked. Isolation or infecting/pollution one has an automatic effect on others. Following of the domestication of plants and animals, the next advance in agriculture come with the control of water. Irrigation arose in the Near-East around the 5000BC and in Mexico shortly after 1000BC. With irrigation more food could be produced by fewer people. Which considerably free the other people in a community or family to work in another sector (Heiser JR 2006)

Bangladesh is a low–lying riverine country. Hundreds of river intersects all over the country including three great rivers the Ganges, Brahmaputra, and Megna (GBM). The importance of rivers in general Bangladeshi lives and culture is inseparable. Some specific types of culture and livelihoods pattern are mutually exclusive with water and food security, i.e. Bede (Nomadic snake charmers) and traditional fishing folks. Polluting water means reduce fish production and availability of fish and also have an impact on other aquatic resources in the water, irrigation with polluted water from Banghsi river claimed to reduce yield production and loss of daily of agriculture labor (Mallick 2011).

By default agriculture all over the world accounts for 70% world water use followed by 20% for industries and 10% domestic use (UN,UNIESCO,FAO 2013). However, global water statistics completely differ with Bangladesh water use trends such as in the year 2008, 88% water of the country's water consumptions was used for agriculture 10% domestic use and only 2% for industrial use vise-versa 79% of the total water withdrawal comes from underground and 21% of surface (BBS 2008, FAO/Aquastar 2010), while Bangladesh called the land of rivers, therefore its clear indication of policy lacks in water use and plan for the country. Again, while the actual water use by industries in Bangladesh 2% but the virtual water use by these industries may be more than 80% as rivers around Dhaka i.e. Water of Buriganga, Shytalakha, Turag, Dwaleshari and Banghsi are completely unusable for any purpose. This assumption gets some authentication by the words of *Charles Depman*, Asia regional coordinator of the New York-based water keeper alliance *"I have never seen such a polluted river, the water looks lifeless and toxic emitting a strong stench in the area"*(the daily Star p 20, Dhaka April 18, 2013)

In many river basins, the rate of socioeconomic change and the accumulation of environmental problems indicate institutional inefficiency. Though environmental policy has had some influence in high-income countries, but has had far less effect so far on the development agenda of poorer countries (FAO 2011) such as Bangladesh does have environmental law river commission and water policy but rivers and wetlands are being polluted and degraded due to indiscriminate disposal of solid and industrial waste into the rivers Bangshi and many others.

According to an FAO study on "The State of the World's Lands and Water Resources for Food and Agriculture" (2011) projected that existing water use trend in agriculture will increase 10% between now and in the year 2050 to feed a growing world population. Further, undermining the interdependency of land water resources and intensively used river basin for commercial purpose i.e. industries and other municipal waste dumping into river Bangshi (Mallick 2011). The interdependency and stability of land and water will not be achieved without more effective natural resource allocation and environmental regulation at national and international level vise-versa existing land and water systems that are threatened by the depletion and degradation of natural resource endowments totally ignored at least in the country's low enforcement of law, absence of governance and from regulation perspective.

In regards to discussions on environmental degradation and food security in Bangladesh, the water issue come into front line, because of its diverse relation with human lives, livelihoods and food security. During 1990s government adopted policy to accelerate country's economy and more employment hence to establish an export processing zone (EPZ) at Savar near river Bangshi. The main objective was to utilize more human energy particularly of the women who constitute almost half of the country's population. While the immediate impact of these exports oriented industries are to create much employment mostly for unskilled women. Vise-versa the long term impacts of pollution released from these unplanned industrialization is to pollute water at river Bangshi, degraded land fertility and reduces yield production.

Thousands acres of productive land go out of cultivation because of industrial pollution. Such as special economic zone (DEPZ) established in a 355 acres hectares of land and there are 300 industries built and many other in process, whereas its seriously polluted more than 1000 acres of highly productive paddy field at Dholai Beel (Roy 2009) is a clear indication of declination of food production, hence to food sovereignty at local level.

The environmental degradation in major river systems and increasing population, increases chances of more food insecurity in the society, again agriculture remain the predominant water user and missing link with non agriculture water use on earth (Coke et al 2009). The development will be constrained if increased demand for irrigation deprives other users and the river system loses capacity due to pollution or over-exploitation.

The behavior and attitude of general people and polluters i.e. industries are factors. The existing policy and policy guidelines for national and international river management and pollution control seems to have inadequacy in control and regulate pollution of rivers. Such as the largest water reservoirs Ganges Brahmaputra is being polluted due to inadequate policy guideline, slow implementations of law, regulations, corruption and unregulated industry (Anwar 2006)

II. VILLAGE GUGUDIA AND THE RIVER BANGSHI:

The River Bangshi is one of the 330 rivers flows throughout the country (FAO 2011). This very river is the source of agriculture and domestic water supply for thousands of people of riverside villages i.e. Sukundi, kunda, Nalm, kakran, Hajipur, Pathalia, Bejir Tek, Chakalgram, Nayrhat, Gupinath pur, Amgachia, Safi pur, Gugudia, Sinduria, Chay baria, Bari gaom, Kauja Kundu, Pura bari, ***Guradia***, Savar, Foot Nagar, Vagalpur, Fulbaria, Kanar Char, Mushuri Khula (Mallick survey , 2011). People of Ghughudia villages and many other are being historically depended on this river for their agriculture watering, fishing, bathing and other use of water, further that, total of 60,000 traditional fishing people (Roy Mohan) were exclusively dependent on the river Bangshi in other words were secured for their water, food and livelihood means.

During 1990s the government of Bangladesh set up a special economic zone called (EPZ) at Savar, near river Bangshi to increase country's GDP and employment. From then, the EPZ along with many other local industries are just discharging their untreated chemical and other waste directly into open water and then drained into the river Bangshi. Gradually fish and other aquatic resources are disappearing. Working in paddy field is irritating and burned and skin disease, agriculture labor loses their daily and employers has to count more money and use of sticky polluted water from the river causes less yields of their crops (Mr. Samad, elderly people, FGD at Ghughudia village).

III. CHANGE IN LAND USE AND THREATENED AGRICULTURE:

Population increase along with many other anthropologic factors i.e. Urbanization, industrialization and pollution of land and water pushes to change. Such as following the establish of the special economic zone (EPZ) near river Banghsi, many other local industries and so many small enterprise developed. Number of new and additional employments were created by these industries i.e. EPZ and other industries. But its impacted land use pattern and traditional livelihoods too. In one hand total agriculture lands reduces and on the other pollution in the fertile cultivable land force to keep uncultivated or other non crops framing i.e. high yields grass, fish cultivation.

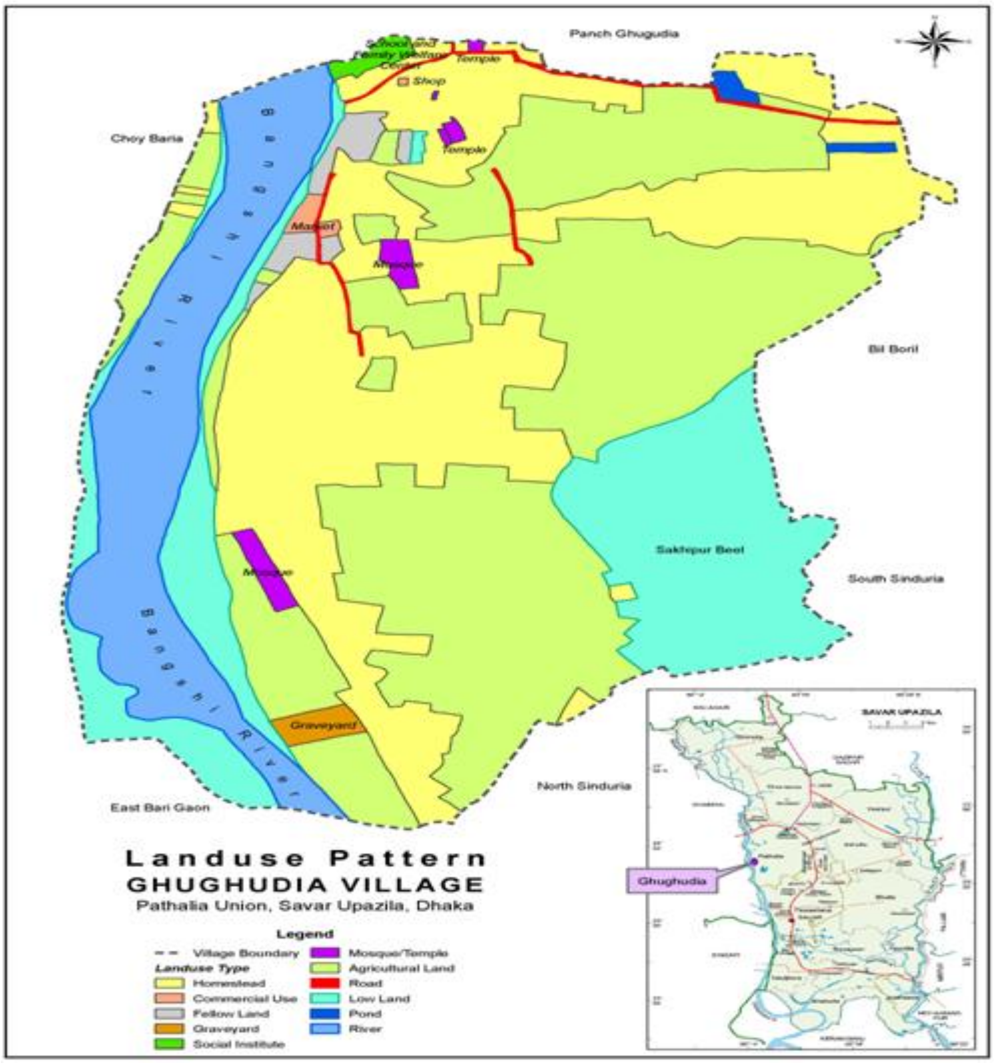

Figure: 1 Land use pattern of Ghughudia

IV. DECREASED AGRICULTURE LAND:

Total demands of foods comply with total population and food consumptions. Availability of cultivable fertile land water is important for food production to meet domestic needs and surplus demands. Again, food security is nevertheless satisfy the availability of food only, rather it has multidimensional impact and cause i.e. Production, distribution and availability of cultivatable land mass too. Increasing population and country's policy and acts are not favorable to conserve country's agricultural or wetland area as encroachment/grabbing are going on. World wide the transnational and national economic actors from various big business sectors (oil and auto, mining and forestry, food and chemical, bioenergy and biotechnology, etc.) Are eagerly acquiring, or declaring their intention to acquire, large swathes of land on which to build, maintain or extend large-scale extractive and agro-industrial enterprises (Saturnino M.et.al 2012). Again these multinationals and corporations i.e. Industries at EPZ are discharging its untreated chemicals and other waste into river Banghsi or its links resulting pollution of water and land.

National governments in 'finance-rich, resource-poor' countries are looking to 'finance-poor, resource-rich' countries to help secure their own food and especially energy needs into the future. The land in global south was attractive historically for multiple reasons, but new momentum building behind the idea is to long-term control of large landholdings beyond states' own national borders is needed to supply the food and energy needed to sustain their population and society into the future (Sturnino M. et al 2012). So, always there are factors behind the seen i.e. local, national, and international factors involved in land grabbing or reduction of total agriculture land. Cultivatable land mass in Ghugudia village are in decreasing trends as it was in other village in the union (the lower unit of governance), significant amount of cultivable lands are lose or transform into other use (fig.2, total land and agriculture land in Patgalia union)

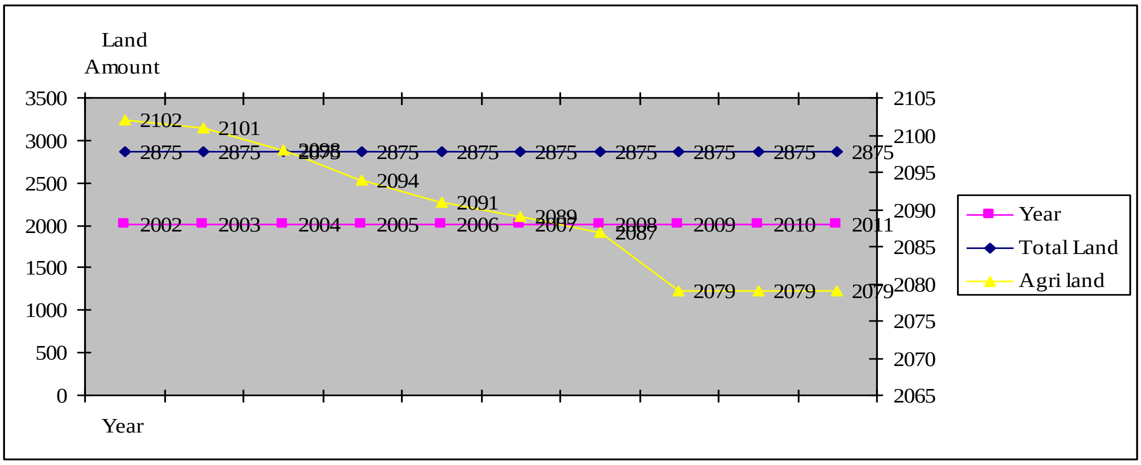

Figure:2 Decreased agriculture land, Mallick filed survey, Source: Savar, Upzila Agriculture office (2012)

In case of agriculture land change at Ghugudia and other villages in savar other than degradation of agricultural lands, immigrations, grabbing of lands by local and national housing company are also a factors. In figure 2 its clearly indicates the agriculture land are gradually decreasing in the area such as in 2002 total agriculture land was 2102 hectors and in the year 2009 its reached in to 2079 hectors. Therefore direct impact on total food production in the country backed with pollution reduces yield productions (Duhlai beel, Ghughudia village) thereafter availability, distribution and accessibility to foods.

V. POLLUTION IMPACTED INDIVIDUAL AND COMMUNITY:

Pollution have both individual community impact such as when any one infected with disease caused by pollution its incurred loss his/her daily and wages. Pollution causes for reduces fish in the river then whole fishing community affected, traditional livelihoods threatened as well as impact on total fish production. In response to questions how pollution affect individual and community following responses where documented. Responses of individual groups i.e. farmer, fishing, small business Goula/milkman and others/students were described in bellow 'Table' 1.

Table: 1. Impact of pollution, N= 30

	Farmers	Fishing	Service	Small business	Guala/ Milkmen	Others/ students	**No of response**
Number of informants	10	6	5	4	3	2	
Reduce water access	8		4	3	3	1	19
Health and disease	6	6	2	1	1	2	16
Livelihoods loss	4	5	3	1	2	2	15
Agriculture	6	6				2	14
Few fishes in the river and fish not eatable	6	5	4	3	2		20
Bad smell/degradation of environment	2		1	2	2	1	8
Land pollution and productivity reduce	2	1	1	1			5
No of response	34	23	15	11	10	10	103

Mallick, survey 2011

Data "Table1" shows that pollution has multidimensional affect on community i.e. reduces accessibility to water/river, affect health and causes to disease, loss of livelihoods of the traditional/fishing livelihood, agriculture that is degradation of land reduces production such as 63% of all respondent groups mentioned that pollution restricted their access to river Bangshi followed by health and diseases 53%. Pollution affected their livelihoods and agriculture mentioned by 50 & 47% respondent of all groups. Availability of fish in the Bangshi is very few and if they catch any are not eatable and overall environment of the riverside village degraded mentioned by 67% and 27% of all respondent groups. Finally degradation of agricultural lands and its consequences is to reduction of yield production none the less insignificant that is 27% of total respondent. Therefore cumulative affect of pollution in the community is degradation of environment and ecological niches affect individual livelihoods and reduced productivity of lands.

VI. CHANGE IN AGRICULTURE AND CROPPING PATTERNS:

High yield commercial grass:

Riverside agriculture plots which use to produce vegetables and other winter crops in Ghughudia trans in to grass field or cultivate high yielding grasses. Farmer opinioned that cultivate paddy, vegetables and other crops require systematic nurturing, use of fertilizers, pesticides and having every things in place there is uncertainty of production of good yields further using polluted water from Banghsi doubled the risk of bad production. In compare with regular crops cultivation of grass is more profiteering and risk free. The estimated cost for growing grass in a 1 decimal of land is about 200-300 taka that, is 4-5 US dollars and sold at around 14 US dollar equivalent Tk. 1120, whereas to cultivate vegetables or other crops in a same amount of land its need almost 21 Us dollar and there were risk of natural calamities (FGD with farmers). But in case of grass cultivation there is very little risk and no problem with polluted water too.

Guava as cash crops:

Guava usually water tolerant and can survive in seasonal flooding when in rainy season, monsoon floods, flooded the riverbank area. Thus the shift framing and crops pattern at Ghughudia and many other villages around river Bangashi, when traditional and usual agriculture is being hampered due to many external factors that is industrial pollution and natural calamities.

Fish pond:

The low land area of Ghughudia and other local village around the river Banghsi which was flooded during monsoon period and used for cultivate paddy one season in a year now converted in to fish ponds as these land are no longer suitable for cultivate paddy because of polluted water intuited in these lands and slug concentratied in the filed. Now huge vast area of lowland area (locally called beel) in Ghughudia and other village around the Bangshi riverside converted in to fish ponds or force to sell to housing company.

Figure: 3 Low land with paddy was converted to fish pond and latter sold to housing company (picture, Shohel Rana, JU 15 Batch)

End note/discussion:

Food security is never the less a unilateral or a single issue, rather it is comprehensive issue and need to address holistically. Degraded environment has immediate and long term impact on food bank that is production, thereafter all other aspects of food security issue.

VII. DISCUSSIONS:

In generally people of this deltaic land are diversely related with rivers. While origin of civilization is link with origin of agriculture, conversely sustainability of agriculture is related with source and availability of water. Therefore inaccessibility or polluting water source is synonym to food insecurity. The river Bangshi is the source of water for domestic and agriculture use for long. It was the means of employment for occupational groups. Contrarily, at present river Bangshi appeared as fate to the people of Gugudia and many other village as pollution in the water just affecting everything i.e. agriculture, health, water access as well as livelihoods of traditional occupational groups.

Local and national politics are involved with the pollution issue. Local people along with organized civil society groups organized protest against pollution, demonstrated in various occasions but was demolished by political influence of government back political people and local administrations. Interestingly problem is being acknowledged by the all government, political party. Again there is law and policy and new law and policy on the table to control pollution and save rivers. Government along with high level Bureaucracy seems very positives about the problems but no fruits yielded at last. Whatever the scenario at national level, local people suffer from the pollution most. The sequence of pollution of land water and generally degraded environment has end link with food insecurity of the country.

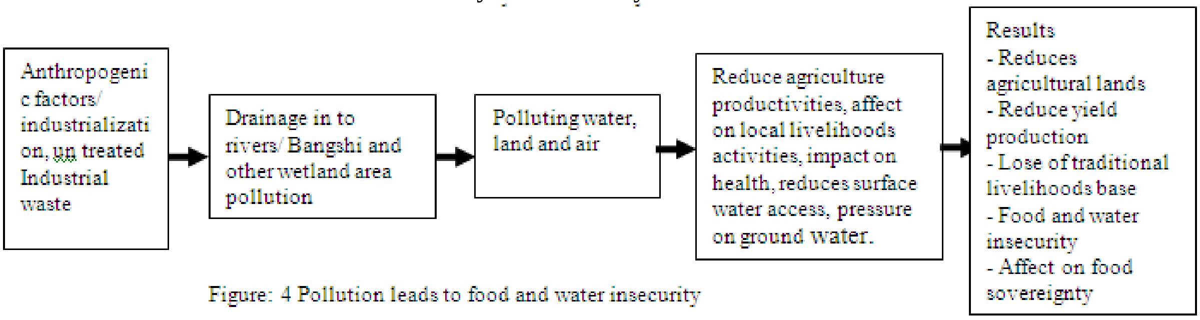

Figure: 4 Pollution leads to food and water insecurity

Waste is a by product of any production and it was not problem until those are not create obstacle or impact on other activities on earth. Industries are creating employment and by processing natural products make people lives easy. Of course responsible and environment friendly industrialization is one step ahead to food security but in regards to above the whole process "fig. 4" show how its sequentially leads to food insecurity.

Industries have ability to reduce pollution by processing of their waste in different way such as use of effluent treatment plants (ETP) doing more responsible and environment friendly business. But the attitudes of industries at least in the focused area are to profit by any means. They just ignoring the rights of people and even violate the existing law of the country by disposed their untreated industrial waste and drainage to the river and nearby water body and wetlands. Consequences are pollution of water, land and air at local area. Once its reach to the farmland in the form of watering for agriculture it's unfertile and toxic the land reduce productivity. Once surface water become toxic and un useable for any purpose, in an alternate people go for ground water use.

The whole pollution chain land water and degradation of ecology are related with food insecurity issue either its at local, national or international aspect. Such as traditional river based livelihoods affected directly when resource depleted in the river either its from natural of anthropogenic cause i.e. fisherman of Bangshi riverside area. Both push and pull factor work for reducing agriculture land in the country such as pollution reduces productivity vise-versa increase population demands for more housing in the area. Ultimate impact is reduction of cultivable land and reduces total food production and food sovereignty in the area.

VIII. CONCLUSION AND RECOMMENDATIONS:

Creation of additional jobs and wage employment is an advantage for food security. However, in the age of globalization and climate change era, every adventure to food production has to very cautious i.e. green revolutions (1940-late 1970) As we have already damage a lot to our motherly earth. According to international plane on climate change (IPCC) the warming we have already dome (co2) will affect us next 30 years if we just start zero emission right now. Climate change will affect just every thing such as due to global warming glacier will molted fast and more. Raise of sea level will inundated more fertile land; salinity in the river water will increase further. Change in the river course is not impossible, which is some time very natural one.

Therefore, polluting of local and national water basin by industrial and other waste is just suicidal. When many of the global issue (global warming, global trade), which we are not part but affecting most. Bangladesh itself is one of the densely populated country in the world such as 1100 people live in per sqm of land and 79% of its population live in rural area (BBS 2010). While in the year 2030, 60% of the world population will live in the urban area (UNFPA 2010) means lose of agricultural land and more demand for domestic water use.

Therefore to have just and sustainable development, there is need of rethinking of whole development approach. Advancement of science and technology still is in hands and use for service to the minority reach people will have to change. Local, national and global policy has to be redefining and change. At local level to control pollution and conservation of agriculture lands, demands stick implementation of exiting law, if not cover new law and policy should be adjusted to meet requirement of the food security.

REFERENCES

[1] Charles B. Heiser JR , Seed to Civilization (The story of food), 2261 Ground floor, Hudson Line, Kingsway Camp Delhi-110 009 (India) 2006

[2] Shahid Mallick, River, Culture and Livelihoods: Water pollution and social around the river Bangshi, Bangladesh, Masters diss. Future Generations Graduate School, Franklin, WV 2012

[3] Bangladesh Bureau of Statistics (BBS) Parishankhyan Bhaban, E-27/A, gargaon Sher-e-Bangla Nagar, Dhaka-1207, Bangladesh. 2008

[4] FAO, The State of world's Land and Water Resources for Food and Agriculture (Managing system at Risk) Rome 2011

[5] Pinaki Roy, Savar in Grave Peril, The Daily Star, May 2007

[6] Simon E Cook et al, Water, food and livelihoods in river basins**,** *Water International, Routledge 34 (1)* 2009, 13–29

[7] Jamal Anwar, Pollution in the Ganges Brhmaputra Delta Plain, SOS-arsenic.net, 2006

[8] Saturnino M. Borasjr and Jennifer C. Franco, Global Land Grabbing and Trajectories of Agrarian Change: A Preliminary Analysis, *Journal of Agrarian Change, 12(1),* 2012, 34–59

[9] Saturnino M. Borras Jr., Jennifer C. Franco, Sergio Go mez, Cristo bal Kay and Max Spoor, Land grabbing in Latin America and the Caribbean, *The Journal of Peasant Studies, Rouledge 39(3-4)* 2012, 845-872

[10] FAO, Scarcity and degradation of land and water: growing threat to food security, 2011

[11] FAO, Climate change, water and food security, Synthesis Paper, Expert Meeting, Rome 26–28 February, 2008

[12] FAO, Water and Food Security, Land and water division, www.fao.org/nr/water, 2009

American Journal of Engineering Research (AJER)
e-ISSN : 2320-0847 p-ISSN : 2320-0936
Volume-02, Issue-06, pp-49-54
www.ajer.org

Research Paper Open Access

Stochastic Modelling of Shiroro River Stream flow Process

Musa, J. J.
Department of Agricultural & Bioresources Engineering, School of Engineering & Engineering Technology, Federal University of Technology, P M B 65, Minna, Nigeria

Abstract: - Economists, social scientists and engineers provide insights into the drivers of anthropogenic climate change and the options for adaptation and mitigation, and yet other scientists, including geographers and biologists, study the impacts of climate change. This project concentrates mainly on the discharge from the Shiroro River. A stochastic approach is presented for modeling a time series by an Autoregressive Moving Average model (ARMA). The development and use of a stochastic stream flow model involves some basic steps such as obtain stream flow record and other information, Selecting models that best describes the marginal probability distribution of flows. The flow discharge of about 22 years (1990-2011) was gotten from the Meteorological Station at Shiroro and analyzed with three different models namely; Autoregressive (AR) model, Autoregressive Moving Average (ARMA) model and Autoregressive Integrated Moving Average (ARIMA) model. The initial model identification is done by using the autocorrelation function (ACF) and partial autocorrelation function (PACF). Based on the model analysis and evaluations, proper predictions for the effective usage of the flow from the river for farming activities and generation of power for both industrial and domestic us were made. It also highlights some recommendations to be made to utilize the possible potentials of the river effectively.

Keywords: - *ARMA, ARIMA, AR, Climate, water, stream flow*

I. INTRODUCTION

There had not been serious attention given to the depleting ozone layer, global warming and climate change until about four decades ago when it became obvious that anthropogenic damage to the earth's stratospheric ozone layer will lead to an increase in solar ultraviolet (UV) radiation reaching the earth's surface, with a consequent adverse impact, (Ghanbarpour, *et. al*., 2010). Climate change is a complex and comprehensive process that can only be understood on the basis of the combined insights from various scientific disciplines (Saremi, *et. al*., 2011). Natural scientists contribute to an improved understanding by looking at issues like the global energy balance, the carbon cycle and changes in atmospheric composition (Gangyan, *et. al*., 2002). At the same time, economists, social scientists and engineers provide insights into the drivers of anthropogenic climate change and the options for adaptation and mitigation, and yet other scientists, including geographers and biologists, study the impacts of climate change (Szilagyi, et. al., 2006; Sharif, et. al., 2007; Krishna, et. al., 2011). They also stated that a key factor of interaction is the availability of water. Water is needed for agriculture, energy production, residential water demand and industry and will be influenced by climate change. These impacts could, certainly locally, be so strong that they would influence the human activities sufficiently to create feedbacks.

Water resources play a crucial role in the economic development of Nigeria. Due to the increasing population growth and resulting demands on limited water resources, an efficient management of exiting water resources needs to be put in place for further use rather than building new facilities to meet the challenge. In the water management communities, it is well known that to combat water shortage issues, maximizing water management efficiency based on stream flow forecasting is crucial.

In design, the hydrologist is most often required to estimate the magnitude of river flow for an ensuing period of hours, days, months or possibly longer. The time sequence of flows during critical periods can be of considerable importance. The operation of a reservoir is necessarily based on anticipated flows into the reservoir and at key points downstream. Reliable flow forecasts are particularly important in the case of multipurpose reservoirs, and they are indispensable to the operation of flood mitigation reservoir systems (Cigizoglu, 2003; Valipour, 2012).

Generation of synthetic sequences of daily hydroclimatic variables like stream flow is often used for efficient short-term and long-term planning, management and assessment of complex water resources systems. Downscaling methods are an important component of the hydrologist's tool kit for generating such flow traces, which should be statistically indistinguishable from the observations (Rajagopalan *et al*., 2010). On the other hand, nonparametric methods require only a limited set of assumptions about the structure of the data, and they may therefore be preferable when *a priori* postulations required for parametric models are not valid (Higgins, 2004).

According to Otache *et al*., (2011), the principal aim of time series analysis is to describe the history of movement in time of some variables such as the rate flow in a dam at a particular size. Time series modeling for either data generation or forecasting of hydrologic variables is an important step in planning and operational analysis of water resource systems.

A stochastic approach is presented for modeling a time series by an Autoregressive Moving Average model (ARMA). This enforces stationarity on the autoregressive parameters and in inevitability on the moving average parameter, thus taking into account the uncertainty about the correct model by averaging the parameter estimates. Several stochastic models have been proposed for modeling hydrological time series and generating synthetic stream flows. These include ARMA models, disaggregation models, models based on the concept of pattern recognition. Most of the time-series modeling procedures fall within the framework of multivariate ARMA models (Otache and Bakir, 2008). Generally, AR models and Autoregressive Integrated Moving Average (ARIMA) models have an important place in the stochastic modeling of hydrologic data. Such models are of value in handling what might be described as the short-run problem; that of modeling the seasonal variability in a stochastic flow series.

The Box-Jenkins methodology, commonly known as the ARIMA model, has already been widely used in a number of related areas such as economic time series forecasting, ecological and weather prediction, medical monitoring, traffic flow prediction, and also physical activity recognition. Generally, the application of ARIMA models is mostly focused on predicting a single univariate time series (Halim, *et al*., 2007). Box and Jenkins (1976) stated that the ARIMA modeling aims at constructing the most appropriate model to fit observed data. Several types of ARIMA modeling methods and their derivatives could be used in the modeling seasonal time series, such as monthly stream flow time series. They are seasonal ARIMA, periodic ARIMA and deseasonalized ARMA model. The deseasonalized ARMA type of modeling strategy was adopted in this study due to its simplicity and effectiveness of modeling. The general form of ARIMA model is expressed as (Vandaele, 1983, Otache, *et. al*., 2011):

$$\varphi(B)y_t = \theta(B)a_t \qquad 1$$

Where

$y_t = (1-B)^d Y_t$ - Stationary series after differencing

$\varphi(B) = 1 - \varphi_1 B - \varphi_2 B^2 - \cdots \ldots . - \varphi_p B^p$ - Non-seasonal autoregressive polynomial

$\theta(B) = 1 - \theta_1 B - \theta_2 B^2 - \cdots \ldots \ldots - \theta_q B^q$ - Non-seasonal moving average polynomial

a_t = white noise process

Y_t = dependent variable

B is the backward shift operator defined as $BX_t = X_{t-1}$

Examination of the Autocorrelation Function (ACF) and Partial Autocorrelation Function (PACF) provides a thorough basis for analyzing the system behavior under time dependence, and will suggest the appropriate parameters to include in the model. The Box and Jenkins (1976) three-stage standard modeling procedure (identification, estimation, and diagnostic check) can be used to develop ARIMA models.

The objective of this study is aimed at analyzing the flow discharge from Shiroro River between 1990-2011 using AR, ARMA and ARIMA Models.

II. MATERIALS AND METHODOLOGY

The study area is located on latitudes $9^0\ 55^1$ and $10^0\ 00^1$N and longitudes $6^0\ 40^1$ and $6^0\ 45^1$E with its elevation ranging between 274 and 305 m. The Shirroro hydro-electricity dam has it source of water supply form river Kaduna. This study makes us of the inflow and outflow information/data form the dam.

The development and use of a stochastic stream flow model involves some basic steps such as obtain stream flow record and other information, Selecting models that best describes the marginal probability distribution of flows in different sections and estimate the models parameters, selecting an appropriate model of the spatial and temporal dependence of the stream flows, verifying the computer implementation of the model, and validating the model for water resources system information.

The ARMA model basically includes the AR, and the seasonal ARIMA models (Vandaele, 1983, Otache, 2011). Box and Jenkins (1976) give the paradigm for fitting ARMA models as

1. Model identification:-Determination of the ARM model orders.
2. Estimation of model parameters:-The unknown parameters in equation 1 are estimated.
3. Diagnostic and Criticism:-the residuals are used to validate the model and interval suggests potential alternative models which may be better.

These steps are repeated until a satisfactory model is found. To enhance the understanding of these paradigms, a brief discussion of the steps is imperative here.

Model Identification

The initial model identification is done by using the autocorrelation function (ACF) and partial autocorrelation function (PACF). Despite this, an alternative procedure for selecting the model order is by using a penalized log likelihood measure. One of the popular measures is the Akaike's information criterion (AIC). This is defined as;

$$AIC(k) = 2\log ML + 2k \qquad 2$$

Where ML is the maximum likelihood and K is the number of independently adjusted parameters within the model.

The best model is the one with the lowest AIC value for ARMA (p, q) models, $k = p + q$, and the AIC value can be calculated as;

$$AIC\ (p,q) = N\log(\delta_t^2) + 2\ (p+q) \qquad 3$$

Where, δ_t^2 is the variance of the innovation process.

III. RESULTS AND DISCUSSION

The analysis was carried out using the MatLab 2009 statistical package. The results are presented in the Autocorrelation Functions (ACF) and Partial autocorrelation function (PACF) graphs to show the iterated variables in a simplified form. The ACF was initially carried on the available data. The stationarity condition here implies that the mean and the variance of the process were constant. The autocovariances model developed is stated in equation 4 below

$$r_k = cov(Z_t, Z_{t-k}) = E\ (Z_t - N)(Z_{t-k} - N) \qquad 4$$

While that of the autocorrelation is obtained as

$$p_k = \frac{cov\,(Z_t, Z_{t-k})}{[v(Z_t)\,.v(Z_{t-k})]^{1/2}} \qquad 5$$

k depends on the lag or time deference since these conditions apply only to the first and second-order or weak stationarity. The autocorrelations p_k are independent of the scale of time series which is considered as a function of k and thus referred to as the autocorrelation function (ACF) or correlogrm. Since $r_k = r - k$ $\big[r_k =$ $cov\ Zt,Zt{-}k{=}cov\ Zt{-}k,Zt{=}cov\ Zt,Zt{+}k{=}r{-}k$ and $pk{=}p{-}k$. It is important to note that only the positive half of the ACF is usually considered. Figures 1 and 2 below shows the ACF for the standardized monthly and unstandardized flow of Shirorro River respectively.

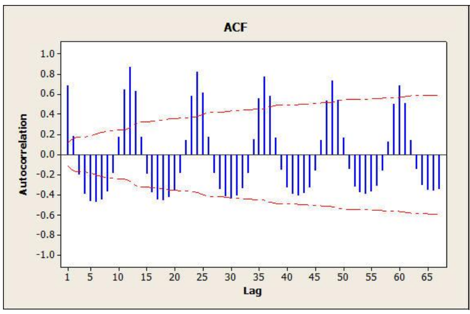

Fig. 1 Autocorrelation for standardized monthly flow

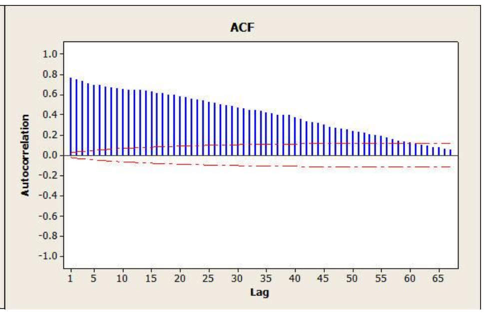

Fig. 2 Autocorrelation for daily flow (unstandardized)

The positive section of the graph shows that there exists seasonality effect on the monthly flow of the river. This further implies that carrying out ACF alone won't satisfy to build our model, thus the need for PACF. The ACF plays a major role in modeling the dependencies among observations, since it characterizes together with the process mean $E(Z_t)$ and variance $r_o = v(Z_t)$, the stationary stochastic process.

The estimate of p_k is given by the lag k sample autocorrelation in equation 6

$$\vartheta_{kk} = \frac{r_k - \sum_{j=1}^{k=1} \vartheta_{k-1,} k_{k-j}}{1 - \sum_{j=1}^{k=1} \vartheta_{k-1,} j r_j} \qquad 6$$

J=0,1,2------------k-1
K=0,1,2------------k-1
For uncorrelated observations the variance of r_k is given by

$$V(r_k) = \frac{1}{n} \qquad 7$$

$$\vartheta_{k,j} = \vartheta_{k-1,j} - \vartheta_{kk}\, \vartheta_{k-1,k-j} \qquad 8$$

The plots of the PACF for the standardized monthly and daily flow of the Shiroro River are given below in the figure 3 and 4 respectively. It was noticed that the PACF is of a particular form. The autocorrelations decrease as the lag k increase indicating that observations closer together are more correlated than the ones far apart. For Ø > 0 the autocorrelations decay geometrically to zero, and for Ø < 0 the autocorrelations decay in an oscillatory pattern.

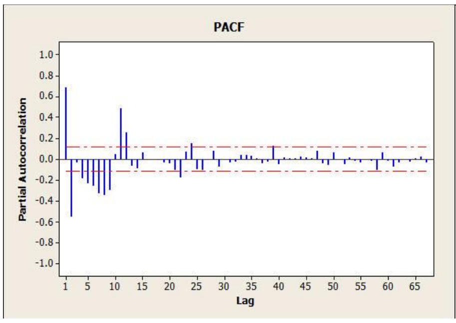

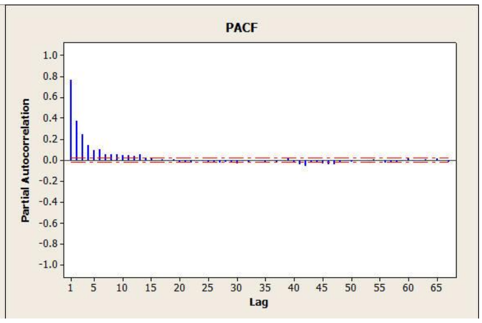

Fig. 3 Partial autocorrelation for standardized monthly flow   Fig. 4 Partial autocorrelation for daily flow (unstandardized)

The standardized data showed some degree of seasonality and thus gave room for the gap in the data points thereby standardizing the data brought which about a uniform decay in our data and the plot is as given in figure 4. From the graph, it was seen that our model is of lag 1 which gave us the basis for selecting our AR (p) model.

The ACF of the residuals in our data reveals addition structure in the data that the regression did not capture. Instead, the introduction of correlation as a phenomenon that leads to proposing the AR and ARMA models. Adding nonstationary models to the mixed leads to the ARIMA model. Adding nonstationary models to the mix leads to the ARMA models popularized by Box and Jenkins (1970).

AR models are based on the idea that the current value of the series, x_t, can be explained as a function of past values, x_{t-1}, x_{t-2},--------, x_{t-p}, where p determines the number of steps into the past needed to forecast the current value.

An AR model of order p, is presented in equation 9

$$X_t = \emptyset_1 x_{t-1} + \emptyset_2 x_{t-2} + ---- + \emptyset_p x_{t-p} + w_t \qquad 9$$

Where x_t is stationary and $Ø_1$, $Ø_2$,----------- $Ø_p$ are constants ($Ø_p \neq 0$). Assuming w_t is a Gaussian white noise series with mean zero and variance δ^2_w, μ= mean of x_t

$$X_t - \mu = \emptyset_1(x_{t-1} - \mu) + \emptyset_2(x_{t-2} - \mu) + ---- + \emptyset_p(x_{t-p} - \mu) + w_t \qquad 10$$

Or

$$X_t = \alpha + \emptyset_1 x_{t-2} + \emptyset_2 x_{t-2} + ---- + \emptyset_p x_{t-p} + w_t \qquad 11$$

Where

α=μ (1-Ø,-------------$Ø_p$)

Equation 11 above have some technical difficulties, because of the regressors, x_{t-1},---- ,x_{t-p}, which are random components, A useful form follows by using the backshift operator to write the AR (p) model, (1) as

$$(1 - \emptyset_1 B - \emptyset_2 B^2 ----- \emptyset_p B^p) x_t = w_t \qquad 12$$

Or

$$\emptyset(B) x_t = w_t \qquad 13$$

Figure 5 shows the ACF of residual daily flow (AR) and figure 6 shows the PACF of residual for daily flow (AR). From the graphs, the value for ACF and PACF in terms of lag is seen to be not significant since it both shows very low lag value, thus, lag 1 was chosen.

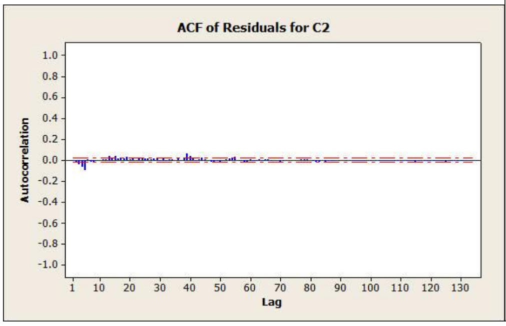

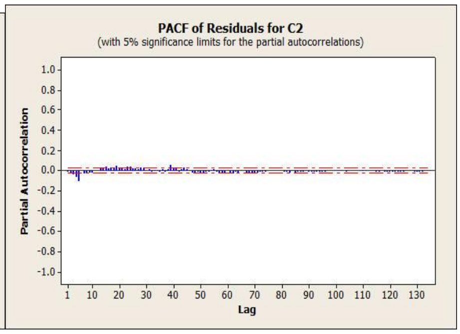

Fig. 5: Autocorrelation functions of residuals for daily flow (AR) Fig. 6: Partial autocorrelation functions of residuals for daily flow (AR)

Proceeding with the general development of autoregressive moving average and mixed ARMA models.

A time series of the form $\{x_t; t = 0, \pm 1, \pm 2, ---- 3\}$ is ARMA (p, q) if it is stationary and

$$X_t = \emptyset_1 x_{t-1} + ----- + \emptyset_p x_{t-p} + w_t + \theta_1 w_{t-1} + --- + \theta_q w_{t-p} \qquad 14$$

With $\emptyset_p \neq 0$, $\Theta_p \neq 0$, and $\delta^2_w > 0$. The parameters p and q are called the autoregressive and the moving average order respectively. If x_t has a nonzero mean μ, we set $\alpha = \mu\,(1-\emptyset_1 ---------- \emptyset_p)$ and write the model as

$$X_t = \alpha + \emptyset_1 x_{t-1} + --- + \emptyset_p x_{t-1} + w_t + \theta_1 w_{t-1} + --- + \theta_q w_{t-q} \qquad 15$$

To aid the investigation of ARAM models it will be useful to write them using the AR operator, and the MA operator. The ARMA (p, q) model can be written in concise form as

$$\emptyset(B) x_t = \theta(B) w_t \qquad 16$$

ARMA models were carried out on the flow data as well and it was observed that the lag values obtained for both ACF and PACF were of very low ranges. This is indicated in the figure below.

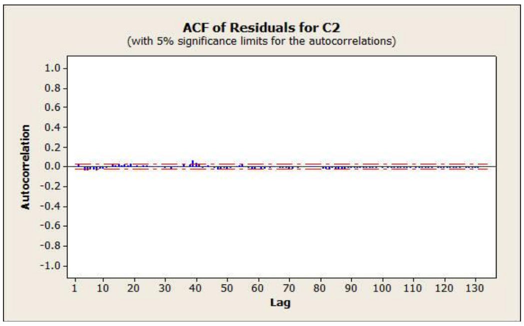

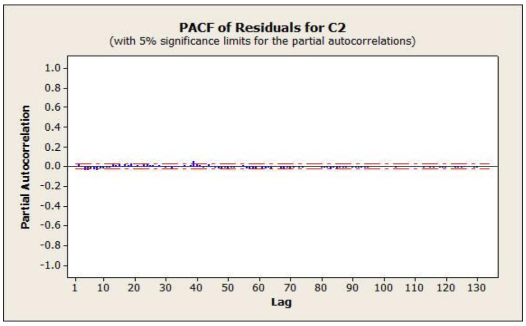

Fig. 7 Autocorrelation functions of residuals for daily flow (ARMA) Fig. 8 Partial autocorrelation functions of residuals for daily flow (ARMA)

It is seen also from the figures 7 and 8 above as analyzed with ARMA model, that the ACF and PACF has very low lag values. Thus, lag 1 is also selected as the best option for the model. Including an integrated domain we have an ARIMA model figure which further show the relations in our river flow. This is shown in the close relations in the data points from figure 9 and 10 respectively.

Since the ACF and PACF shows some seasonality in the ARIMA model due to the closeness in their data points, thus, ARIMA model is similar to both AR and the ARMA model, but only has a difference in its components. The ARIMA plots for both ACF and PACF are as given below figure 9 and 10 respectively;

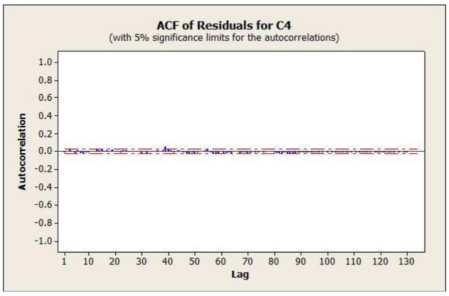

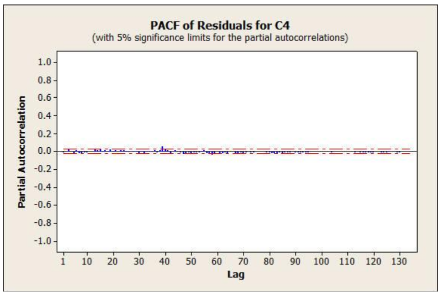

Fig. 9 Autocorrelation functions of residuals for daily flow (ARIMA) Fig. 10 Partial autocorrelation functions of residuals for daily flow (ARIMA)

IV. CONCLUSIONS

The study was able to conclude that the Shiroro river shows some correlated properties, but can still be used all year round with some degree of scheduling. This is because the amount of flow from the dam in each month of the year is still sufficient enough for optimum usage, though irrigation has to be regulated during the dry season, so as not to affect the dam reservoir level. Thus, in conclusion, the Shiroro River can be used for agriculture activities all year round but with some scheduling during the PICK dry season.

With proper regulations, there is a chance that if another dam is built along the down-stream after some contributing tributaries, there will be sufficient water to still produce Hydro power and water supply for the surrounding areas and Niger state as a whole.

REFERENCE

[1] Box, G. E. P., and Jenkins, G. M., (1976): Time Series Analysis Forecasting and Control, Holden-Day, San Francisco, CA.

[2] Cigizoglu, H. K., (2003): Incorporation of ARMA models into flow forecasting by artificial neural networks. *Environmetrics; 14: 417–427*

[3] Gangyan, Z., Goel, N. K., and Bhatt, V. K. (2002): Stochastic modeling of the sediment load of the upper Yangtze River (China). *Hydrological Sciences-Journal, 47: 93 – 105*

[4] Ghanbarpour, M. R., Abbaspour, K. C., Jalalvand, G., and Moghaddam, G. A (2010): Stochastic modeling of surface stream flow at different time scales: Sangsoorakh karst basin, Iran. *Journal of Cave and Karst Studies, v. 72, no. 1, p. 1–10*

[5] Halim, S., Bisono, I.N. Melissa, and Thia, C., (2007): Automatic Seasonal Auto Regressive Moving Average Models and Unit Root Test Detection, *IEEE International Conference on Industrial Engineering and Engineering Management*, Singapore. Pp. 1129-1133.

[6] Higgins, J. J., (2004): Introduction to Modern Nonparametric Statistics (Brooks/Cole, Pacific Grove, CA, 366 pp).

[7] Krishna, B., Satyaji Rao, Y. R., and Nayak, P. C., (2011): Time Series Modeling of River Flow Using Wavelet Neural Networks. *Journal of Water Resource and Protection, 3, 50-59*

[8] Otache Y.M, M.A. Sadeeq, and I.E Ahaneku (2011), ARMA modeling River flow Dynamics: Comparative study of PAR model. *Open Journal of Modern hydrology, vol. 1 no. 1, pp 1-9*

[9] Otache Y.M., and Bakir M., L, Z (2008): Analysis of stochastic characteristics of the Benue River Flow process. *Chin J. oceanol Limnol 26 : 151*

[10] Rajagopalan, B., Salas, J.D., and Lall, U., (2010): Stochastic methods for modeling precipitation and stream flow. In: *Advances in Data-based Approaches for Hydrologic Modeling and Forecasting.* B. Sivakumar and R. Berndtsson, Eds., World Scientific, Singapore, 17-52.

[11] Saremi, A., Pashaki, M. H. K., Sedghi, H., Rouzbahani, A., and Saremi, A., (2011): Simulation of River Flow Using Fourier Series Models. *International Conference on Environmental and Computer Science vol.19: 133 - 138*

[12] Sharif, H. O., Crow, W., Miller, N. L., and Wood, E. F., (2007): Multidecadal High-Resolution Hydrologic Modeling of the Arkansas–Red River Basin. *Journal of Hydrometeorology, Vol 8: 1111 – 1127*

[13] Szilagyi, J., Balint, G., and Csik, A., (2006): Hybrid, Markov Chain-Based Model for Daily Stream flow Generation at Multiple Catchment Sites. *Journal of Hydrologic Engineering. Pp. 245 -256*

[14] Valipour, M. (2012): Parameters Estimate of Autoregressive Moving Average and Autoregressive Integrated Moving Average Models and Compare Their Ability for Inflow Forecasting. *Journal of Mathematics and Statistics 8 (3): 330-338*

[15] Vandaele, W. (1983): *Applied time series and Box-Jenkins models* (Academic Press, New York).

American Journal of Engineering Research (AJER)
e-ISSN : 2320-0847 p-ISSN : 2320-0936
Volume-02, Issue-06, pp-55-59
www.ajer.org
Research Paper Open Access

Comparitive analysis of some important physicochemical parameters of surface soil and underground water samples of fluorotic areas of Agastheeswaram Union, South India

A.Anita Joshi Raj[1], V.Umayoru Bhagan[2]
[1](Department of Chemistry, Ponjesly College of Engineering, Anna University, India)
[2](N. I. College of Arts and Science, M.S University, India)

Abstract: - This paper analyses the fluoride concentration and some other important physicochemical parameters of 51 surface soil samples and 51 underground water samples of ten fluorotic areas of Agastheeswaram Union, South India. In all the fluorotic areas the surface soil samples were having fluoride levels greater than the undgerground water samples. The fluoride concentration in the soil was ranging between 2 to 3.5 ppm and in the water samples it was ranging between 1.3 to 2.7 ppm. Both the levels were found to be above the permissible limit. Other parameters such as p^H, alkalinity, total hardness, calcium, magnesium, chloride, salinity and sodium were also measured. Alkalinity and p^H were found to be higher than the permissible limit in all the soil and water samples at various seasons. Finally it was predicted that leaching of minerals from the soil is responsible for high fluoride content in water samples and this inturn is responsible for the prevalence of fluorosis in the study area.

Keywords: - *Fluoride, Fluorosis, Fluorotic, leaching, Physicochemical*

I. INTRODUCTION

Some elements are essential in trace amount for human beings, while higher concentration of these elements causes toxic effects, and fluoride is one among them. Concentration of fluoride between 0.6 to 1.0 ppm in potable water protects tooth decay and enhances bone development [1]. While higher levels greater than 1.5 ppm in drinking water pose a threat to human health [2]. Chronic fluorosis is a world wide problem nowadays [3]. The presence of fluoride content in the ground water samples can be attributed to geological deposits, geochemistry of location and extensive application of fertilizers like rock phosphates [4] and also depends on some physicochemical parameters such as p^H, alkalinity and temperature [5]. So the study was carried out to assess some important physicochemical parameters along with fluoride in surface soils and underground water samples in the ten fluorotic areas of Agastheeswaram Union and correlate them with the severity of fluorosis.

II. MATERIALS AND METHODS

First a door to door survey was conducted to determine the presence or absence of fluorosis using Dean's index. Next 51 underground water samples from ten fluorotic areas were collected in precleaned containers. Fluoride level was analysed using a fluoride ion selective electrode (Orion 9609 BNWP) along with TISAB-II solution in a 1:1 volume ratio with the samples.Then the analysis involved the determination of p^H using p^H meter of systronics made, calcium, magnesium and total hardness using complexometric titrations, alkalinity by normal titration, chloride by argentometric method and sodium using flame photometer of systronics made. Then 51 air dried surface soil samples from the same ten fluorotic areas were collected. Water extracts were prepared by mixing 40g of each samples with 100ml of distilled water. Then the extracts were analysed for fluoride and other physicochemical parameters by the same above said procedures.

III. RESULTS AND DISCUSSION

According to the survey report the overall prevalence of dental fluorosis in the study area was found to be 50.02%. Based on the prevalence of fluorosis the study area was classified into three categories as less endemic, moderately endemic and highly endemic.

3.1 Fluorotic areas I and II

Fluorotic area I (Azhagappapuram) and II (Anjugramam) come under highly endemic areas. Tables 1 and 2 shows the minimum and maximum values of physicochemical parameters in surface soil and underground water samples of fluorotic area I and II. In fluorotic areas I and II the surface soil contained higher values of fluoride and p^H than the underground water samples. The values of electrical conductivity, total hardness, calcium, magnesium, chloride, salinity and alkalinity of surface soils were lower than the underground water samples. The intensity of fluorosis was found to be proportional to the fluoride levels in the surface soils. Rice and coconut are cultivated in these areas. Rice is the staple food for the people of the study area. Phosphate fertilizers are used in large scale in these agricultural fields. The rock phosphate fertilizers and minerals present in soil undergo dissolution due to heavy rainfall during the monsoon seasons And increases the fluoride levels in soil and water sources gradually [6] in the study areas.

Table : 1 Values of physicochemical parameters in fluorotic area - I

S.No.	Parameter	Surface Soil		Underground Water Samples	
		Minimum	Maximum	Minimum	Maximum
1	Fluoride (ppm)	3.1	3.5	1.5	2.5
2	pH	8.6	9.1	7.2	8.9
3	Electrical Conductivity (mho/cm)	1146	1362	1540	1720
4	Total alkalinity (ppm)	127	354	236	495
5	Total hardness (ppm)	85	92	101	174
6	Calcium (ppm)	53	70	61	135
7	Magnesium (ppm)	15	37	11	81
8	Chloride (ppm)	8	14	8	92
9	Salinity (ppm)	12	22	14	166
10	Sodium (ppm)	30	69	25	92

Table : 2 Values of physicochemical parameters of fluorotic area II

S.No	Parameter	Surface Soil		Underground Water Samples	
		Minimum	Maximum	Minimum	Maximum
1	Fluoride (ppm)	2.9	3.0	2.0	2.6
2	pH	8.7	9.0	7.3	8.7
3	Electrical Conductivity (mho/cm)	410	562	938	1340
4	Total alkalinity (ppm)	156	211	310	489
5	Total hardness (ppm)	72	87	67	205
6	Calcium (ppm)	61	71	43	185
7	Magnesium (ppm)	11	16	22	55
8	Chloride (ppm)	25	35	36	123
9	Salinity (ppm)	46	64	65	223
10	Sodium (ppm)	107	198	83	316

3.2 Fluorotic areas III, IV and V

Fluorotic areas III (Marungoor), IV (Mylady), V (South Thamaraikulam) come under moderately endemic areas. Tables 3, 4 and 5 show the minimum and maximum values of physicochemical parameters of surface soil and underground water samples of fluorotic areas III, IV and V respectively. In fluorotic areas III, IV and V the surface soils contained higher values of fluoride and p^H than the underground water samples. All the other physicochemical parameters of the surface soils were found to be lower than the underground water samples. The values of fluoride and alkalinity in both the surface soil and underground water samples of those study areas were found to be higher than the prescribed limit. Normally higher alkalinity of water promotes leaching of fluoride and thus affects the concentration of fluoride in the ground water [7]. Agriculture and stone polishing were the major occupations for the people of those areas. Many of those affected working adults consume an average of 5 litres of water per day. This increases the fluoride level in the people as the fluoride content of the water they consume is greater than the permissible limit.

Table : 3 Values of physicochemical parameters of fluorotic area III

S.No.	Parameter	Surface Soil		Underground Water Samples	
		Minimum	Maximum	Minimum	Maximum
1	Fluoride (ppm)	3.2	3.4	1.6	2.1
2	pH	8.9	9.1	7.3	8.7
3	Electrical Conductivity (mho/cm)	356	623	1299	1624
4	Total alkalinity (ppm)	112	316	220	595
5	Total hardness (ppm)	42	102	62	183
6	Calcium (ppm)	33	72	50	130
7	Magnesium (ppm)	6	32	7	81
8	Chloride (ppm)	103	120	201	206
9	Salinity (ppm)	186	354	362	372
10	Sodium (ppm)	40	103	52	241

Table : 4 Values of physicochemical parameters of fluorotic area IV

S.No.	Parameter	Surface Soil		Underground Water Samples	
		Minimum	Maximum	Minimum	Maximum
1	Fluoride (ppm)	2.1	2.4	1.6	2.2
2	pH	8.3	8.9	6.9	8.6
3	ElectricalConductivity (mho/cm)	862	963	1430	1817
4	Total alkalinity (ppm)	183	297	326	605
5	Total hardness (ppm)	72	102	90	201
6	Calcium (ppm)	61	90	61	161
7	Magnesium (ppm)	9	15	17	89
8	Chloride (ppm)	76	103	103	120
9	Salinity (ppm)	137	186	186	216
10	Sodium (ppm)	197	200	201	285

Table : 5 Values of physicochemical parameters of fluorotic area V

S.No.	Parameter	Surface Soil		Underground Water Samples	
		Minimum	Maximum	Minimum	Maximum
1	Fluoride (ppm)	2.0	2.5	1.5	2.0
2	pH	8.7	8.8	6.8	8.7
3	ElectricalConductivity (mho/cm)	336	852	1620	1871
4	Total alkalinity (ppm)	218	322	344	695
5	Total hardness (ppm)	79	102	100	239
6	Calcium (ppm)	50	77	53	177
7	Magnesium (ppm)	12	32	21	97
8	Chloride (ppm)	40	130	129	229
9	Salinity (ppm)	73	239	236	413
10	Sodium (ppm)	91	151	98	206

3.3 Fluorotic areas VI, VII, VIII, IX and X

Fluorotic areas VI (Theroor), VII (Mahadhanapuram), VIII (Theraikalpudur), IX (Kottaram) and X (Nallur) come under less endemic areas. Tables 6,7,8,9 and 10 shows the minimum and maximum values of physiochemical parameters of the surface soil and underground water samples of the fluorotic areas VI, VII, VIII, IX and X. In all those fluorotic areas the amount of fluoride in the surface soils and underground water samples exceeds the prescribed limit. Several processes namely dissolution of fluoride bearing minerals, ion exchange and evaporation concentration can locally account for high fluoride concentration in ground water of the study areas [8]. People of these study area were affected by fluorosis because of the fact that the people consumed locally available rice, coconut, vegetables and fruits which contain more fluoride level. Moreover they entirely depend upon borewell water containing higher fluoride.

Table : 6 Values of physicochemical parameters of fluorotic area VI

S.No.	Parameter	Surface Soil		Underground Water Samples	
		Minimum	Maximum	Minimum	Maximum
1	Fluoride (ppm)	2.4	3.2	1.6	2.1
2	pH	8.6	8.8	7.3	8.5
3	Electrical Conductivity (mho/cm)	425	936	913	1223
4	Total alkalinity (ppm)	228	342	231	584
5	Total hardness (ppm)	76	82	97	164
6	Calcium (ppm)	58	59	43	138
7	Magnesium (ppm)	18	23	22	63
8	Chloride (ppm)	132	140	132	184
9	Salinity (ppm)	238	257	238	332
10	Sodium (ppm)	52	76	73	133

Table : 7 Values of physicochemical parameters of fluorotic area VII

S.No.	Parameter	Surface Soil		Underground Water Samples	
		Minimum	Maximum	Minimum	Maximum
1	Fluoride (ppm)	2.6	2.7	1.9	2.1
2	pH	8.7	8.8	7.5	8.5
3	ElectricalConductivity (mho/cm)	574	745	1001	1521
4	Total alkalinity (ppm)	256	272	174	628
5	Total hardness (ppm)	73	86	141	341
6	Calcium (ppm)	55	61	98	250
7	Magnesium (ppm)	12	31	15	118
8	Chloride (ppm)	19	24	127	184
9	Salinity (ppm)	35	43	230	332
10	Sodium (ppm)	14	19	14	90

Table : 8 Values of physicochemical parameters of fluorotic area VIII

S.No.	Parameter	Surface Soil		Underground Water Samples	
		Minimum	Maximum	Minimum	Maximum
1	Fluoride (ppm)	2.0	2.1	1.5	1.7
2	pH	8.8	8.9	7.4	8.5
3	ElectricalConductivity (mho/cm)	963	978	1002	1691
4	Total alkalinity (ppm)	252	256	234	652
5	Total hardness (ppm)	86	96	110	163
6	Calcium (ppm)	70	78	90	146
7	Magnesium (ppm)	16	18	16	37
8	Chloride (ppm)	70	127	132	158
9	Salinity (ppm)	128	230	238	283
10	Sodium (ppm)	76	86	75	78

Table : 9 Values of physicochemical parameters of fluorotic area IX

S.No	Parameter	Surface Soil		Underground Water Samples	
		Minimum	Maximum	Minimum	Maximum
1	Fluoride (ppm)	2.9	3.0	1.4	2.0
2	pH	8.7	8.8	7.5	8.5
3	Electrical Conductivity (mho/cm)	530	726	1360	1559
4	Total alkalinity (ppm)	230	262	154	565
5	Total hardness (ppm)	86	105	101	270
6	Calcium (ppm)	71	82	15	230
7	Magnesium (ppm)	15	23	20	95
8	Chloride (ppm)	127	129	127	208
9	Salinity (ppm)	230	237	230	375
10	Sodium (ppm)	1.96	2.96	130	238

Table : 10 Values of physicochemical parameters of fluorotic area X

S.No.	Parameter	Surface Soil		Underground Water Samples	
		Minimum	Maximum	Minimum	Maximum
1	Fluoride (ppm)	2.0	2.3	1.3	1.9
2	pH	8.6	8.8	7.2	8.4
3	Electrical Conductivity (mho/cm)	1126	1141	1108	1326
4	Total alkalinity (ppm)	256	259	145	632
5	Total hardness (ppm)	95	97	110	159
6	Calcium (ppm)	74	75	62	120
7	Magnesium (ppm)	21	22	30	56
8	Chloride (ppm)	200	201	193	208
9	Salinity (ppm)	367	369	354	375
10	Sodium (ppm)	172	189	173	225

IV. CONCLUSION

Fluoride content and some important physicochemical parameters of 51 surface soil samples and underground water samples of Agastheeswaram Union, South India were evaluated. Almost all the surface soil samples were having higher fluoride and p^H values than the water samples. Both soil and water samples do not meet the quality parameters such as fluoride, alkalinity and p^H. Most of the people depend on vegetables and food grains cultivated in the study area. And they also depend upon the borewell water containing higher fluoride which is not suitable for consumption without prior treatment. The above said two reasons are responsible for the prevalence of fluorosis in the study area. People of Agastheeswaram Union should be educated about the hazards of consumption of high fluoride bearing water and they should be encouraged to defluoridate water before consumption.

REFERENCES

[1] N. Kundu, M.K. Panigrahi, S. Tripathy, S. Munshi, M. A. Powell and B.R. Hart, Geochemical appraisal of fluoride contamination of ground water in the Nayagarh district, Orissa, *Environmental Geology, 41*, 2001, 451-450.

[2] B. Mayer, K. Kim, S. Kim, J.K. Won, K. Kim and Y. Koh, Fluorine geochemistry in bed rock ground water of South Korea, Science, *Total Environ, 385*, 2007, 272-283.

[3] R. Srikanth, K.S. Vishwanath, F. Khasai, A. Fitsahatsion and M. Asmallash, Fluoride in ground water of selected villages in Eritrea, *Environmental Monitoring and Assessment, 75 (2)*, 2002, 169-177.

[4] K. Karthikeyan, K. Nanthakumar, P. Velmurugan, S. Tamilarasi, P. Lakshmanaperumalsamy, *Environmental Monitoring Assessment, 160*, 2010,141-155.

[5] Garg, Kavitha, Renuka and Anjumalik, Ground water quality in some villages of Haryana, India, Focus on fluoride and fluorosis, *Journal Hazard mater, 106*, 2004, 85-97.

[6] B. Rao, Nagamalleswor, S.V.R. Rao and G.V.V.S. Chowdary, *Ind. Journal. Env. Protection, 10 (5)*, 1990, 160-162.

[7] V.K. Saxena and S. Ahmed, Disssolution of fluoride in ground water, water rock interaction study, *Environmental Geology, 40*, 2001, 1084-1087.

[8] V.K. Saxena and S. Ahmed, Inferring the chemical parameters for the dissolution of fluoride in groundwater . *Environmental Geology, 43*, 2003, 731-736.

American Journal of Engineering Research (AJER)
e-ISSN : 2320-0847 p-ISSN : 2320-0936
Volume-02, Issue-06, pp-60-68
www.ajer.us

Research Paper Open Access

Experimental study of Nusselt number and Friction factor in solar air heater duct with Diamond shaped rib roughness on absorber plate

S. S. Pawar[1], Dr. D. A. Hindolia[2], Dr. J. L. Bhagoria[3]
[1]*Research scholar, Rajeev Gandhi Prodhyogiki Vishwvidhyalaya, Bhopal (M.P.) 462026, India.*
[2]*Principal, Jai Narayan College of Technology, Bhopal (M.P.) 402046, India.*
[3]*Professor, Mechanical Engineering department, M.A.N.I.T., Bhopal, (M.P.) 462046, India.*

Abstract:- Solar air heater is used to heat air but it has low thermal efficiency because of low thermal conductivity between air and absorber plate. Thermal efficiency of solar air heater can be improved by creating artificial roughness on absorber plate which causes higher temperature to absorber plate and hence maximum thermal losses occurs to atmosphere. There are number of parameters which enhances the thermal conductivity such as relative roughness height (e/D_h), relative roughness pitch (P/e), Reynolds number (Re), and angle of attack (α).Experimental investigations were carried out to study heat transfer enhancement using diamond shape rib on absorber plate of solar air heater. Absorber plate is heated with the solar radiation in outdoor experiment whereas electric heater is used for indoor experiment. Setup is isolated from the three sides with Thermocol. The relative roughness pitch (p/e) varies from 10 to 25 mm. The roughened wall has relative roughness height (e/D_h) of 0.023mm and 0.028mm, angle of attack (α) is 0° degree, rib height (e) is 1 mm and 1.25 mm. Duct aspect ratio (W/H=8), rate of air flow corresponds to Reynolds no. (Re) ranging from 3000-14000.Finally comparison of heat transfer and friction factor from both smooth and roughened plate under the similar condition of air flow is made.

Keyword: - *Solar air heater, diamond shape rib, heat transfer enhancement, pitch and Reynolds number, rib height, friction factor.*

I. INTRODUCTION

The Artificial roughness is used as turbulence promoters on a surface. It is also the technique to enhance the rate of heat transfer to the flowing fluid in a testing duct. The surface roughness can be created by number of methods such as welding, fixing small ribs, fixing small diameter of wires, machining, and sand blasting, casting and forming. Several investigators [15, 21, 22, and 24] create artificial roughness in the form of fine wires and ribs of different shapes to enhance the heat transfer coefficient. It results to increase in frictional losses which cause more power required by blower. To keep friction losses at a minimum level, the turbulence should be created very close to the duct surface i.e. laminar sub layer. Flowing air strike with ribs and break laminar sub layer which creates local wall turbulence causes flow separation and reattachment between consecutive ribs which reduce the thermal resistance and increases the heat transfer. Various studies [7, 8, 11, 13, 18, 20, 21, and 22] have shown that V-shaped ribs perform better than angled ribs. Formation of two secondary flow cells in case of V-ribs instead of one cell in case of angled rib has been cited as reason for the superior performance of V-ribs. Application of the artificial roughness in a solar air heater owes its origin to several investigations carried out for enhancement of cooling of turbine blades' passage. Several investigations have been carried out to study effect of artificial roughness on heat transfer and friction factor for two opposite roughened surfaces by Han [6], Han et al. [4,6,7], Lau et al. [8,9], Han and Zhang [11] , Taslim et al. [13] and Wright et al. [21] have developed correlations. Prasad and Saini [5], Gupta et al. [14], Karwa et al. [20], Bhagoria et al. [23], Momin et al. [25], Karwa [18] have carried out investigations on rib roughened absorber plates of solar air heaters which have only one roughened heated wall and three smooth walls. Correlations for heat transfer coefficient and friction factor have been developed for such systems. Prasad and Saini [5] used transverse small diameter wire as roughness element. Gupta et al. [14] investigated effect of relative roughness height, angle of attack on heat transfer and friction factor for inclined circular wire ribs. Karwa et al. [20] investigated effect of rib chamfer angle (U), duct aspect ratio on heat transfer and friction factor using integral chamfered ribs. Prasad and Saini [5] investigated the effect of relative roughness height (e/D_h) and relative roughness pitch (p/e) on heat transfer and friction factor using circular wire roughness. It also observed that increase in the relative roughness height results decrease in the rate of heat transfer. Increase in the relative roughness pitch results in a decrease in the rate of both heat transfer and friction factor. Nusselt number and friction factor were enhancing maximum as 2.38 and 4.25 times than that of smooth duct, respectively. Gupta et al. [12] investigated the effect of relative roughness height, angle of attack and Reynolds number on heat transfer and friction factor in rectangular duct having circular wire ribs on the absorber plate. It was found as result that the heat transfer coefficient in roughened duct improved by a factor up to 1.8 and the friction factor found as result is increased by 2.7 times that of the smooth duct. The heat transfer coefficient and friction factor were found maximum at an angle of attack of 60 and 70 respectively.Saini and Saini [14] investigate the effect of metal matrix geometry on the heat transfer coefficient and friction factor in a large aspect ratio rectangular duct, having one wall artificially roughened by an expanded metal matrix. The maximum values of Nusselt number and friction factor corresponds to angle of attack values of 61.9 and 72.The maximum enhancement in Nusselt number and friction factor values are of the order of 4 and 5, respectively. Muluwork et al. [15] compared the thermal performance of staggered discrete V-apex up and down with corresponding transverse staggered discrete ribs. The relative roughness length ratio (B/S) had been considered as dimensionless geometric parameter of roughness element to compare three different configurations. It was observed that the Stanton number increases with the increase of relative roughness length ratio. The Stanton number for V-down discrete ribs was higher than the corresponding V-up and transverse discrete roughened surfaces. The Stanton number ratio enhancement was found 1.32–2.47 in the range of parameters covered in the investigation. It was also observed that the friction factor increases with an increase in the relative roughness length ratio. Further for Stanton number, it was seen that the ribbed surface friction factor for V-down discrete ribs was highest among the three configurations investigated.Karwa et al. [16] performed experimental study to predict the effect of rib chamfer angle (Uc) and duct aspect ratio on heat transfer and friction factor in a rectangular duct roughened with integral chamfered ribs. As compared to the smooth duct, the presence of chamfered ribs on the wall of duct yields up to about two fold and three fold increases in the Stanton number and the friction factor in the range of parameters investigated. The highest heat transfer as well as highest friction factor exists for a chamfer angle (Uc) of 15°. The minima of the heat transfer function occur at roughness Reynolds number of about 20. As the aspect ratio (H/D) increases from 4.65 to 9.66, the heat transfer function also increases and then attains nearly a constant value. The roughness function decreases with the increase in the aspect ratio (H/D) from 4.65 to 7.75 and then attains nearly a constant value.Verma and Prasad [17] investigated the effect of geometrical parameters of circular wire ribs on heat transfer and friction factor. It was observed that the value of heat transfer enhancement factor (Nur/Nus) varies from 1.25 to 2.08 within the range of parameters.Momin et al. [20] experimentally investigate the effect of geometrical parameters of V-shaped ribs on heat transfer and fluid flow characteristics in rectangular duct of solar air heater. The investigation covered Reynolds number range of 2500–18,000, relative roughness height of 0.02–0.034 and angle of attack of flow of 30– 90 for a fixed relative pitch of 10. For this geometry it was observed that the rate of increase of Nusselt number with an increase in Reynolds number is lower than the rate of increase of friction factor. The maximum enhancement of Nusselt number and friction factor as result of providing artificial roughness had been found as 2.30 and 2.83 times to smooth surface respectively, for an angle of attack of 60_. It was also found that for relative roughness height of 0.034 and angle of attack of 60, the V-shaped ribs enhance the value of Nusselt number by 1.14 and 2.30 times over inclined ribs and smooth plate, respectively. It was concluded that V shaped ribs gave better heat transfer performance than the inclined ribs for similar operating conditions. Bhagoria et al. [19] performed experiments to determine the effect of relative roughness pitch, relative roughness height and wedge angle on the heat transfer and friction factor in a solar air heater roughened duct. The presence of ribs yields Nusselt number up to 2.4 times while the friction factor rises up to 5.3 times as compared to smooth duct in the range of parameters investigated. A maximum enhancement in heat transfer was obtained at a wedge angle of about 10_. The heat transfer was found maximum for a relative roughness pitch of about 7.57. The friction factor decreased as the relative roughness pitch increased. M.M.Sahu and Bhagoria [22] experimentally investigate on broken transverse ribs in solar air heaters that Reynolds number range of 3000–12,000, roughness pitch of 10–30 mm, height of the rib 1.5 mm and the aspect ratio of 8. It was found that the maximum Nusselt number attained for roughness pitch (p/e) of 20 and decreased with the increase in roughness pitch. Roughened absorber plates increased the heat transfer coefficient by 1.25–1.4 times as compared to smooth rectangular duct under similar operating conditions at higher Reynolds number.

II. INDOOR EXPERIMENTAL PROGRAM

2.1 Experimental apparatus

An indoor setup consist of long duct 2040 mm which is divided into number of parts .These are inlet section 177 mm, test section 1500 mm, mixing section and exit section 353 mm, baffles spacing 87 mm. A blower, single phase 240 volts, control valve, orifice plate and other devices such as milli voltmeter measures temperature, micro manometers measures pressure head for Reynolds no. (ASHRAE 1977) and inclined manometer for pressure measurement .A roughened absorber plate placed of length 1500 mm, on the top of the test section. Actual experimental setup shown in fig.-1.

Fig.1 Actual setup of experiment

Exit section is provided after this test section i.e.354 mm in length. The reason is to provide the exit section is to reduce the end effect in the test section to find uniform temperature at the out let, three baffles at 87 mm at equidistance are provided to mix the hot air coming out from duct. Inclined manometer is placed between blower and exit section of the duct and a control valve also provided beside the orifice plate to control the Reynolds no. The setup is covered with 25 mm thick thermocol sheet from inlet section of the duct to orifice plate to avoid heat losses. The heated GI 1mm thick sheet have diamond shaped roughness create with the help of pasting repeated diamond shaped on one side of the sheet and other side painting with black paint and fixed thermocouples on the back side of the sheet. These couples give the temperature at the different locations, the mass flow rate measures with the help of providing the inclined manometer across the orifice plate. A schematic diagram shown in fig.-2.

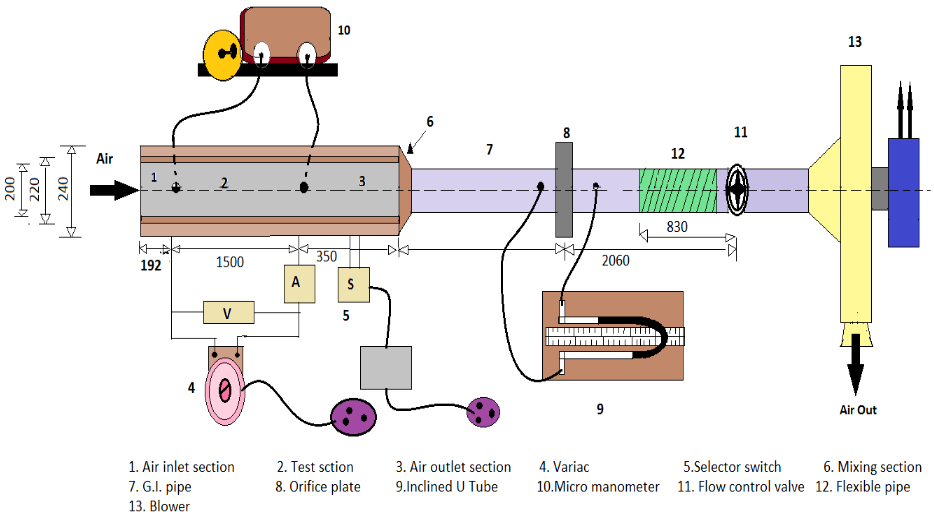

Fig.2 Schematic diagram of setup

TABLE 1 EXPERIMENTAL CONDITION

Parameter	Values
Reynolds number(Re)	3000 – 14,000
Channel aspect ratio(W/H)	8.0
Test length (L)mm	1500
Roughness height(e)mm	1 and 1.25
Relative roughness height (e/ D_h)	0.023 and 0.034
Hydraulic Diameter(D_h)mm	44.44
Roughness pitch(P)mm	10,15,20 and 25
Insulation(I) W/m^2	900-950

2.2 Absorber plates

Absorber plate made up of G.I. 1mm thickness. Roughness created by pasting regular diamond shaped of 5mm pieces and 1mm rib height on the absorber plate. Other side of the absorber plate painted by black paint also affixed thermocouples on this side. Some difficulties were experienced in getting plates manufactured to the exact dimensions. One smooth and other was artificially roughness. Figure no.-3 shows the photograph of rough plate. Fig no.4 shows the geometry of the absorber plate with diamond shape of roughness.

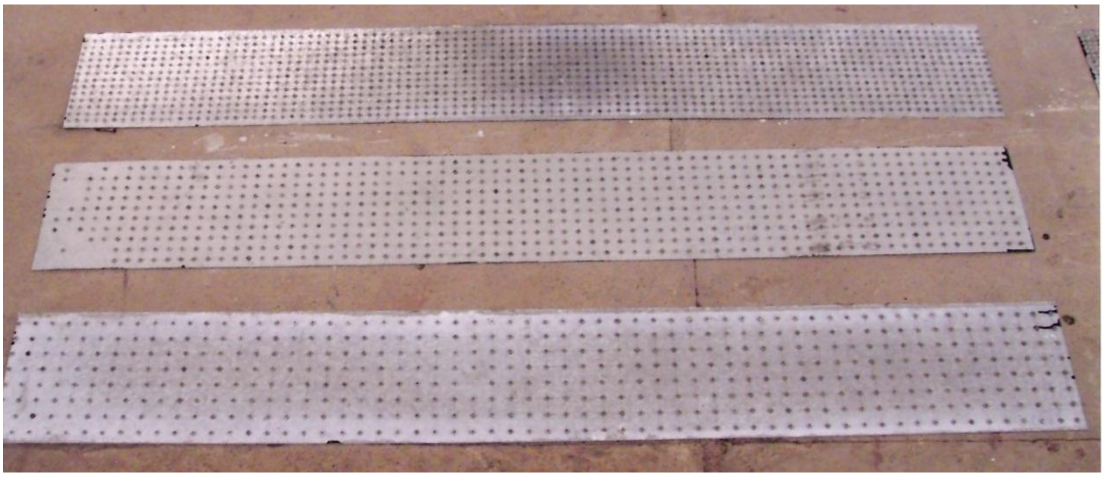

Fig.3 Rough plate of different pitches

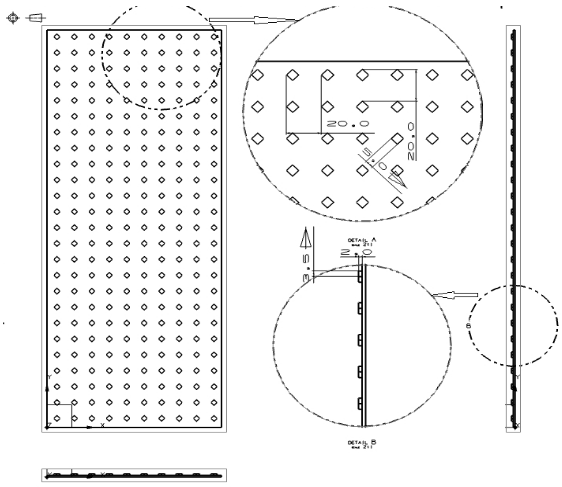

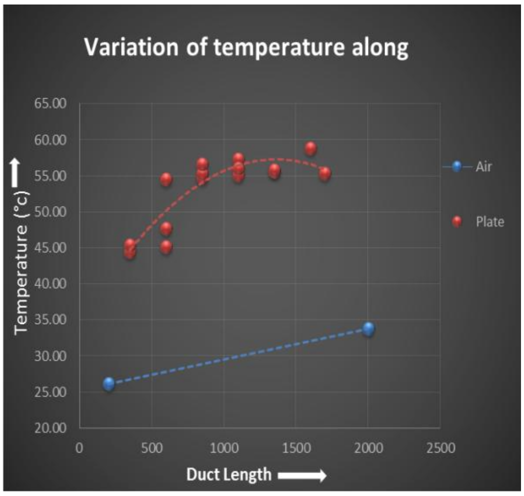

Fig. 4 Geometry of rough plate with 20mm pitch and Graph for variation of temperature along the test length

2.3 Experimental procedure

Instrument should check whether all equipment is in proper working before starting the setup. Also check all the instruments are connecting in proper way and correct. The leakage of the joints can be checked by soap and bubble treatment .Micro manometer is connected to measure pressure drop across the duct. Thermocouples are used to measure temperature of plate. Flow of air can be control with the help of control valve for the proper value of the Reynolds no. Switch on to run the blower and heater. Set the rate of flow of air according to Reynolds no. Wait for half an hour if the steady state condition reaches. Collect all the relevant data concern with setup and required data for each rib configuration and the various Reynolds no.3000-14000. This gives the various parameters which are to be measured during experiments. The parameters are needed to record is

1. Inlet temperature of air at entrance of duct.
2. Outlet temperature of air at exit section of the duct.
3. Intermediate temperature of the collector.
4. Pressure drop across orifice plate measure with the help of inclined manometer.
5. Solar insulation

2.4 Validation test

Validation curve with smooth plate is taken by S.S.Pawar et al. [28] and the value of Nussselt no. and friction factor is obtained from experimental data .These data is compared with value of DittusBoelter and modified Blasius equation respectively.

DittusBoelter equation $Nu_s = 0.024Re^{0.8}Pr^{0.4}$ (1)

Modified Blasius equation $fs = 0.085Re^{-0.25}$ (2)

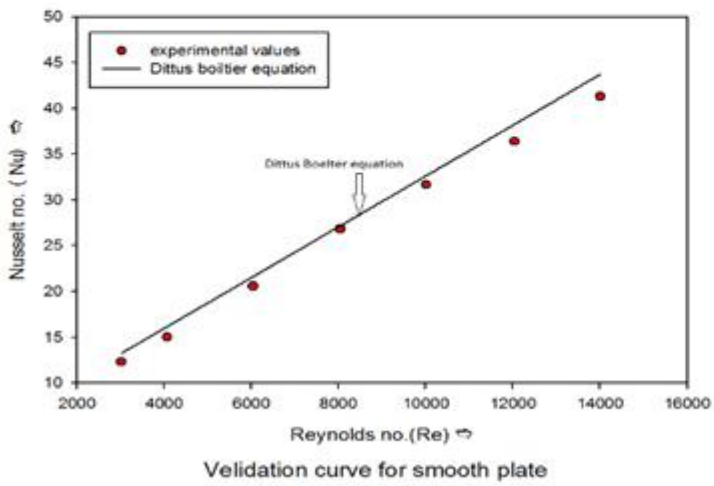

Fig.5 Graph no.-1

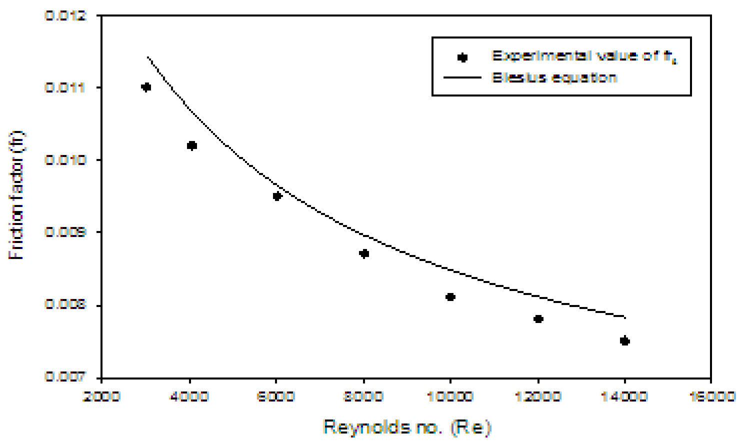

Fig.6 Graph no.-2

2.5 Variation of temperature along test duct

Setup consist four section i.e. entering section, heating section, mixing section and exit section .Air enters at atmosphere temperature in the entering section, heat added in heating section ,air mixed in mixing sections temperature reduced .Finally uniform temperature received after mixing section. Temperatures of all the four sections are noted down and are plotted as shown in graph in fig-4.

III. DATA REDUCTION

3.1 Data analysis

Table – 1 shows the experimental parameter and table 2 -3 shows the experimental data for smooth and roughened plate.

3.2 Mean Air & Plate Temperature

The mean air temperature is the simple arithmetic mean of the measure values at the inlet and exit of the test section. Thus

$T_{fav} = (t_i + t_{oav}) /2$

The mean plate temperature, t_{pav} is the weighted average of the reading of all points located on the absorber plate.

3.3 Pressure Drop Calculation

Pressure drop measurement across the orifice plate by using the following relationship:

$\Delta P_o = \Delta h \times 9.81 \times \Delta_m \times 1/5$

Where

ΔP_o = Pressure difference

$\Delta\rho_m$ = Density of the fluid (Mercury) i.e. $13.6\text{x}10^3$

Δh = Difference of liquid head in U-tube manometer, m

3.4 Mass Flow Measurement

Mass flow rate of air has been determined from pressure drop measurement across the orifice plate by using the following relationship:

$m = C_d \times A_0 \times [2\,\rho\Delta P_0 / (1 - \beta^4)]^{0.5}$

Where

m = Mass flow rate, kg / sec.

C_d = Coefficient of discharge of orifice i.e. 0.62

A_0 = Area of orifice plate, m^2

ρ= Density of air in Kg/m^3

β= Ratio of dia. (d_o / d_p) i.e. 26.5/53 = 0.5

3.5 Velocity Measurement:

$V = m / \rho WH$

Where,

m = Mass flow rate, kg / sec

ρ = Density of air in Kg/m^3

H = Height of the duct in m

W = Width of the duct, m

3.6 Reynolds Number

The Reynolds number for flow of air in the duct is calculated from:

$R_e = VD / v$

Where,

ν= Kinematics viscosity of air at t_{fav} in m^2/sec

$D_h = 4WH / 2\,(W+H) = 0.04444$ m

3.7 Heat Transfer Coefficient

Heat transfer rate, Q_a to the air is given by:

$Q_a = m\, c_p\, (t_o – t_i)$

The heat transfer coefficient for the heated test section has been calculated from:

$h = Q_a / A_p\, (t_{pav} - t_{fav})$

A_p is the heat transfer area assumed to be the corresponding smooth plate area.

3.8 Nusselt Number

The Heat Transfer Coefficient has been used to determine the Nusselt number defined as;

$$Nu = h\,D_h / K$$

Where k is the thermal conductivity of the air at the mean air temperature and D_h is the hydraulic diameter based on entire wetted parameter.

3.9 Thermal Efficiency

The Thermal efficiency for test section is calculated from:

$$\eta = Q_a / A_p I$$

Where, I = Heat Flux i.e. 900 W/m^2

IV. RESULT AND DISCUSSION

Heat transfer coefficient and friction factor compared roughened plate with smooth plate under similar fluid flow condition. Roughness creates by pasting regular diamond shaped rib to see the enhancement in heat transfer coefficient. Fig.3 shows the roughened plate of different pitches. Figure-4 shows the geometry of roughened plate. These graph shows as Nusselt number increases with increases in Reynolds numbers. Comparison of two rib height results takes place in this experiment. These are 1mm and 1.25mm.finally compared for higher heat transfer coefficient.

The Nusselt number found maximum at the pitch value of 15mm with Rib height 1mm.Also indicate that heat transfer coefficient is maximum at 15 mm pitch roughened plate.

It is nothing but the ratio of conductive resistance to convective resistance of heat flow and as Reynolds number increases thickness of boundary layer decreases and hence convective resistance decreases which in term increases the Nusselt number.

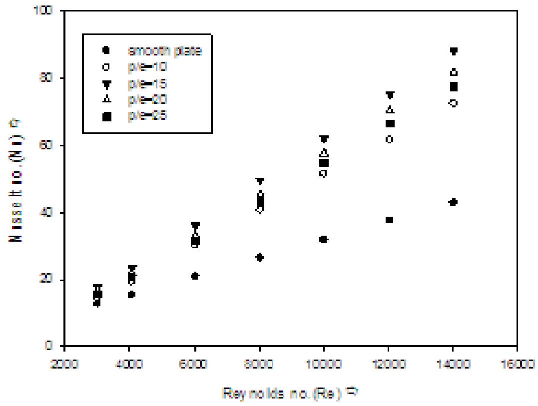

Graph of Nusselt no.(Nu) v/s Reynolds no.(Re) for e=1mm

(a)

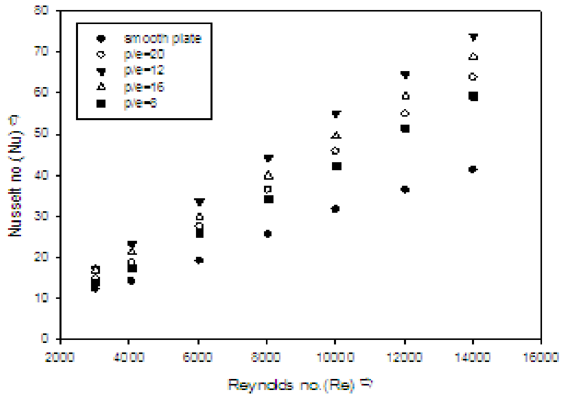

Graph of Reynold no.(Re) V/s Nusselt no. (Nu) for 1.25 mm

(b)

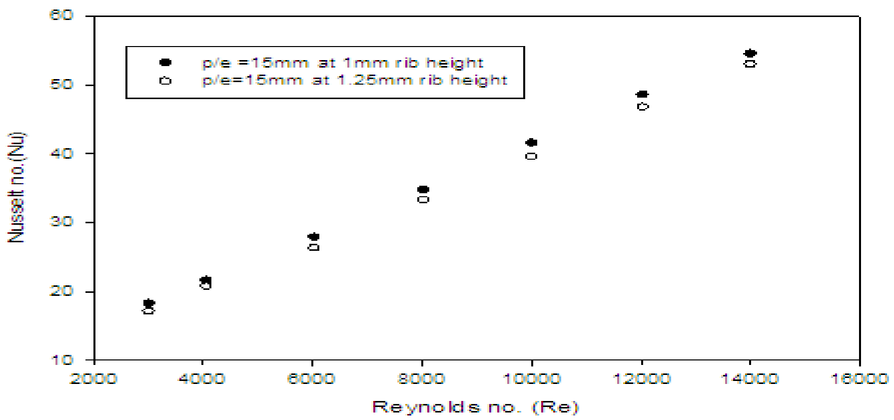

Graph compare the maximum values in two rib height 1mm & 1.25 mm

(C)

Fig. 7 (a) Nu vs Re for e=1mm (b) Nu vs Refor e=1.25mm (c)Nu vs Refor e=1mm&for e=1.25mm (c)

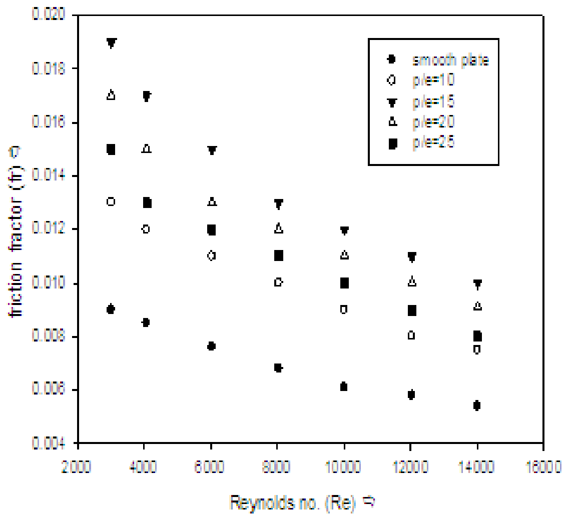

Graph of Renould no.(Re) with friction factor (fr) of 1mm rib height.

(a)

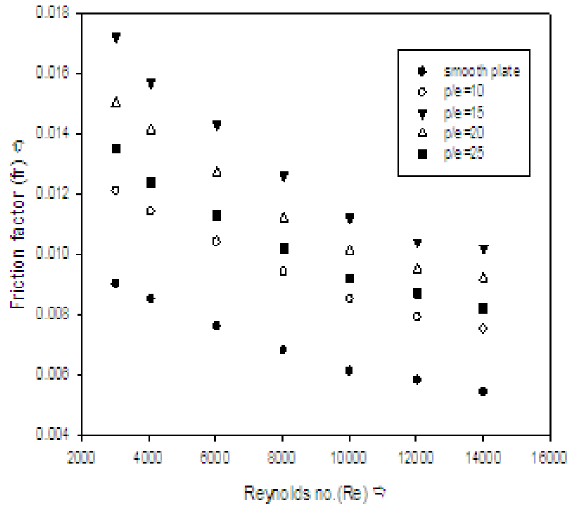

Graph for friction factor (fr) versus Reynolds no. (Re) of 1.25mm rib height at 0 deg.angle of attack

(b)

Graph for Comperation of result for 1mm and 2mm rib height

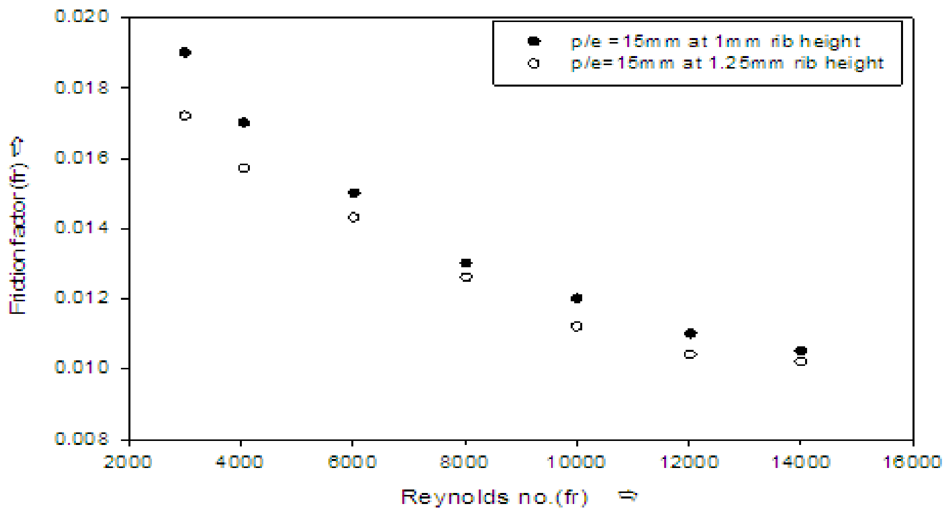

(c)

Fig. 7 (a) fvs Re for e=1mm (b) fvs Re for e=1.25mm (c) fvs Re for e=1mm & for e=1.25mm

V. CONCLUSIONS

The major conclusions of this article are as follows:

1. Presence of diamond shaped rib on the absorber plate is an effective technique to enhance the rate of heat transfer as compared to the smooth solar air heaters.
2. The Nusselt no. (Nu) and friction factor (f_r) are strongly dependent on the relative roughness pitch (P/e) and relative roughness height (e/D_h) of diamond shaped rib together with the flow Reynolds number.
3. It has been found that Nu increases with the increase in Re.
4. Maximum value of Nusselt no. (Nu) has been found to be 84.72 at a Reynolds no. (Re) of 14012.
5. It has been found that friction factor (f_r) decreases with the increase in Reynolds no. (Re)
6. Maximum value of friction factor (f_r) has been found to be 0.0194 at a Reynolds no. (Re) is 3010.

REFERENCES

[1] Kline SJ, McClintock FA. Describing uncertainties in single sample experiments. *MechEngg.* 1953; *75*:3–8

[2] Dipprey DF, Sabersky RH. Heat and momentum transfer in smooth and rough tubes at various Prandtl numbers. *Int J Heat Mass Transfer* 1963*; 6*:329–53.

[3] ASHARE standard 93–97. Method of testing to determine the thermal performance of solar collector; 1977

[4] J.C. Han, L.R. Glickman, W.M. Rohsenow, An investigation of heat transfer and friction for rib roughened surfaces, *International Journal of Heat and Mass Transfer*1978 *21 (8)* 1143–1156.

[5] Prasad BN, Saini JS. Effect of artificial roughness on heat transfer and friction factor in a solar air heater.*Solar Energy* 1988; *41*:555–560.

[6] J.C. Han, Heat transfer and friction characteristics in rectangular channels with rib tabulators, ASME Transactions, *Journal of Heat Transfer 110 (2)* (1988) 321–328.

[7] J.C. Han, Y.M. Zhang, C.P. Lee, Augmented heat transfer in square channels with parallel, crossed, and V-shaped angled ribs, ASME Transactions, *Journal of Heat Transfer113 (3)* (1991) 590–596

[8] S.C. Lau, R.T. Kukreja, R.D. McMillin, Effects of V-shaped rib arrays on turbulent heat transfer and friction of fully developed flow in a square channel, *International Journal of Heat and Mass Transfer34 (7)* (1991) 1605–1616.

[9] S.C. Lau, R.D. McMillin, J.C. Han, Turbulent heat transfer and friction in a square channel with discrete rib turbulators, ASME Journal of Turbomachinery*113* (1991) 360–366

[10] Nikuradse J. Law of flow in rough pipes. National Advisory Committee for aeronautics Technical Memorandum 1292; 1950.

[11] J.C. Han, Y.M. Zhang, High performance heat transfer ducts with parallel broken and V-shaped broken ribs, *International Journal of Heat and Mass Transfer 35 (2)* (1992) 513–523.

[12] Gupta D, Solanki SC, Saini JS. Heat and fluid flow in rectangular solar air heater ducts having transverse rib roughness on absorber plates. *Solar Energy* 1993; *51*:31–37.

[13] M.E. Taslin, T. Li, D.M. Kercher, Experimental heat transfer and friction in channels roughened with angled, V-shaped and discrete ribs on two opposite walls, *ASME Journal of Turbo machinery118* (1996) 20–28.

[14] Saini RP, Saini JS. Heat transfer and friction factor correlations for artificially roughened ducts with expanded metal mesh as roughness element, *Int. J Heat Mass Transfer* 1997; 40:973–86.

[15] Muluwork KB, Saini JS, Solanki SC. Studies on discrete rib roughened solar air heaters. In: Proceedings of National Solar Energy Convention, Roorkee, 1998, 75–84.

[16] R. Karwa, S.C. Solanki, J.S. Saini, Heat transfer coefficient and friction factor correlations for the transitional flow regime in rib-roughened rectangular ducts, *International Journal of Heat and Mass Transfer42 (9)* (1999) 1597–1615.

[17] Verma SK, Prasad BN. Investigation for the optimal thermo hydraulic performance of artificially roughened solar air heaters. *Renewable Energy* 2000; *20*:19–36.

[18] Momin E, Saini JS, Solanki SC. Heat transfer and friction in a solar air heater duct with V-shaped rib roughness on absorber plate. *Int J Heat Mass Transfer* 2002; *45*:3383–96.

[19] Bhagoria JL, Saini JS, Solanki SC. Heat transfer coefficient and friction factor correlations for rectangular solar air heater duct having transverse wedge shaped rib roughness on the absorber plate. *Renewable Energy* 2002;*2*5:341–369.

[20] A.M.E. Momin, J.S. Saini, S.C. Solanki, Heat transfer and friction in solar air heater duct with V-shaped rib roughness on absorber plate, *International Journal of Heat and Mass Transfer45 (16)* (2002) 3383–3396.

[21] Wright LM, Fu WL, Han JC. Thermal performance of angled, V-shaped and W-shaped rib tabulators in rotating rectangular cooling channels (AR: 4:1), *ASME. J Turbo Machinery* 2004; *126(4)*:604–614.

[22] Sahu MM, Bhagoria JL. Augmentation of heat transfer coefficient using 90_ broken transverse ribs on absorber plate of solar air heater. *Renewable Energy* 2005; *30(13)*:2057–73.

[23] Jaurker AR, Saini JS, Gandhi BK. Heat transfer and friction characteristics of rectangular solar air heater duct using rib-grooved artificial roughness. *Solar Energy* 2006;*80(8)*:895–907.

[24] Layek A, Saini JS, Solanki SC. Heat transfer and friction characteristics of artificially roughened ducts with compound turbulators. *Int J Heat Mass Transfer* 2007; *50*:4845–54.

[25] Karmare SV, Tikekar AN. Heat transfer and friction factor correlation for artificially roughened duct with metal grit ribs. *Int J Heat Mass Transfer* 2007; *50*:4342–51.

[26] Aharwal KR, Gandhi BK, Saini JS. Experimental investigation on heat-transfer enhancement due to a gap in an inclined continuous rib arrangement in a rectangular duct of solar air heater.*Renewable Energy* 2008; *33(4)*:585–96.

[27] Varun, Saini RP, Singal SK. Investigation of thermal performance of solar air heater having roughness elements as a combination of inclined and transverse ribs on the absorber plate. *Renewable Energy* 2008; *33(6):*1398–405.

[28] Pawar S.S.,HindoliaD.A,Bhagoria J.L.” Enhancement of heat transfer coefficient using Diamond shaped roughness on the absorber plate of solar air heater “International journal of engineering research and application Vol.-2, Issue -3, March-April 2013; pp-968-974.

American Journal of Engineering Research (AJER)
e-ISSN : 2320-0847 p-ISSN : 2320-0936
Volume-02, Issue-06, pp-69-75
www.ajer.org

Research Paper Open Access

Faults Detection in Power Systems Using Artificial Neural Network

Eisa Bashier M Tayeb
School of Electrical and Nuclear Engineering, College of Engineering
Sudan University of Science &Technology; Khartoum – SUDAN

Abstract:- Electrical power systems suffer from unexpected failures due to various random causes. Unpredicted faults that occur in power systems are required to prevent from propagation to other area in the protective system. The functions of the protective systems are to detect, then classify and finally determine the location of the faulty line of voltage and/or current line magnitudes. Then at last, for isolation of the faulty line the protective relay have to send a signal to the circuit breaker. The ability to learn, generalize and parallel processing, pattern classifiers is powerful applications of NN used as an intelligent means for detection. This paper presents neural network NN architecture for fault detection in a transmission line power system. It aims to implement complete scheme for distance protection that subdivided into different neural networks zones. Single phase to ground, double phase and double phase to ground faults are considered. As a result a protection relaying system for the power transmission line systems can be done using the NNBP architecture.

Keywords:* - *Power *system protection, fault identification, neural network architecture, Transmission lines protection.*

I. INTRODUCTION

The electrical system faults are the greatest threat to the continuity of electricity supply. Faults on electric power systems are an unavoidable problem. Hence, a well-coordinated protection system must be provided to detect and isolate faults rapidly so that the damage and disruption caused to the power system is minimized. The clearing of faults is usually accomplished by devices that can sense the fault and quickly react and disconnect the faulty section. It is therefore an everyday fact of life that different types of faults occur on electrical systems, however infrequently, and at random locations. Faults can be broadly classified into two main areas which have been designated as active and passive [1].

Electrical power systems control centers contain a large number of alarms received as a result of different types of faults. To protect these systems, the faults must be detected and isolated accurately. Majority of short-circuit faults tend to occur on overhead lines [2]. The operators in the control centers have to deal with a large amount of data to get the required information about the faults.

Through the years artificial neural networks [3, 4], have been invented with both biological ideas and control applications in mind, and the theories of the brain and nervous system have used ideas from control system theory [5].

The neural network represents a network with a finite number of layers consisting of solitary elements that are similar to neurons with different types of connection between layers. The number of neurons in the layers is selected to be sufficient for the provision of the required problem solving quality. The number of layers is desired to be minimal in order to decrease the problem solving time [1, 6].

Basically, we can design and train the neural networks for solving particular problems which are difficult to solve by the human beings or the conventional computational algorithms. The computational meaning of the training comes down to the adjustments of certain weights which are the key elements of the ANN. This is one of the key differences of the neural network approach to problem solving than conventional computational algorithms. This adjustment of the weights takes place when the neural network is presented with the input data records and the corresponding target values.

Due to the possibility of training neural networks with off-line data, they are found useful for power system applications. The neural network applications in transmission line protection are mainly concerned with improvements in achieving more effective and efficient fault diagnosis and distance relaying [7 - 9]. NN used for overhead transmission lines [10, 11], as well as in power distribution systems [12, 13].

This paper presents a method for detection and identification of the fault type and its zone in the line. Backpropagation neural network approach is studied and implemented. Voltages and currents signals of the line are observed to perform these three tasks. The detailed coefficients of all phase current signals that are collected only at the sending end of a transmission line are selected as parameters for fault classification [14].

The transmission line models are constructed and simulated to generate information which is then channeled using the software MATLAB (Version 7) and accompanying Power System Block Set (Version 2.1). Besides Neuroshell-2 software used to provides back-propagation neural networks.

II. TRANSMISSION LINE MODEL

Pi model network for AC overhead transmission lines is used to model 110 kV transmission line system connects two cities (namely; EL FAU and GEDAREF). The line length is 145 Km, this line is used to develop and implement the proposed architectures and algorithms for this problem. Fig. 1 shows a single-line diagram of the system used to train and test the neural networks. The system consists of two Substations one in each city at the beginning and the end of the transmission line [15].

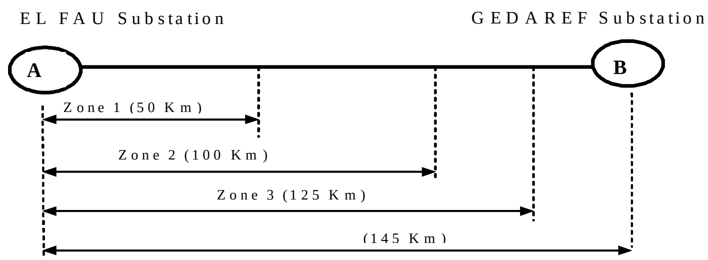

Fig. 1 ELFAU GEDAREF Transmission Line

In Fig. 1 the three-phase voltages and currents, V = $[Va\ Vb\ Vc]^T$ and I = $[Ia\ \ Ib\ Ic]^T$ are measured at substation A. The three simulations categories (phase to ground faults; phase to phase faults and double-phase to ground faults are presented.

III. CONVENTIONAL BACKPROPAGATION ALGORITHM

Recently, multilayer neural networks have been applied successfully to solve lots of difficult and diverse problems through employing various supervised learning procedures among which the error Backpropagation (BP) learning algorithm appears to be the most popular. This algorithm is an iterative gradient based algorithm proposed to minimize an error between the actual output vector of the network and the desired output vector. The term back propagation refers to the manner in which the gradient is computed for nonlinear multilayer neural networks [16]. The output of all hidden layers and the output layer are obtained by propagating the training patterns through the network. Let us define the matrix:

$$O^{\ell} = A^{\ell} W^{\ell} \qquad \ldots\ldots\ldots\ldots (1)$$

The entries of $A^{\ell+1}$ for all layers (ℓ = 1,2..., *L-1*) are evaluated as:

$$a_{p,j}^{\ell+1} = f(O_{p,j}^{\ell}) \qquad \ldots\ldots\ldots\ldots (2)$$

Where; $p = 1,....,P$ and $\mathrm{j} = 1,2,\ldots\ldots \mathrm{n}_{\ell+1}$

An algorithm is required to adjust the weights so that the network learns how to map the input patterns to the output patterns. The most widely used algorithm for training feedforward neural networks is the BP algorithm. Learning is achieved by adjusting the weights such that the network output, A^L is as close as possible or equal to the target, T^L. The error is given as:

$$E = \frac{1}{2P} \sum_{p=1}^{P} \sum_{j=1}^{n_L} (t_{p.j} - a_{p,j}^{L})^2 \qquad \ldots\ldots\ldots (3)$$

So, we need to minimize the error E, with respect to the weight changes $W_{i,j}$. We follow the delta rule to incorporate the learning rate η, along with the gradient descent algorithm techniques to define the weight change. The changes of weights are proportional to the error gradient [17]. Mathematically,

$$\Delta W_{ij}^{\ell} = -\eta . \frac{\partial E}{\partial W_{ij}}; \qquad 0 < \eta \le 1 \quad \text{.........} (4)$$

If the gradient $\frac{\partial E}{\partial W_{i,j}}$ is positive then the weight change should be negative and vice versa. Hence, a minus sign is added at the right hand side of (4).

The weight changes $\Delta W_{i,j}^{L-1}$ for the weights connecting to the final layer are obtained by:

$$\Delta W_{i,j}^{L-1} = -\frac{\eta}{2P} \sum_{p=1}^{P} \sum_{j=1}^{n_L} \frac{\partial}{\partial W_{i,j}^{L-1}} (t_{p.j} - a_{p,j}^{L})^2 \qquad \ldots (5)$$

Notice that for a given *j*, only $a_{p,j}^{L}$ has a relation with $W_{i,j}^{L-1}$, we get:

$$\Delta W_{i,j}^{L-1} = \frac{\eta}{P} \sum_{p=1}^{P} (t_{p.j} - a_{p,j}^{L}) \frac{\partial a_{p,j}^{L}}{\partial W_{i,j}^{L-1}} \qquad \ldots\ldots (6)$$

The partial derivative $\frac{\partial a_{p,j}^{L}}{\partial W_{i,j}^{L-1}}$ can be evaluated using the chain rule. From equations (5) and (6)

$$\Delta W_{i,j}^{L-1} = \frac{\eta}{P} \sum_{p=1}^{P} (t_{p.j} - a_{p,j}^{L}) f'(o_{p,j}^{L-1}) a_{p,i}^{L-1} = \frac{\eta}{P} \sum_{p=1}^{P} \delta_{p,j}^{L-1} a_{p,i}^{L-1} \qquad \ldots\ldots. (7)$$

Where; $\delta_{p,j}^{L-1} = (t_{p.j} - a_{p,j}^{L}) f'(o_{p,j}^{L-1})$ and $f'(o_{p,j}^{L-1}) = \frac{\partial a_{p,j}^{L}}{\partial o_{i,j}^{L-1}}$

By analogy the weights change for other lower layers of weights are:

$$\Delta W_{i,j}^{\ell} = \frac{\eta}{P} \sum_{p=1}^{P} \delta_{p,j}^{\ell} a_{p,i}^{\ell} \qquad \ell = 1, \ldots, L-1$$

and

$$\delta_{p,j}^{\ell} = \sum_{k=1}^{n_{\ell+1}} \left[\delta_{p,k}^{\ell+1} w_{j,k}^{\ell+1} \right] f'(o_{p,j}^{\ell}) \quad \ell = 1, \ldots, L-1$$

The learning procedure therefore consists of the network starting with a random set of weight values, choosing one of the training patterns and evaluating the output(s) using that pattern as input in a feedforward manner. Using the BP procedure, all the weight changes for that pattern are evaluated. This procedure is repeated for all the patterns in the training set so that for all the weights ($\Delta w_{i,j}$) are obtained. Then corrections to the weights are made.

It has been proven that BP learning with sufficient hidden layers can approximate any nonlinear function to arbitrary accuracy. This makes BPNN learning neural network a good candidate for signal prediction and system modeling.

IV. DESIGN OF ANN FOR TRANSMISSION LINE

Artificial neural network (ANN) is an interconnected group of artificial neurons that uses a mathematical model or computational model for information processing based on a connectionist approach to the computation [1].

Transfer function in the ANN is an important key element to invoke the nonlinear relationships that maps the input(s) to the output(s). In the process of learning the neural network presented with pairs of input and output data then teached how to produce the output when the corresponding input is presented. Through iterative training procedure the network's weights are adjusted by the error signal in a way that the network output tries to follow the desired output as close as possible. The learning procedure continues until the error signal is close to zero or below a predefined value. The sum of errors over all the training samples can be considered as a kind of network performance measure, which is a function of free parameters of the

system. Such function can be visualized a multidimensional error surface where network free parameters serves as coordinates. During the course of learning the system gradually moves to a minimum point along an error surface. The error surface is determined by the network architecture and the cost function [17, 4].
Data generated from the transmission line system are collected, trained and tested. The detection of a fault situation in the system is the first step. Following that is the investigation of the fault class and finally location of the faulty zone to be isolated.

4.1 NEURAL NETWORK DESIGN FOR FAULT DETECTION

Extensive simulations of the output error at the network output have been made using data of table (1). Fig 2 shows three layers BPNN used for fault detection. NN were tried with different neurons in each layer. Fig 3 shows the output errors obtained for NNs with 6-2-1, 6-3-1 and 6-4-1 neurons in each layer. As a result of these errors; it was decided to select the network which has an input layer with 6 neurons and one hidden layer with three hidden neurons beside an output layer with one neuron. The activation function at input layer is linear (-1, 1) function while at hidden layer and output layer is logistic function [15].

TABLE 1 PER UNIT VOLTAGE AND CURRENT TRAINING SET

Case NO.	Input Vector (P.U)						Fault Type
	Va	Vb	Vc	Ia	Ib	Ic	
1	.997	.9991	.9985	.9978	.9988	.9984	No fault
2	0.334	1.194	1.172	3.335	0.981	0.979	A to Grd
3	1.172	0.334	1.194	0.981	3.335	0.979	B to Grd
4	1.194	1.172	0.334	0.981	0.979	3.335	C to Grd
5	0.471	0.650	.986	5.379	5.379	0.983	A to B
6	0.986	0.471	0.650	0.984	5.379	5.379	B to C
7	0.471	.986	0.650	5.379	0.984	5.379	A to C
8	0.205	0.205	1.188	7.187	7.855	0.985	A to B to Grd
9	1.188	0.205	0.205	0.985	7.187	7.855	B to C to Grd
10	0.205	1.188	0.205	7.187	0.985	7.855	A to C to Grd

The selected network is then tested with a new set of data which was not used before created to analyze its performance. The performance of network for input/output is shown in fig.4.

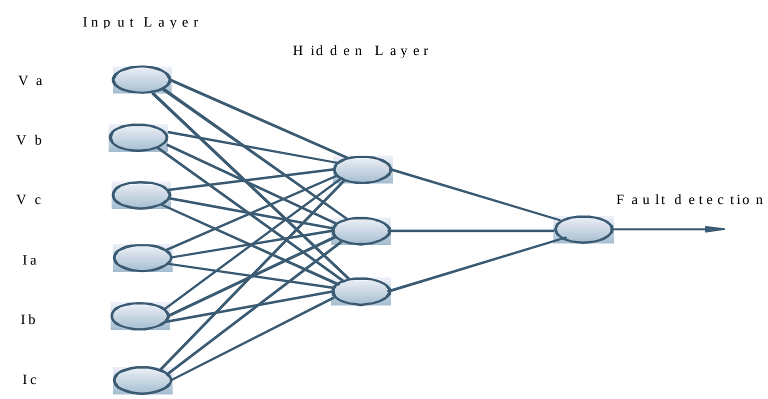

Fig.2. BPNN for Fault Detection

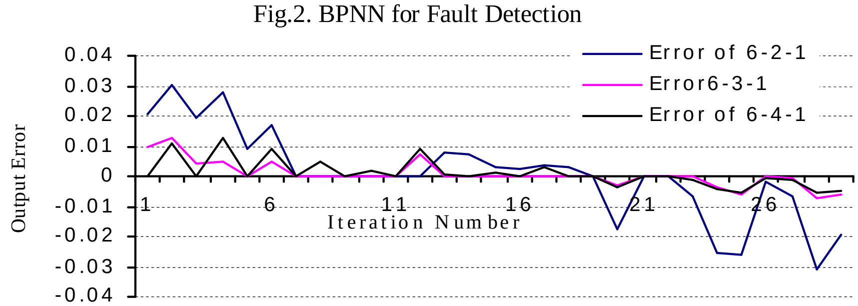

Fig.3. Output error for the BPNN with 6-2-1; 6-3-1and 6-4-1 neurons

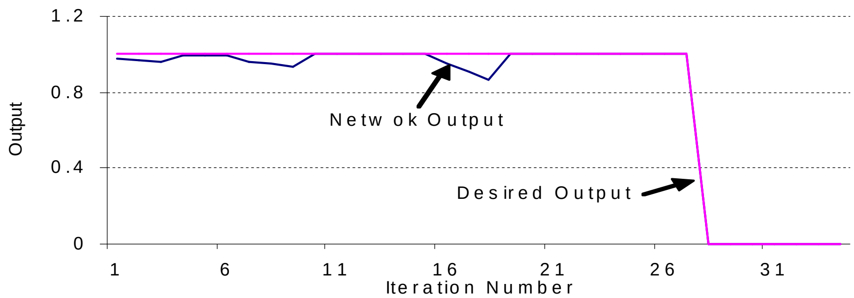

Fig.4. Testing Samples Network output versus desired output for the BPNN 6-3-1

4.2 NEURAL NETWORK DESIGN FOR FAULT CLASSIFICATION

There are three phases (A, B, C) and neutral or ground G or Grd. their combinations are subjected to faults. The data required to differentiate between these types of faults are the three phase voltages and currents. This data generates four output statuses associated with the four fault categories. The outputs contain variables whose values are given as either 0 or 1 corresponding to the existence of that class of fault.

The proposed NN should classify if the specific phases involved in the fault scenario or not. The combinations generate nine different categories of faults as illustrated in Table 2. This designed NN should be able to distinguish between them.

TABLE 2 BPNN CLASSIFICATION NETWORK TRUTH TABLE

Fault Situation	A	B	C	G
A-G	1	0	0	1
B-G	0	1	0	1
C-G	0	0	1	1
A-B	1	1	0	0
B-A	0	1	1	0
C-A	1	0	1	0
A-B-G	1	1	0	1
B-C-G	0	1	1	1
C-A-G	1	0	1	1

A large number of three layers networks were extensively simulated and studied. The input and output layers has fixed six (three phase voltages and currents) and four neurons, respectively. The hidden layer is tried with different neurons numbers. The most suitable network size for the classification task was found to be hidden layer with five hidden neurons as shown in Fig.5. The activation function at input layer is linear (-1, 1) function while at hidden layer and output layer is logistic function. Error plot of the testing set is shown in fig.6. The selected network was able to recognize correctly the type of the fault category.

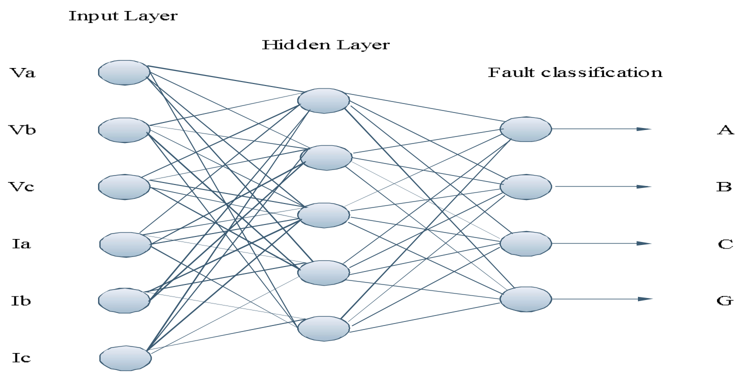

Fig.5 Back Propagation NN for Fault Classification

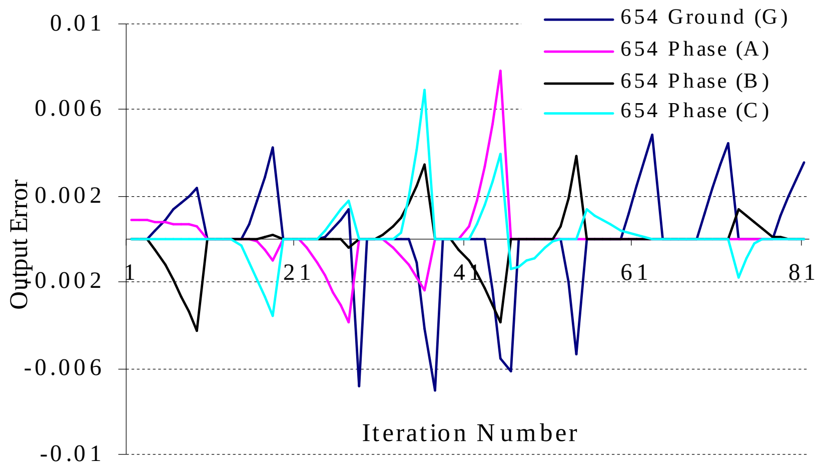

Fig.6 Testing samples output error BPNN 6-5-4

4.3 NEURAL NETWORK DESIGN FOR FAULT LOCATION

Detection of fault location has to be done for the purpose of isolating the faulty section of the system. The network is expected to identify the location of the fault by classifying the identified fault into one of the three fault zones, namely Zone 1, 2 and 3. The proposed neural networks here should isolate the specific zone involved in the fault network as shown in the network training Table 3.

TABLE 3 ISOLATION NN TRAINING SET

Fault	**Networks Output**		
Location	**Z1**	**Z2**	**Z3**
Zone 1	1	0	0
Zone 2	0	1	0
Zone 3	0	0	1

A large number of BPNN with different structures were studied and analyzed. This time network which has two hidden layers is tried. The training includes some of the selected networks structures (6-5-5-3, 6-6-6-3, 6-7-6-3 and 6-5-4-3). It is found that through trial and error that a BP network with two hidden layers provides the best training performance. The first hidden layer has 5 neurons and the second hidden layer has 4 neurons. Again the activation function at input layer is linear (-1, 1) function while at hidden layer and output layer is logistic function. This network is illustrated in Fig.7.

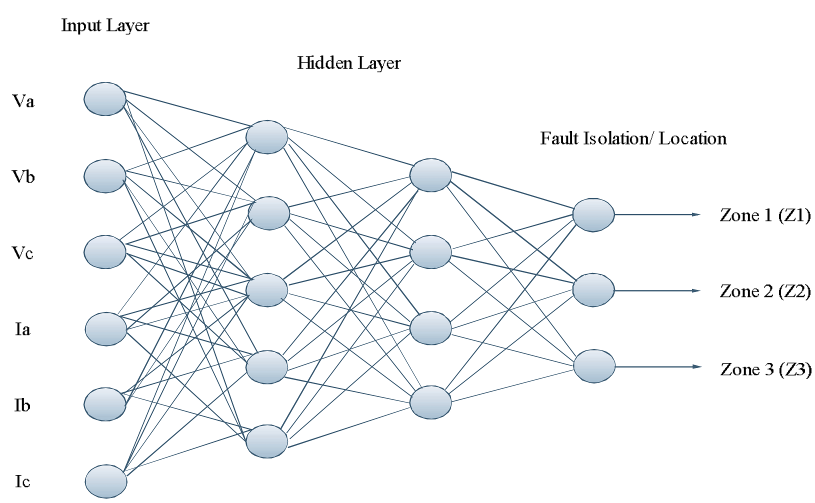

Fig.7 Back Propagation NN chosen for fault isolation

A new set of test data samples was created to analyze the performance of the proposed network. A fault cases for each location of fault were utilized in the test set. Output error plot of the testing set is shown in fig 8. The selected network from the previous section was able to recognize correctly the location of the fault.

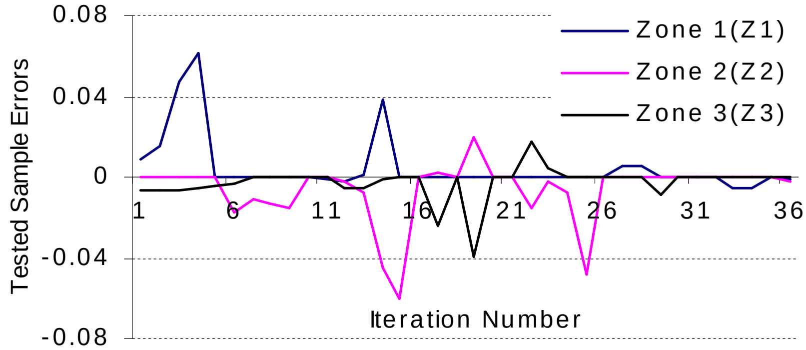

Fig. 8 Testing samples output error for the BPNN 6-5-4-3

V. CONCLUSION

This paper fault detection, classification and location in a transmission line system have been investigated using neural network backpropagation (BP) algorithm. MATLAB-7, Power System Block Set-2.1and Neuroshell-2 software were used for simulation of the transmission line models. Data generated is used for single phase to ground faults, double phase faults and double phase to ground faults. The multi-layer neural networks were trained with the generated data. When real values are then used as an input to trained NN; fast evaluation of errors obtained. The results obtained for transmission line fault detection, classification and locations finding all were highly satisfactory using BPNN architecture.

REFERENCES

[1] Laurene V. Fausett, *Fundamentals of Neural Networks: Architectures, Algorithms, and Applications* Prentice Hall, 1993.
[2] Nasser D. Tleis, *Power Systems Modeling and Fault Analysis Theory and Practice* Elsevier Ltd, 2008.
[3] H. Bourlard and C. Wellekens. *Speech pattern discrimination and multilayer perceptrons* Computer Speech and Language ,3:1-19, 1989.
[4] N. Morgan and H. Bourlard. Continuous speech recognition using multilayer perceptrons and Hidden Markov Models. *In Proceedings of the ICASSP,* pages 413-416, Albuquerque, New Mexico, April 1990.
[5] Omid M. Omidvar, David L. Elliott *Neural systems for Control* Elsevier Science & Technology Books 1997.
[6] Hagan MT, Demuth HB, Beale MH, *'Neural network design* PWS Publishing, 1996.
[7] Kevin Gurney, *An Introduction to Neural Networks* UCL Press, 1997.
[8] Upendar, J., Gupta, C.P., Singh, G.K., Ramakrishna, G., PSO and ANN-based fault classification for protective relaying. Iet Generation Transmission & Distribution 4, (2010) 1197-1212.
[9] Tsuji, K. Protection Relaying Scheme Based on Fault Reactance Operation Type. *Electrical Engineering in Japan* 168, (2009) 29-40.
[10] Eisa, A.A.A., Ramar, K. Accurate one-end fault location for overhead transmission lines in interconnected power systems. *International Journal of Electrical Power & Energy Systems* 32, (2010) 383-389.
[11] Nahman, J.M., Salamon, D.D. Ieee Safety Analysis at overhead Line Towers in Close Proximity to the Substation. *Transactions on Power Delivery* 25, (2010) 1508-1515.
[12] Peretto, L., Sasdelli, R., Scala, E., Tinarelli, R. Performance Characterization of a Measurement System for Locating Transient Voltage Sources in Power Distribution Networks. *IEEE Transactions on Instrumentation and Measurement* 58, (2009) 450-456.
[13] Salim, R.H., Resener, M., Filomena, A.D., de Oliveira, K.R.C., Bretas, A.S. Extended Fault-Location Formulation for Power Distribution Systems. *IEEE Transactions on Power Delivery* 24, (2009) 508-516.
[14] Upendar, J., Gupta, C.P., Singh, G.K. Fault Classification Schemes Based on the Adaptive Resonance Theory Neural Network for protection of Transmission Lines. *Electric Power Components and Systems* 38, (2010) 424-444.
[15] O A A Elmubark, *"Fault Detection, Classification and Location in Power Transmission Line System Using Artificial Neural Network," M.Sc. dissertation, Dept. Electrical Engineering, Sudan Univ. of Science & Technology-Khartoum, March 2011.*
[16] R. Kamyab Moghadas and S. Gholizadeh "A New Wavelet Back Propagation Neural Networks for Structural Dynamic Analysis" *IAENG, Engineering Letters,* February 2008.
[17] TommyW S Chow and Siu-Yeung Cho "Neural Networks and Computing" Imperial College Press 2007.

American Journal of Engineering Research (AJER)
e-ISSN : 2320-0847 p-ISSN : 2320-0936
Volume-02, Issue-06, pp-76-78
www.ajer.org

Research Paper Open Access

The Solve of Laplace Equation with Nonlocal and Derivative Boundary Conditions by Using Non Polynomial Spline

Abas Taherpour[1], Azadeh Hosseinpour[2]
Lila Abasabadi[3], Arezoo Hosseinpour[4]
[1]Department of Mathematics, Kermanshah Branch, Islamic Azad University, Kermanshah, Iran
[2]Department of Mathematics, Science and Research Branch, Islamic Azad University, Kermanshah, Iran
[3]Young Researchers Club, Kermanshah Branch, Islamic Azad University, Kermanshah, Iran
[4]Department of Mathematics, Science and Research Branch, Islamic Azad University, Kermanshah, Iran

Abstract: - In this paper we consider a non polynomial spline function where it to depend on parameter τ, such that it interpolated *u(x)* in points of grid. By using this function we solve the Laplace equation with nonlocal and derivative boundary conditions. The method is applied in this paper is a implicit method. We know superiority of implicit methods is stability of them, because most of them are unconditionally stable.

Key Words: - *Non polynomial function, Cubic spline, Laplace equation, Implicit method, Nonlocal and derivative boundary conditions.*

I. INTRODUCTION

The Laplace equation is a elliptic equation that occur in many branches of applied mathematics. In this paper we consider the Laplace equation $\frac{\partial^2 u}{\partial_{x^2}} + \frac{\partial^2 u}{\partial_{y^2}} = 0$ with the following initial-boundary conditions

$$u_x(1,y) = g(y) \qquad 0 < y < Y \qquad (1)$$

$$\int_0^1 u(x,y)dx = m(y) \qquad 0 < y < Y \qquad (2)$$

$$u(x,0) = f(x) \qquad 0 < y < Y \qquad (3)$$

Where $f(x), g(y)$ and $m(y)$ are known, while the function $u(x,y)$ is to be determined, the boundary value problem arises in a large variety of applications in engineering, physics and other science. Study in this filed is very important. You can see some methods for solve of these problems [3, 4, 5]. In many problems boundary conditions are as integral equations. These problems are a kind of nonlocal problems and have important applications in other branches of pure and applied science [6, 7, 8, 9]. In this paper we want to solve a type of nonlocal problem by using a non polynomial spline function. Rashidinia and Jalilian used a non polynomial spline function to smooth the approximate solution of the second order boundary value problems [2]. In addition they used quintic non polynomial spline functions to develop numerical methods for approximation to the solution of a system of fourth order boundary value problems associated with obstacle, unilateral and contact problems [1].

II. THE PRESENTATION NON POLYNOMIAL SPLINE FUNCTIONS

Note that grid points P are given by $x_i,\ i = 0,1,\dots,n\ as\ follows$

$$P = \{a = x_0 < x_1 < \cdots < x_n = b\}$$

Where $x_i = a + ih,\ i = 0,1,\dots,n\ and\ h = (b-a)/n.$

Consider non polynomial function $Sp(x) \in C^2[a,b]$ such that depend on parameter τ and interpolate $u(x)$ in grid points. When $\tau \to 0$ this function is converted to ordinary cubic spline in [a,b].

For all subinterval $[x_i, x_{i+1}],\ i = 0,1,\dots,n-1$ non polynomial function $Sp(x)$ is defined as follow

$$Sp(x) = a_i + b_i(x - x_i) + c_i \sin\tau(x - x_i) + d_i \cos\tau(x - x_i) \qquad i = 0,1,\dots,n-1 \qquad (4)$$

Where a_i, b_i, c_i and d_i are constant numbers, and τ is a ordinary parameter. u_i is considered as a approximation $u(x_i)$ where is got by spline function that pass through points (x_i, u_i) and (x_{i+1}, u_{i+1}).
Now we obtain necessary conditions to presentation coefficients in E.q. (4). First must function $Sp(x)$ satisfies in interpolation conditions in points x_i and x_{i+1}, namely $Sp(x_i) = u_i$ and $Sp(x_{i+1}) = u_{i+1}$. We know that the first derivative of function Sp is continued in common points x_i and x_{i+1} with M_i and M_{i+1} respectively. Namely $S"p(x_i) = M_i$ and $S"p(x_{i+1}) = M_{i+1}$. It follows from E.q. (4) that

$$a_i = u_i + \frac{M_i}{\tau^2} \qquad d_i = -\frac{M_i}{\tau^2} \tag{5}$$

Since $s(x_{i+1}) = u_{i+1}$ and $s"(x_{i+1}) = M_{i+1}$ we obtain

$$b_i = \frac{u_{i+1} - u_i}{h} + \frac{M_{i+1} - M_i}{\tau\theta} \qquad c_i = \frac{M_i \cos\theta - M_{i+1}}{\tau^2 \sin\theta}, \quad i = 1,2,..,n-1 \tag{6}$$

where $\theta = \tau h$. Noting that $S'^{p_{i-1}}(x_i)$, hence we have

$$b_{i-1} + \tau c_{i-1} \cos\tau (x - x_{i-1}) - \tau d_{i-1} \sin\tau (x - x_{i-1}) = b_i \tau c_i \cos\tau (x - x_i) - \tau d_i \sin\tau (x - x_i)$$
(7)

substituting E.q.s (5) and (6) into E.q. (7) by simplifying implies that

$$\frac{1}{\theta^2}[\theta \csc\theta - 1]M_{i+1} + \frac{2}{\theta^2}[1 - \theta \cot\theta]M_i + \frac{1}{\theta^2}[\theta \csc\theta - 1]M_{i-1} = \frac{1}{h^2}[u_{i+1} - 2u_i + u_{i-1}]$$

Finally, by letting $\alpha = \frac{1}{\theta^2}(\theta \csc\theta - 1)$ and $\beta = \frac{1}{\theta^2}(1 - \theta \cot\theta)$ we obtain

$$\alpha M_{i+1} + 2\beta M_i + \alpha M_{i-1} = \frac{1}{h^2}(u_{i+1} - 2u_i + u_{i-1}) \tag{8}$$

if $\tau \to 0$ then $\theta \to 0$, therefore

$$\alpha = \lim_{\theta \to 0} \frac{\theta \csc\theta - 1}{\theta^2} = \frac{1}{6} \qquad \beta = \lim_{\theta \to 0} \frac{1 - \theta \coth\theta}{\theta^2} = \frac{1}{3}$$

Thus $(\alpha, \beta) \to (\frac{1}{6}, \frac{1}{3})$, and (8) changed into ordinary cubic spline

$$\frac{h^2}{6}(M_{i+1} + 4M_i + M_{i-1}) = u_{i+1} - 2u_i + u_{i-1}$$

III. FINIT DIFFERENCE SCHEME FOR LAPLACE EQUATION

Cover the domain $[0,1] \times [0,\infty]$ by $\Omega_h \times \Omega_k$, where $\Omega_h = \{x_i | x_i = ih, i = 0,1, \dots N\}$ and $\Omega_k = \{y_i | y_i = jh,\ j = 0,1,2, \dots\}$. In which N is a positive integer and h is step size in space.
The notations u_i^j and M_i^j are used for the finite difference approximations of $u(x_i, y_j)$ and $s"(x_i, y_j)$, respectively. We approximate the derivative u_{yy} in Laplace equation by

$$(u_{yy})_i^j = \frac{u_i^{j+1} - 2u_i^j + u_i^{j-1}}{h^2}$$

And the derivative of space u_{xx} by non polynomial cubic spline function. Therefore the finite difference scheme for Laplace equation is as follows:

$$\frac{1}{h^2}(u_i^{j+1} - 2u_i^j + u_i^{j-1}) = M_i^j \tag{9}$$

from (8) and (9) we have

$$\alpha u_{i+1}^{j+1} + 2\beta u_i^{j+1} + \alpha u_{i-1}^{j+1} = (2\alpha - r^2)u_{i+1}^j + (4\beta + 2r^2)u_i^j + (2\alpha - r^2)u_{i-1}^j$$
$$-[\alpha u_{i+1}^{j-1} + 2\beta u_i^{j-1} + \alpha u_{i-1}^{j-1}] \tag{10}$$

and $r = k/h$. previously parameters α and β are defined.
Differentiating E.q. (2) with respect to y and then using Laplace equation, we have condition:

$$u_x(0, y) = g(y) + m"(y) \qquad 0 < y < Y \tag{11}$$

We approximate u_x at $x=0$ and $x=N$ by a central difference formula. Then the boundary conditions can be represented by

$$\frac{u_1^j - u_{-1}^j}{2h} = u_0^j \qquad \frac{u_{N+1}^j - u_{N-1}^j}{2h} = u_N^j$$

u_{-1}^j and u_{N+1}^j are unknown that they obtain by boundary conditions E.q. (1) and (11). By using these equations, linear system of equations is as follows

$$\begin{pmatrix} 2\beta - 2\alpha h & 2\alpha & & & \\ \alpha & 2\beta & \alpha & & \\ & \ddots & \ddots & \ddots & \\ & & \alpha & 2\beta & \alpha \\ & & & 2\alpha & 2\beta + 2\alpha h \end{pmatrix} \begin{pmatrix} u_0^{j+1} \\ u_1^{j+1} \\ \vdots \\ u_{N-1}^{j+1} \\ u_N^{j+1} \end{pmatrix} =$$

$$\begin{pmatrix} a & 2(2\alpha - r^2) & & & \\ 2\alpha - r^2 & 4\beta + 2r^2 & 2\alpha - r^2 & & \\ & \ddots & \ddots & \ddots & \\ & & 2\alpha - r^2 & 4\beta + 2r^2 & 2\alpha - r^2 \\ & & & 2(2\alpha - r^2) & b \end{pmatrix} \begin{pmatrix} u_0^j \\ u_1^j \\ \vdots \\ u_{N-1}^j \\ u_N^j \end{pmatrix} -$$

$$\begin{pmatrix} 2\beta - 2\alpha h & 2\alpha & & & \\ \alpha & 2\beta & \alpha & & \\ & \ddots & \ddots & \ddots & \\ & & \alpha & 2\beta & \alpha \\ & & & 2\alpha & 2\beta + 2\alpha h \end{pmatrix} \begin{pmatrix} u_0^{j-1} \\ u_1^{j-1} \\ \vdots \\ u_{N-1}^{j-1} \\ u_N^{j-1} \end{pmatrix}$$

where $a = (4\beta + 2r^2) - 2(2\alpha - r^2)h$, $b = (4\beta + 2r^2) + 2(2\alpha - r^2)h$, giving

$$AU^{j+1} = BU^j + CU^{j-1} \tag{12}$$

where A, B and C are as displayed, U^{j+1} is a vector of unknown values and U^{j} and U^{j-1} are vector of known values. The finite difference approximation of a Laplace equation needs three space-levels. For solve the first set of equation for $u_{i,2}$ it is necessary to calculate a solution along the first space-level by some other method, it being assumed that the initial data along $y=0$ are known.
We get different methods for solve Laplace equation by suitable choosing parameters α and β. With condition $0 \le \alpha \le \beta$ the matrix A is a diagonally dominate matrix. Therefore from E.q. (12) we get

$$U^{j+1} = A^{-1}BU^{j} + A^{-1}CU^{j-1}$$

Error, stability and compatibility conditions are presented in the next section.

IV. STABILITY AND COMPATIBILITY OF METHOD AND ERROR

We let the solution of E.q. (10) in point (x_i, y_j) is as follows

$$u_i^j = \xi^j e^{i\sqrt{-1}\theta} \qquad (13)$$

θ is real and ξ is complex. By using (10) and (13) we get

$$2(\alpha\cos\theta + \beta)\xi^2 - 2[(2\alpha - r^2)\cos\theta + (2\beta + r^2)]\xi + 2[\alpha\cos\theta + \beta] = 0$$

by putting $A = 2(\alpha\cos\theta + \beta)$ and $B = 2[(2\alpha - r^2)\cos\theta + (2\beta + r^2)]$ we obtain

$$A\xi^2 - B\xi + A = 0 \qquad (14)$$

we assume that the roots of E.q. (14) are ξ_1 and ξ_2 , therefore $\xi_1.\xi_2 = 1$. We have two states:

1) $|\xi_1| \ne |\xi_2| \ne 1$ thus $|\xi_1| = 1/|\xi_2|$ so $|\xi_1| < 1$, $|\xi_1| > 1$ (or $|\xi_1| > 1$, $|\xi_2| < 1$) therefore in this case our scheme is not stable.

2) $|\xi_1| = |\xi_2| = 1$, in this case $\cos\theta = 0$ so $\theta = 0, 2\pi, \ldots$. We know $\theta = 0$ is not acceptable, hence we admit $\theta = 2\pi$.

For study of error and compatibility, we let $D_x = \frac{\partial}{\partial_x}$ and $D_y = \frac{\partial}{\partial_y}$. Then by Taylors expansion of terms in E.q. (10) we obtain

$$2(\alpha+\beta)k^2D_y^2 + \frac{1}{3!}(\alpha+\beta)k^4D_y^4 + \frac{1}{180}2(\alpha+\beta-1)k^6D_y^6 + \alpha h^2k^2D_x^2D_t^2 + r^2h^2D_x^2 + \frac{1}{4!}(2r^2 - 4\alpha)h^4D_x^4 + \ldots$$

Thus by suitable choosing of parameters α and β we obtain different error. In addition our difference scheme is compatible for Laplace equation.

V. CONCLUSIONS

Our purpose in this article is solving partial differential equation. We presented an explicit method for solving this equation, and we considered necessary conditions for stability of this method.

VI. ACKNOWLEDGEMENTS

The authors wish to thank from the Islamic Azad University for supporting projects. This research was supported by Islamic Azad University, Kermanshah Branch, Kermanshah, Iran.

REFERENCES

[1] J. Rashidinia and R. Jalilian, Non polynomial spline of fourth order obstacle boundary value problems, Word Academy of Science, Engineering and Technology. 52 (200) 200-206.
[2] J. Rashidinia and R. Jalilian, Spline solution of two point boundary value problems, Appl. Comput. Math. 9 (2010) 258-266.
[3] W.A. Day, Extension of a property of the heat equation to linear thermo elasticity and other theories, Quart. Appl. Math. 40 (1982) 319-330.
[4] W.A. Day, A decreasing property of solutions of parabolic equations with applications to thermo elasticity, Quart. Appl. Math. 41 (1983) 468-475.
[5] Y. Lin, An inverse problem for a class of quasilinear parabolic equations, SIAM J. Math. Anal. 22 (1991) 146-156.
[6] N.I. Yurchuk, Mixed problem with an integral condition for certain parabolic equation, Differential Equations. 22 (1986) 2117-2126.
[7] Y.Liu, Numerical solution of the heat equation with nonlocal boundary conditions, J. Comp. Appl. Math. 110 (1999) 115-127.
[8] Zhi Zhong Sun, A high order difference scheme for a nonlocal boundary value problem for the heat equation, J. Comp. Meth. Appl. 1 (2001) 398-414.
[9] M. Akram and M. A. Pasha, A numerical for the heat equation with nonlocal boundary condition, Int J. Inf. Sys. Sci. 1 (2005) 162-171.

American Journal of Engineering Research (AJER)
e-ISSN : 2320-0847 p-ISSN : 2320-0936
Volume-02, Issue-06, pp-79-93
www.ajer.org
Research Paper Open Access

Use Of Dynamic Resistance And Dynamic Energy To Compare Two Resistance Spot Welding Equipments For Automotive Industry In Zinc Coated And Uncoated Sheets.

Márcio Batista[1], Sérgio Duarte Brandi[1].
[1]Escola Politécnica, University of São Paulo, Dept. of Metallurgy and Materials - São Paulo, SP - Brasil.

***Abstract:* -** Resistance spot welding is a fabrication process highly used in the structures assembly. This fact evidences the importance of this welding process control, due to its efficiency, productivity speediness and straightforward simple automation. This work aimed to study the weldability of zinc coated and uncoated steel sheets for automotive industry, comparing the performance of two welding equipments with two current output kinds: alternating current (AC) and medium frequency direct current (DC). The welding parameters were kept constant: 260 kgf (force), 150 ms (time) and 7.0 kA (welding current), based upon an optimization parameters methodology. The joints were characterized using optical metallography (spot diameter, indentation depth and weld penetration depth), mechanical tensile-shear tests and electrical measurements: contact electrical resistance, dynamic resistance and dynamic energy. The results showed that welding in medium frequency direct current was more efficient in generating heat in zinc coated sheets and uncoated sheets than alternating current equipment. In welding using AC and DC equipments in zinc coated sheets, the spot weld time formation was 25ms longer than uncoated steel sheets spot weld time. The burn of zinc during welding did not damage the spot weld formation with AC or DC equipments. The electrical contact resistance increased with the roughness and also presented 52% higher in uncoated sheets than in zinc coated sheets. Finally, the increase in dynamic resistance and dynamic energy augmented the spot weld diameter for both welding equipments. As a final conclusion, the medium frequency direct current equipment presented better results than wave alternating current.

***Key-words:* -** resistance spot welding; zinc coated steel sheet; uncoated steel sheet; dynamic contact resistance; automotive industry.

I. INTRODUCTION

The resistance spot welding is widely used in the modern vehicles auto-body assembling process. Each spot weld presents different conditions due to misalignment of the electrodes, gap between the plates and plates surface conditions. The optimum welding parameter condition during welding has to consider the electric current magnitude intensity and duration, the force between the electrodes; the electrodes shape geometry, the electrodes materials and properties, and presence of coating sheets material. Therefore, the resistance spot welding process behavior control is extremely important to all welded structure productivity and quality [1].

Automotive industry must match the desires of customers to deal with global competition, such as resistance to chassis corrosion, high resistance welded joints when exposed to mechanical stresses, impact absorption ability, low cost and comfort.

1.1. Resistance Spot Welding Process

The joining of two pieces using the electrical resistance spot welding is done by heat generation due to the passage of electrical current and by applying pressure. During the process, the pieces are heated and fusion occurs at the contact point located on the faying surface [2].

Through the movement of electric current between the electrodes in contact with the parts, enough heat is generated (by Joule effect) in the contact resistance between the surfaces to start the sheet metals fusion [3]. As the electrodes apply force between the parts, the merging surrounding solid metal is under pressure,

preventing liquid metal expulsion by through contact faying surface. This produces a joint with metallurgical characteristics similar to the forging process. Liquid metal loss avoidance is crucial since the process has no metal addition, and a drop in mechanical resistance may occur. The electrode pressure also controls the contact resistance between the materials. The electrodes are water cooled due to the high temperature achieved during welding at the electrode/sheet faying surface and at the contact surface area with the work piece. The cooling inefficiency causes premature electrodes wear and influences mechanical properties of the spot weld. This electrode cooling also helps the spot weld. After fusion, the electrodes remain exerting a force between pieces to allow the solidification of metal. [4].
The secondary circuit of a spot welding machine and plates to be welded are composed in a series of resistances, as shown, schematically, in Figure 1.
There are at least five resistors connected in series, producing the joint warming. The sum of the resistances is expressed in the formula below [5]:

$$R = R_{eletrode-pieceA} + R_A + R_{Weld} + R_B + R_{eletrode-pieceB} \quad (1)$$

The most important resistance formation required for the spot weld is located at the interface of the plates to be welded (R_{weld}). The magnitude of this contact resistance depends on the roughness surface of the material base metal and on the size, strength, and electrode contact face geometry and pressure applied between the electrodes. This is the most important point for the generation of heat to produce the spot weld. The electrode/sheet faying surface also has a significant contact resistance, which should be kept lower than sheet/sheet faying surface contact resistance to avoid melting at electrode/sheet contact resistance. This is one reason for using copper as an electrode material and also the electrode water cooling system, but the contact surfaces of the electrodes do not reach the melting temperature during the passage of current due to high thermal conductivity of the electrodes and the fact that they are usually cooled by water.
The resistance R in equation (1) is influenced by the welding pressure and the effect of contact resistance of the interface between the pieces. The pieces to be welded must be firmly fixed to enable the passage of current flow. If the force of the electrode increases, it will be necessary to increase the current to compensate the decrease in the contact electrical resistance drop at the sheet/sheet faying surface [5].

1.2. Heat Generation

The heat required in the process of spot welding is produced by electrical contact between the pieces to be welded, as shown in Figure 2. Due to the small value of these resistances (depicted in figure 1) relatively high currents are required to develop the heat necessary for welding [6]. The magnitude of heat generated depends on three factors:
- welding current (Amps); - electrical resistance set (ohms); - current flow time interval (seconds).

The heat generated during the welding process can be calculated by equation (2) [2]:

$$Q = k\int_0^t R(t).I^2.dt \quad (2)$$

Where:
Q = Heat generated [(cal]),
R = equivalent set of electrical resistance, [(ohms)],
t = current flow time (seconds),
I = welding current [Amps],
k = Joule equivalent constant = 1 / 4. 185

1.3. Welding Parameters

Industries often use internal standards to define the spot welding parameters and spot characteristics. The values adopted by these standards depend on the acceptance quality criteria and also the welding electrodes shape. It becomes necessary to define the process parameters to control the amount of heat generated in the transformation of electrical energy into heat in the materials that will be welded. The main process variables are: electrode pressure (force), electric current, welding cycles (time), and equipment electrical output type.

The welding pressure is produced by an external force applied by the electrodes on the joints and affects the value of total contact resistances, in particular the contact resistance at the faying surface. The parts to be welded must be well fixed in the region where the operator will do the weld to ensure the passage of current. An increase in electrode pressure results in a total electrical resistance decrease and, consequently, a

decrease of the generated welding heat, keeping all other parameters constant. Thus, electric current or the number of welding cycles (time) must be increased to compensate the reduction of the electrical resistance [7].
In the beginning of the nugget formation the welding current flows through the micro contacts between the two sheets [4] up to start to melting to build up the nugget. The welding current is the most important welding parameter since it has a greater influence in the nugget size than other parameters. An electrode diameter increase reduces the current density and the heat generated during welding, which can cause significant decrease in the nugget size, decreasing the mechanical strength of the welded spot. Excessive current density causes liquid metal expulsion at the faying surface, that can result in internal voids or cracks in the nugget, which impairs the weld mechanical properties [7].

The welding time (cycles) determines the total heat amount per spot since the other parameters remain constant. The electrical resistance during welding should cause, together with the welding time (number of cycles), an adequate heating in the welded joint to produce a suitable nugget size.

The original electrode geometry for a specific weld changes with the amount of produced welds. To increase electrode life is important to control electrode overheating to avoid geometry damage and, consequently, the nugget size. The geometrical electrode losses are caused mainly by the pressure, number of cycles, welding current, electrode water cooling system, and the presence of zinc sheet coating. . The losses increase with increasing welding time and temperature of the metal [1]. The equipment current output type is important to control the heat generated during welding. Actually, these equipments can produce alternating or medium frequency direct current.

1.4. Contact electric resistance

Contact electric resistance can be explained as the surface roughness micro contacts between conductors which cause electrical current flow [8], as illustrated in figure 2. The electrode pressure applied to establish these micro contacts between the conductors and electrode cross-sectional area defines the value of the contact resistance. There is a correlation between the contact resistance, the pressure in the electrode surface and the condition of the sheet to be welded [9]. Usually, contact resistance between the faying surfaces is the highest one.

1.5. Dynamic electrical resistance

The electrical contact is responsible for Joule effect heating at the faying surface and, consequently, by the formation of the weld nugget during the steel sheet welding. The contact electric resistance at this place changes rapidly during the welding time and, therefore, is dynamic in nature [10]. Figure 3 shows a schematic picture of a dynamic electrical resistance during welding.
Based on figure 3 there are five stages of the electrical dynamic resistance during the formation of a nugget [11]:
Stage I: Surface oxides fragmentation and roughness collapse, producing the micro contacts.
Stage II: Heating concentrated at the sheets faying surfaces. Electrical resistance decreases with increasing contact areas and the resistivity increases with temperature. The competition between these two mechanisms defines the point 'α' in figure 3.
Stage III: Resistivity increases with increasing temperature up to the formation of the first liquid that determines the transition to Stage IV, in the curvature inflection, defining point 'β' in figure 3.
Stage IV: Three mechanisms take place at this stage: (1) temperature of the material continues to rise, increasing its electrical resistivity; (2) fusion at the faying surface increases the cross-sectional area, decreasing the electrical resistance; (3) the sheet material strength decreases with increasing temperature, and mechanical collapse happens in the roughness reducing electrical resistance.
Stage V: Nugget grows and expulsion of liquid metal might happen.

1.6. Heat generation comparison between the types of welding current equipment output

Figure 4 shows a comparison of heat generation between the welding equipment with alternating current (AC) and medium frequency direct current (DC). The greater heat production is observed in the welded joint with the welding equipment in medium frequency direct current. For this reason, the behavior of contact resistance R_{weld} in function of time is different for the two equipments [8].

The difference between welding nugget size produced by these two equipment types is better observed at lower current magnitudes. For current values close to liquid metal expulsion the size of the nugget between DC and AC are quite similar [12].

The DC welding current allows a faster effective heat generated. In other words, a constant increase in the current concentrates more heat in less time in the weld zone than AC welding equipment, allowing lower welding currents, and expands the capability of welding with different steel types and sheet coatings [9].

II. MATERIALS AND METHODS

In this work, two plain steel sheet types were used: uncoated and zinc coated sheets, both of them with a thickness of 0.8 mm. The sheets were overlapped and welded with two different welding equipments, AC and DC medium frequency. Welding parameters were optimized and fixed with 260 kgf of electrodes force, welding time of 150 ms (9 cycles) and welding current of 7 kA. The dimensions of the tensile test specimens used were based on EN ISO 14273 standard, as depicted in Figure 5.

A digital oscilloscope differential probe tip was used to measure the magnitudes of voltage. To acquire the magnitude of current, a coil-type Rogowski flexible, with the integration of the signal of the coil executed in MM315 Miyachi Weld Tester, was utilized. Figure 6 shows the differential probe tip to measure the voltage during welding. These data were processed by a specially developed program to obtain the dynamic resistance and energy during welding.

As an acceptance criterion for this paper, for coated and uncoated sheets of 0.8 mm thick, the minimum nugget diameter was 3.1mm and the minimum force to the tensile test was 230kgf. The nugget size was measured by a macrograph, using optical microscopy. Tensile-shear tests were done in a testing machine under laboratory conditions. The tensile speed was remained constant during test. Analysis of electrical resistance versus contact surface roughness of Zn coated and uncoated sheets were carried out at the roughness measuring instrument (Mitutoyo, USA) under laboratory conditions.

III. RESULTS AND DISCUSSION

3.1 Dynamic resistance and dynamic energy in DC and AC welding in uncoated steel sheets

Figure 7 shows the comparison between the RMS dynamic resistance and RMS dynamic energy of the spot weld made with the same welding parameters, using DC and AC welding equipments and uncoated steel sheets, as a function of time. The red line refers to DC medium frequency equipment and the blue line represents the result of AC equipment.

It can be observed in figure 7(a) that the dynamic resistance at DC was greater than AC dynamic resistance during welding with the same parameters in uncoated sheet. This result is related to the most efficient heat produced in DC due to a higher dynamic resistance and to electrical constructive characteristics of the welding equipments, as shown in figure 4(a).

Regarding the comparison of the values of the AC and DC welding dynamic energies of uncoated sheets, the total dynamic energy during welding in DC was 9% higher compared to the total dynamic energy in AC welding. This result is also related to the difference in dynamic resistance for the two welding conditions.

3.2 Dynamic resistance and dynamic energy in DC and AC welding in zinc coated steel sheets

Figure 8 depicts the comparison between the RMS dynamic resistance and RMS dynamic energy of the spot weld made with the same welding parameters, using DC and AC welding equipments and zinc coated steel sheets, as a function of time. The red line refers to DC equipment and the blue line represents the result of AC equipment.

As a remarkable result the dynamic resistance at DC during welding was greater when compared with the dynamic resistance in CA. Comparing figures 7 and 8, the dynamic resistance of uncoated sheet is higher than zinc coated sheet dynamic resistance. This is due to the difference between electrical resistivity of steel (180 nΩ.m) and zinc (59 nΩ.m), which is approximately 1/3 of the steel resistivity, as can be noted in the result of figures 7(a) and 8(a).

Comparing figures 7(a) and 8(a), the shape of dynamic resistance is also different for uncoated and zinc coated steel sheet. Figure 8(a) for DC current and zinc coated steel presented two minimum resistance values, identified as numbers 1 and 3, and two dynamic resistance peaks, named 2 and 4. After minimum resistance 1, the solid zinc is heated up to reach dynamic resistance peak 2, where zinc started to melt and vaporize, decreasing the dynamic resistance up to point 3 in the figure. After reaching point 3, the zinc was melted and vaporized, starting the micro contact and collapse of steel roughness, up to reach point 4. Figure 9 shows a schematic drawing of the zinc burn represented by the stages 2 and 3 of the dynamic resistance of figure 8 (a). It can be observed that the zinc coating fills all the roughness of the sheets. This filling in the valleys and peaks of the sheets roughness does not allow a complete deformation of the steel roughness, giving a dynamic resistance close to zinc value. After the zinc burn (melting, vaporization and diffusion), the peaks and valleys of the sheets roughness meet and the micro contact collapse happens. This collapse increases the contact area decreasing the dynamic resistance.

Regarding the comparison of the DC and AC welding dynamic energies values in zinc coated sheets, the total dynamic energy during DC welding was 16.7% higher than the total dynamic energy in AC welding. This result is related to the most efficient heat generation in the DC welding compared to the AC welding with the same welding parameters, and presented in figure 4(a).

3. 3 Comparison between dynamic resistances and energies in AC welding for uncoated and zinc coated sheets

Figure 10 shows the comparison between the dynamic resistances (a) and energies (b) in AC welding of the weld made with zinc coated and uncoated sheets.

It can be observed that the dynamic resistance during welding in AC with zinc coated sheet presents lower values if compared with the dynamic resistance in AC with uncoated sheet. This result is related to the fact that zinc coating has lower resistance to current flow, approximately 1/3, as presented previously in this paper, when compared to carbon steel. This explains the drop in dynamic resistance at time zero in figures 7(a) and 8(a).

Observing the Fe-Zn phase diagram, zinc is a strong ferrite stabilizer. Assuming a part of zinc coating is dissolved into the nugget, producing an iron-zinc alloy, the nugget became ferritic (bcc) in a large temperature range when compared to uncoated steel, which is mainly austenitic (fcc) in high temperature. As ferrite has a lower resistivity than austenite [WW], the dynamic resistance of zinc coated sheet is lower than uncoated sheet, as presented in figure 10 (a).

One can also note the formation of the nugget on AC welding with zinc coated sheet begins with a delay of approximately one and a half cycle after the formation of the uncoated sheet nugget, as shown at stages 1 and 2. This is due to the zinc effect, similar to the previous explanation.

Regarding the comparison of the values of the dynamic energies in zinc coated and uncoated steel sheets in AC welding, uncoated sheets presents 15% higher dynamic energy than zinc coated sheets. This result is also related to the greatest efficiency in heat production in uncoated sheet AC welding. As the zinc coated sheet has a lower resistivity, the dynamic resistance is lower and the Joule heating effect is reduced, decreasing the dynamic energy for zinc coated sheets.

3.4 Comparison between dynamic resistances and energies in DC welding for uncoated and zinc coated sheets

Figure 11 shows the comparison between the dynamic resistance and dynamic energy of the spot weld made with the same DC welding parameters in zinc coated and uncoated sheets.

It can be observed in figure 11(a) that the dynamic resistance during DC welding with zinc coated sheet was lower than the dynamic resistance with uncoated sheet. This result is similar to figure 10(a), and has the same explanation.

One can also note that the formation of the DC weld spot with zinc coated sheet begins with a delay of approximately one and a half cycle after the formation of spot welds in uncoated sheets, as stages 1 and 2 in figure 11(a) have shown. The values of the dynamic energies in DC welding of uncoated sheet where 7.3% higher than those of zinc coated sheet. This result is related to the most efficient heat generation in DC welding of uncoated sheets.

3.5 Analysis of electrical resistance versus contact surface roughness of Zn coated and uncoated sheets

Figure 12 represents a schematic view of surface roughness measurement in the region where the electrode pressure is applied compared to the as-received surface roughness sheets. As a consequence, there is a surface roughness difference between these two regions. The lower surface roughness is found in the region of applied force compared to the outside region of original sheets. This is due to the collapse of the peaks of the roughness in these regions.

Table 1 depicts the comparison of mean surface roughness inside and outside the electrode pressure region for zinc coated and uncoated sheets, measured in three samples. Analyzing table 1 one can note different mean values, with zinc coated sheet presenting the highest mean value and lower dispersion in values.

Table 1 - Comparison of surface roughness inside and outside the electrode pressure region in Zn coated and uncoated sheets.

	Rz roughness on the sheet surface		**Rz roughness on the electrode pressure region**	
	Uncoated	**Zinc coated**	**Uncoated**	**Zinc coated**
Mean (μm)	**3.526 ± 0,475**	**4.066 ± 0,363**	**3.156 ± 0,549**	**3.374 ± 0,504**
Variation (%)	**13.5**	**8.9**	**17.4**	**14.9**

Figure 13 shows the graph of contact electrical resistance (R cont.) versus surface roughness (Rz) inside the Zn coated spot region and uncoated sheet, using a constant force between electrodes of 260 kgf.

It can be observed in Figure 13 a comparison between electrical contact resistance inside the spot region for Zn coated and uncoated steel sheets. It can be observed, in table 2, that the mean value of the contact electrical resistance in uncoated sheet is 52% greater than the mean of contact electrical resistance in zinc coated sheets.

Table 2 - Comparison of electrical contact resistance inside the spot in zinc coated and uncoated sheets.

	Electrical contact resistance (µ□)	
	Uncoated	Zinc coated
Mean (µm)	299.37 ± 25.28	109.87 ± 5.16
Variation (%)	11.0	4.7

Analyzing table 2, it is possible to observe that the variation and standard deviation of electrical contact resistance in uncoated sheet was higher than in Zn coated sheets. This result is related to the roughness variations, outside and inside the spot region, and the resistivity of zinc compared with carbon steel.

3.6 Comparison of spot weld dimensions and mechanical strength welded with AC or DC for uncoated sheets.

Table 3 shows the measured dimensions from macrographs and mechanical strength by tensile-shear tests of the uncoated sheets AC/DC spot weld.

Table 3 –Spot welding dimensions for AC/DC for uncoated sheets.

					Welding parameters		
	d (mm)	p (mm)	Indentation (mm)	Tensile force (kgf)	Electrode force (kgf)	Welding time (ms)	Welding current (kA)
AC uncoated sheet	4.4	1.1	1.3	473.5	260	150	7.0
DC uncoated sheet	4.6	1.2	1.4	487.0			

It can be observed in this table that the spot diameter and tensile force in the welding on DC output equipment present in welded sheets were higher when compared to welding in AC output equipment. These results are related to the most efficient heat production in DC welding, with the same welding parameters. This higher heat generation efficiency is showed in figure 7 for total dynamic energy showing a result of 9% higher in DC welding in uncoated sheet. This produces a spot with large dimensions, influencing the tensile-shear test result.

3.7 Comparison of spot weld dimensions and mechanical strength welded with AC / DC for zinc coated sheets.

Table 4 shows the measured dimensions from macrographs and mechanical strength by tensile-shear tests of the zinc coated sheets AC/DC spot weld.

Table 4 –Spot welding dimensions for AC/DC for zinc coated sheets.

					Welding parameters		
	d (mm)	p (mm)	Indentation (mm)	Tensile force (kgf)	Electrode force (kgf)	Welding time (ms)	Welding current (kA)
AC Zn coated sheet	3.2	1.0	1.1	336.5	260	150	7.0
DC Zn coated sheet	4.1	1.1	1.4	339.5			

In this table the spot diameter and tensile force of DC welding presented higher values in zinc coated sheets than welding in AC output. These results are related to the most efficient heat generation in DC welding with the same welding parameters. This higher heat generation efficiency is showed in the plot of total dynamic energy in figure 8, which shows a result of 16.7% higher energy generation in DC welding in zinc coated sheet. These results also influenced the nugget geometry.

3.8 Comparison of spot weld dimensions and mechanical strength welded with AC in uncoated and zinc coated sheets.

Table 5 shows the measured dimensions from macrographs and mechanical strength by tensile-shear tests of the uncoated and zinc coated sheets AC spot weld.

Table 5 –Spot welding dimensions for AC welding for uncoated and zinc coated sheets.

					Welding parameters		
	d (mm)	p (mm)	Indentation (mm)	Tensile force (kgf)	Electrode force (kgf)	Welding time (ms)	Welding current (kA)
AC uncoated sheet	4.4	1.1	1.3	473.5	260	150	7.0
AC Zn coated sheet	3.2	1.0	1.1	336.5			

It can be seen by analyzing table 5 that the spot diameter and tensile force of AC welding presented higher values in uncoated sheets than zinc coated sheets. These results are related to the most efficient heat generation in uncoated sheet AC welding with the same welding parameters. This higher heat generation efficiency is showed in the plot of total dynamic energy in figure 10, which shows a result of 15.0% higher energy generation in AC welding in uncoated sheet. This result also influenced the nugget geometry, which produce a higher nugget diameter for AC welding uncoated sheet.

3.9 Comparison of spot weld dimensions and spot mechanical strength with DC in uncoated and zinc coated sheets.

Table 6 shows the measured dimensions from macrographs and mechanical strength by tensile-shear tests of the uncoated and zinc coated sheets DC spot weld.

Table 6 – Spot welding dimensions for DC welding for uncoated and zinc coated sheets.

					Welding parameters		
	d (mm)	p (mm)	Indentation (mm)	Tensile force (kgf)	Electrode force (kgf)	Welding time (ms)	Welding current (kA)
DC uncoated sheet	4.6	1.2	1.4	487.0	260	150	7.0
DC Zn coated sheet	4.1	1.1	1.4	339.5			

Analyzing table 6, the spot diameter and tensile force of DC welding presented higher values in uncoated sheets than in zinc coated sheets. These results are related to the most efficient heat generation in uncoated sheet DC welding with the same welding parameters. This higher heat generation efficiency is showed in the plot of total dynamic energy in figure 11, which shows a result of 7.3% higher energy generation in DC welding in uncoated sheet. This result also influenced the nugget geometry, which produce a higher nugget diameter for DC welding uncoated sheet.

IV. FIGURES

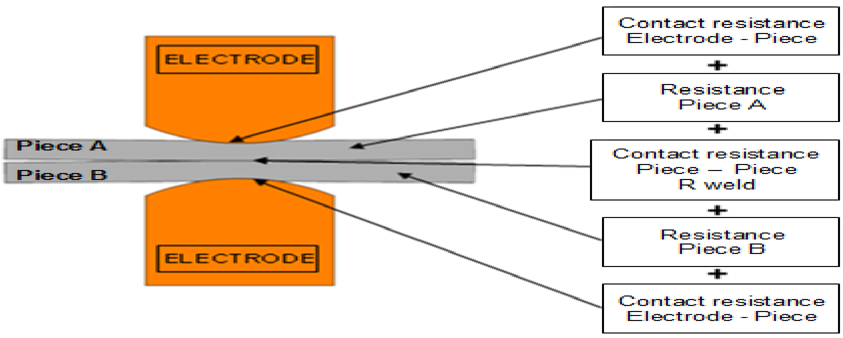

Figure 1- Scheme of electrical resistance between the electrodes in resistance spot welding.

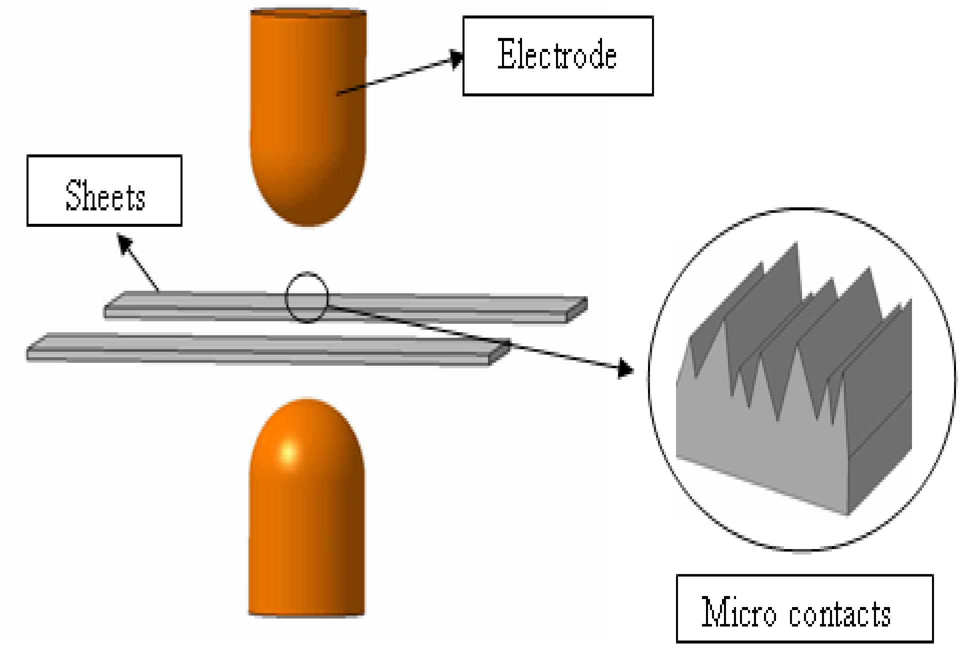

Figure 2 - Sheet surface roughness which defines the contact resistance.

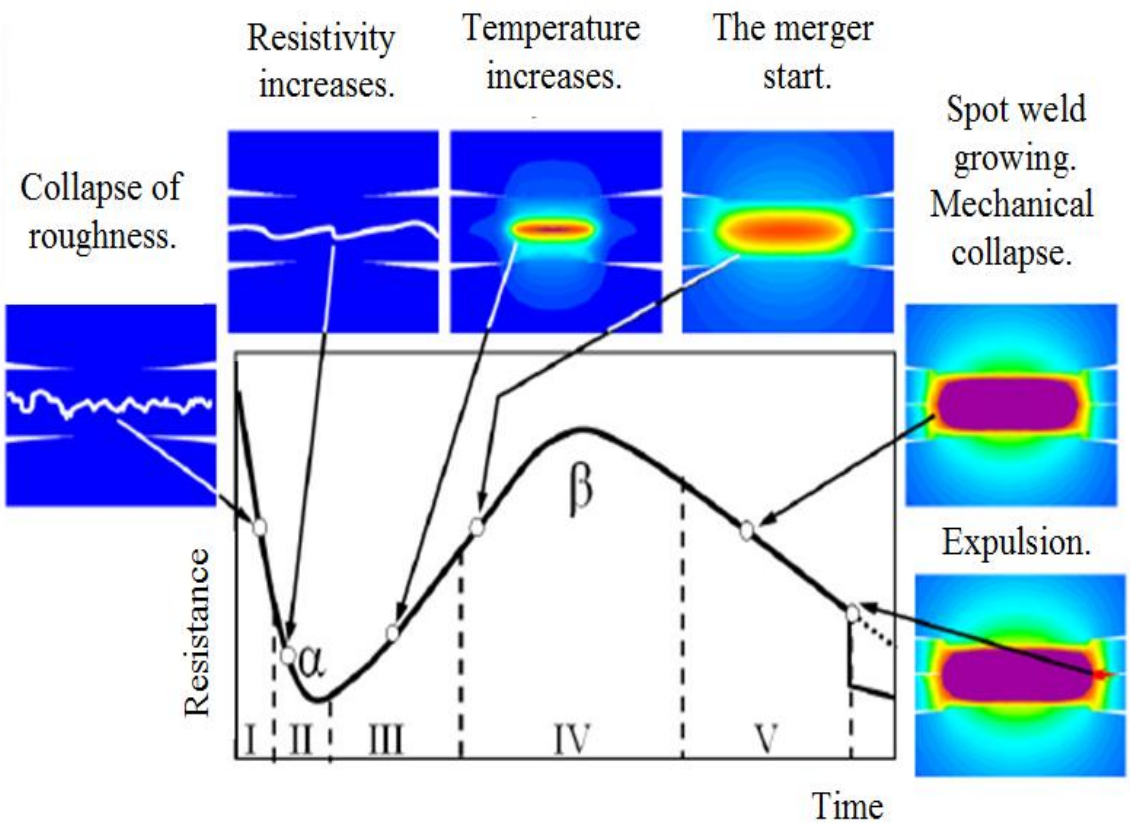

Figure 3 - Scheme of the dynamic electrical resistance during the formation of a nugget. Adapted from reference [11].

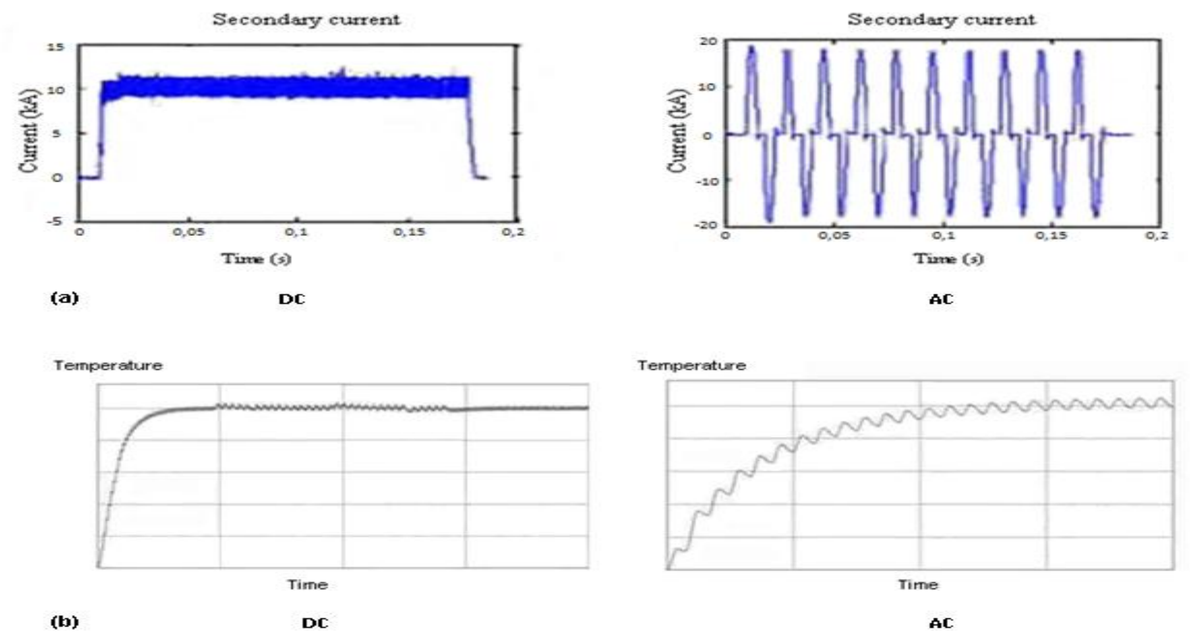

Figure 4. (a) Shape of the DC and AC current outputs [12]; (b) Heat generation in DC and AC welding equipments [8].

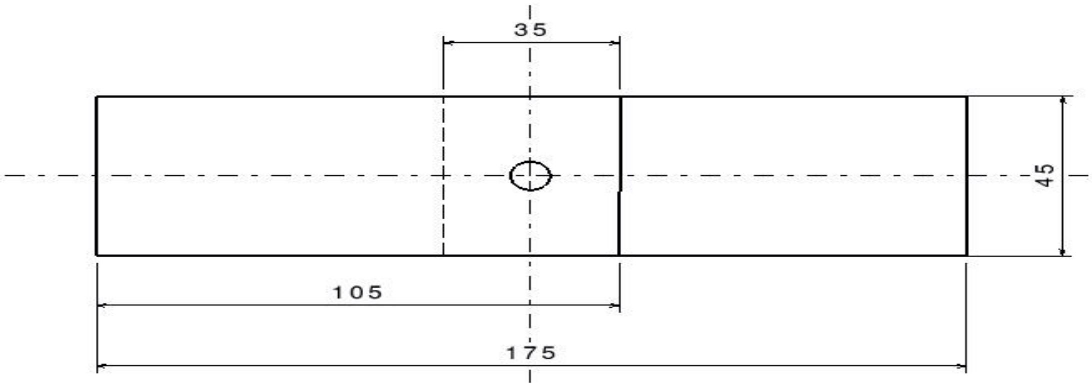

Figure 5- Dimensions of specimen in accordance to standard EN ISO 14273.

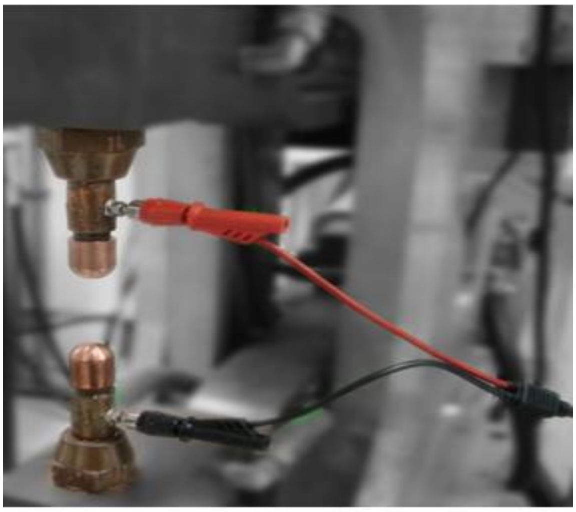

Figure 6 - Differential probe tip to measure the voltage during welding.

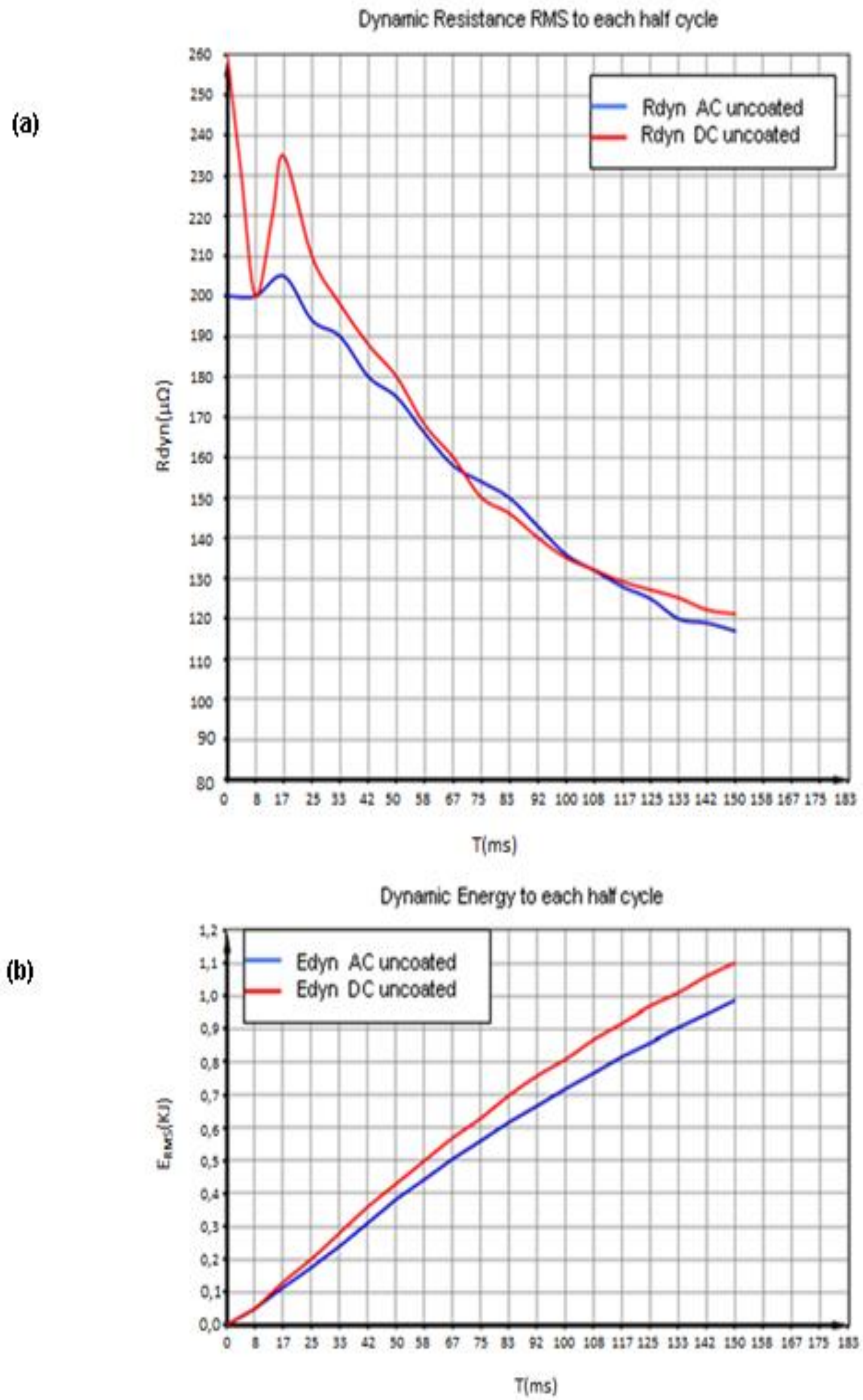

Figure 7 – (a) RMS dynamic resistances (μΩ) and (b) RMS dynamic energies (kJ) in AC and DC welding in uncoated steel sheets, as a function of time (ms).

(a)

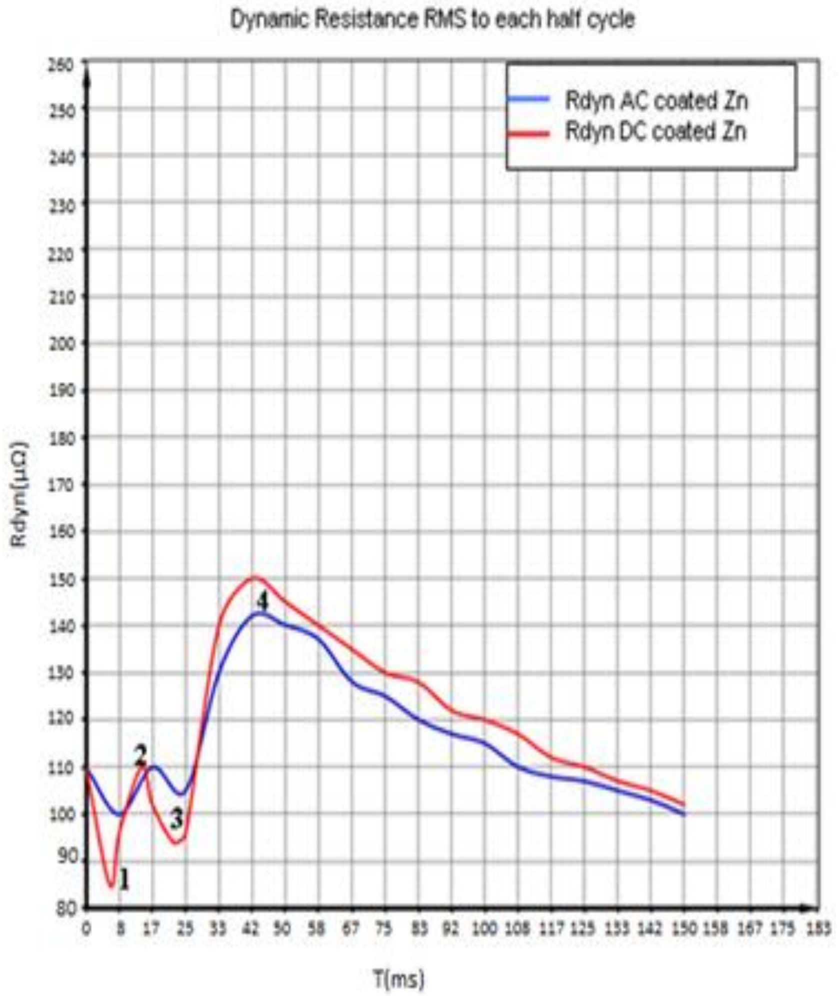

(b)

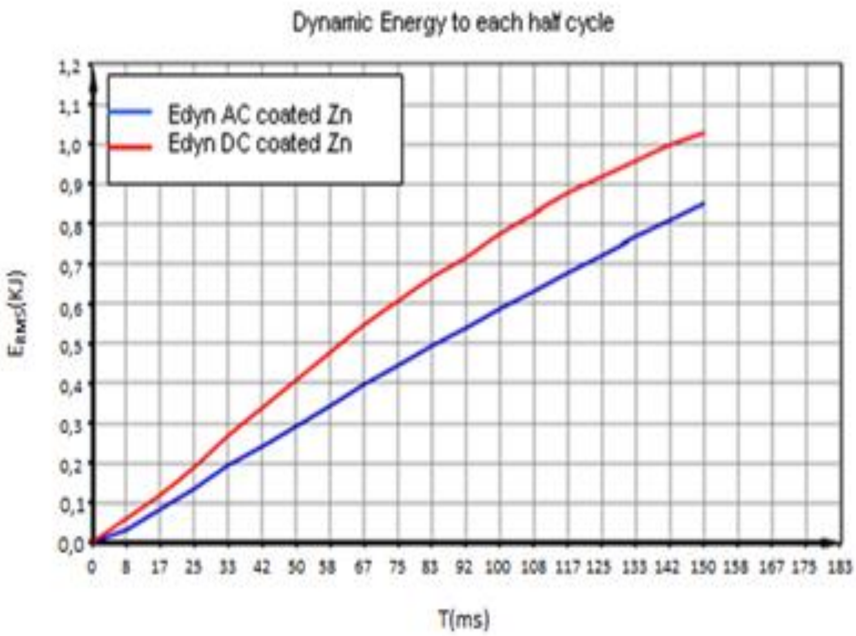

Figure 8 – (a) RMS dynamic resistances (μΩ) and (b) RMS dynamic energies (kJ) in AC and DC welding in zinc coated steel sheets, as a function of time (ms).

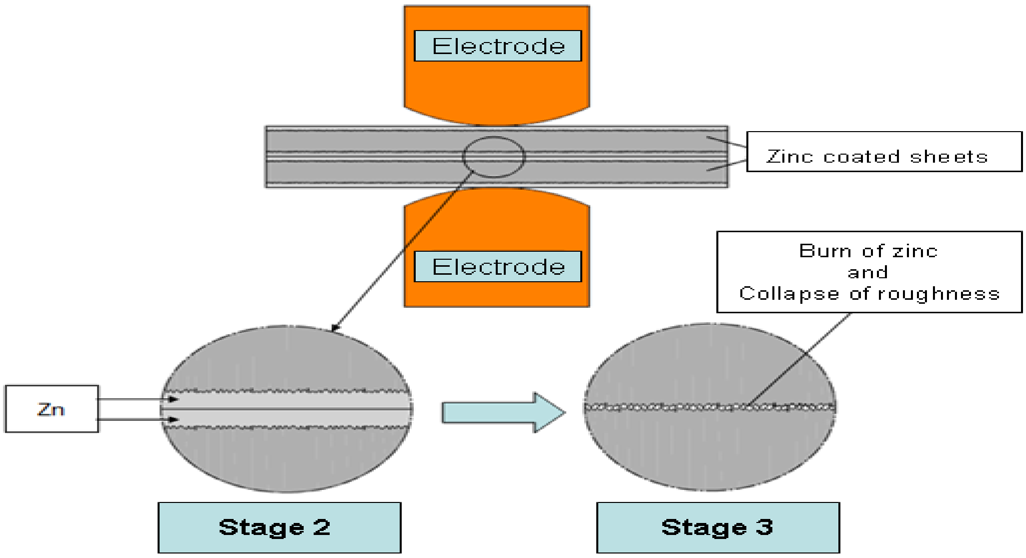

Figure 9 - Schematic drawing of the zinc burn (melting, vaporization and diffusion) represented by stages 2 and 3 of figure 8(a).

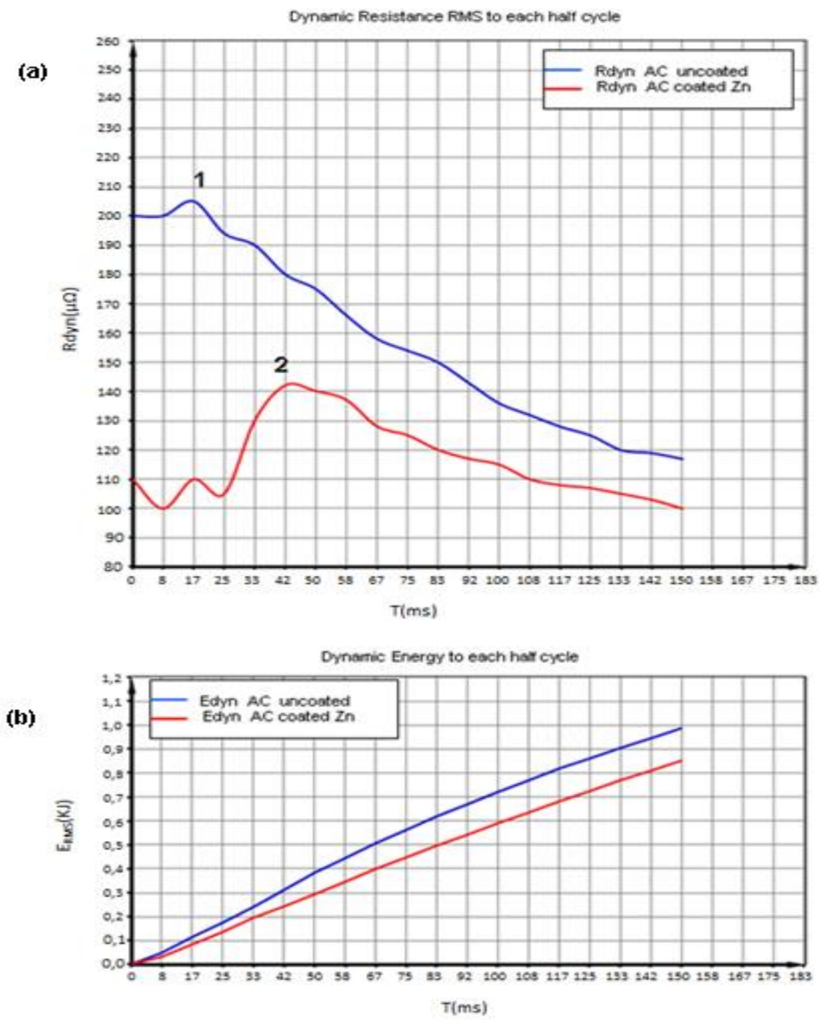

Figure 10 - (a) RMS dynamic resistances (μΩ) and (b) RMS dynamic energies (kJ) in AC welding in zinc coated and uncoated steel sheets, as a function of time (ms).

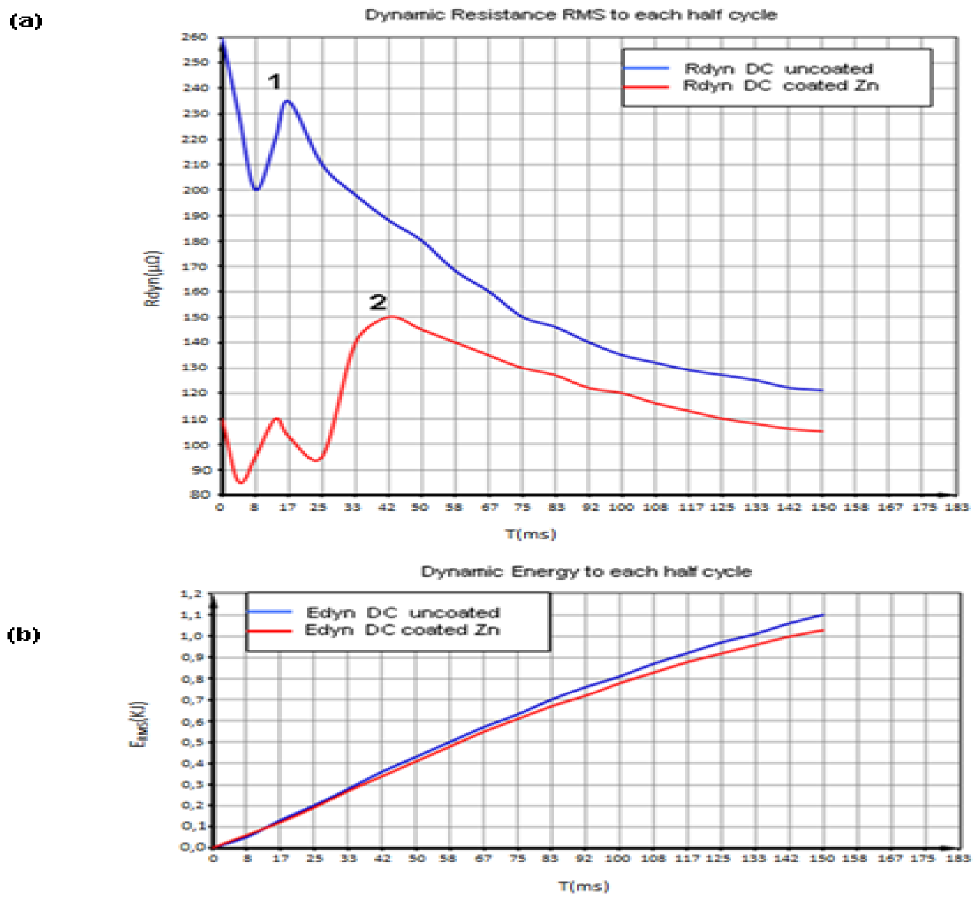

Figure 11 - (a) RMS dynamic resistances (μΩ) and (b) RMS dynamic energies (kJ) in DC welding in zinc coated and uncoated steel sheets, as a function of time (ms).

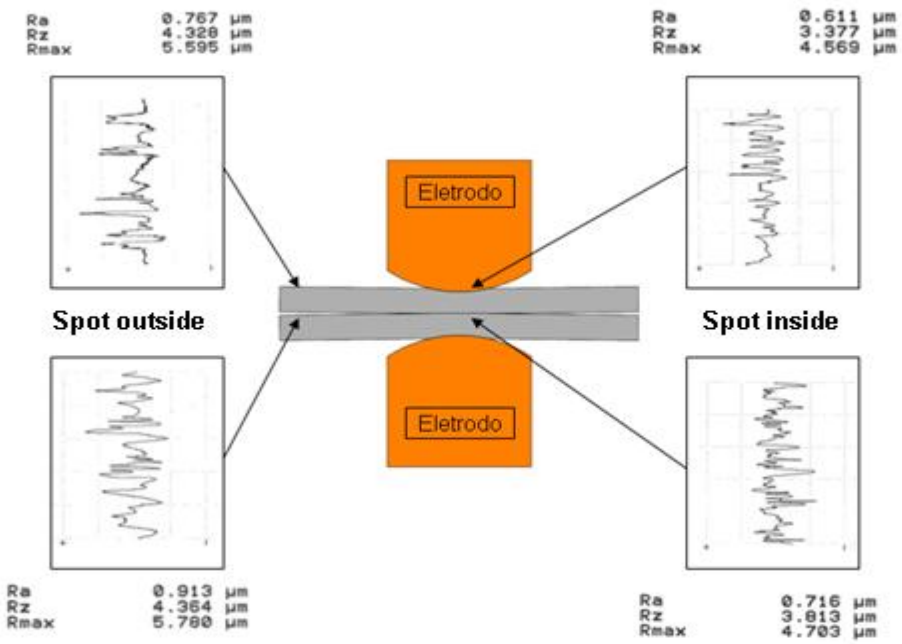

Figure 12 - Example of surface roughness of steel sheets inside and outside of the action line of the force exerted by the electrodes, with a force of 260 kgf.

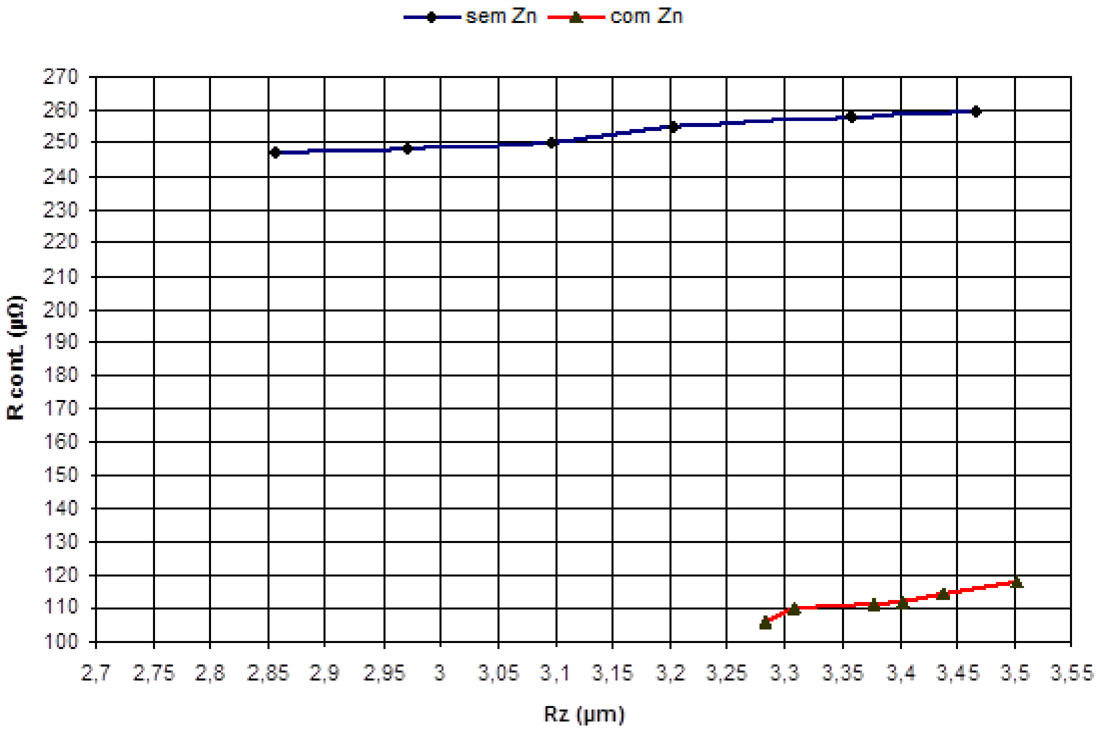

Figure 13 - Contact electrical resistance (R cont. µΩ) versus surface roughness (Rz-µm) inside the spot in Zn coated and uncoated sheets using an electrode force of 260kgf.

V. CONCLUSIONS

Based on the materials and experimental methodology used in the experiments carried out is possible to conclude:

a) The resistance and dynamic energy in DC welding with uncoated sheets were 8.6% and 9.0% higher than in AC welding, respectively. It can be concluded that DC welding with uncoated sheets, with same conditions and welding parameters, is more efficient in generating heat when compared to AC welding uncoated sheets.
b) The resistance and dynamic energy in DC welding with zinc coated sheets were 3.4% and 16.7% higher than in AC welding, respectively. It can be concluded that DC welding with zinc coated sheets, with same conditions and welding parameters, is more efficient in generating heat when compared to AC welding zinc coated sheets.
c) Dynamic resistance during welding, AC and DC with zinc coated sheets showed a small decrease in dynamic electric resistance for a short period of time, approximately half of a cycle. It can be concluded that with zinc burning, the steel surface roughness of the sheets touch and, therefore, their collapse happens. This fact increases the contact area and decreases the dynamic electrical resistance. It can be also conclude that zinc burning does not affect the formation of the nugget during the welding process.
d) The contact electrical resistance increases with surface roughness increase. It can be concluded that with increasing roughness the micro contacts decrease and, consequently, the contact resistance increases. This fact increases the electrical resistance to passage of current.
e) The resistance and dynamic energy in AC welding with uncoated sheets were 31.0% and 15.0% higher than zinc coated sheets AC welding, respectively. The AC welding nugget formation with zinc coated sheets starts about 25ms after the nugget formation with uncoated sheets. It can be concluded that the Joule effect at the interfaces in zinc coated sheet is lower due to the better electrical conductivity of zinc coating.
f) The resistance and dynamic energy in DC welding with uncoated sheets were 34.6% and 7.3% higher than in zinc coated sheets DC welding, respectively. The nugget formation in DC with zinc coated sheets starts about 25ms after the nugget formation with uncoated sheets. It can be concluded that the Joule effect at the interfaces in coated sheet is lower due to the better electrical conductivity of zinc coating.
g) The electrical contact resistance in uncoated steel sheets with constant welding parameters (electrode force of 260 kgf) was 52% higher than in zinc coated sheets. It can be concluded that the surface electrical contact resistance is lower because the zinc coating have a lower electrical conductivity.

h) The nugget diameters showed to be higher when the resistance and dynamic energies were higher. It can be concluded that the higher the resistance and dynamic energy higher will be the efficiency in heat generation to the spot weld formation.

VI. ACKNOWLEDGMENTS

The authors appreciate Welding Science Co. for dynamic resistance and dynamic energy measurements.

REFERENCES

[1] ASLANLAR, S. et al. Welding time effect on mechanical of automotive sheets in electrical resistance spot welding. Journal Materials and Design, v.29, p.1427-1431, Oct. 2007.
[2] BRANDI. S.D. Soldagem por resistência. In: WAINER, E. et al. Soldagem: Processos e Metalurgia. São Paulo: Edgard Blücher Ltda, 1992. p.217-242. (in portuguese)
[3] KEARNS, W.H. Welding Handbook: Resistance and Solid-State Welding and Other Joining Processes. Miami: American Welding Society, 1984.
[4] ZHANG, H; SENKARA, J. Resistance Welding: Fundamentals and Applications. 1. ed. London: Taylor & Francis, 2006. p.461.
[5] ASLANLAR, S. The effect of nucleus size on mechanical properties in electrical resistance spot welding of sheets used in automotive industry. Journal Materials and Design, Turkey, v.27, p.125-131, Nov. 2006.
[6] FURLANETTO,V. Proposta e validação experimental de um modelo para máquina de solda a ponto CA: 2005.88p. Dissertação (Mestrado) – Escola Politécnica, Universidade de São Paulo, São Paulo.(in portuguese)
[7] ZIEDAS, S; TATINI, I. Coleção Tecnologia SENAI: Soldagem. São Paulo: SENAI, 1997.p.245-254.
[8] WELDING SCIENCE. Manual de treinamento de soldagem por resistência. 2009. p.82. (in portuguese)
[9] HAMMOND, R. Automatic Welding, 1 ed. London: Alvin Redman Limited, 1963.p.447.
[10] SHOME, M. Effect of dynamic contact resistances on advanced high strength steels under medium frequency DC spot welding conditions. Science and Technology of Welding and Joining, India, v. 14, n .6, p.533-541, Dec. 2008.
[11] DICKINSON, D. W.; FRANKLIN. J.E.; STANYA, A. Characterization of Spot Welding Behavior by Dynamic Electrical Parameter Monitoring Welding Research Council, New York, v. 59, n.6, p. 170-176, June 1980.
[12] FENG, E. et al. Energy consumption in AC and DC resistance spot welding. In: Sheet Metal Welding Conference XI, Washington, 2004.p.12.

American Journal of Engineering Research (AJER)
e-ISSN: 2320-0847 p-ISSN : 2320-0936
Volume-2, Issue-06, pp-94-102
www.ajer.org

Research Paper Open Access

Evolutionary approach to restoration service of electric power distribution networks

Jan Stępień[1], Sylwester Filipiak[2]
[1](Electrical Engineering Automatics and Computer Science Faculty, University of Technology Kielce, Poland)
[2](Electrical Engineering Automatics and Computer Science Faculty, University of Technology Kielce, Poland)

Abstract:- *In the literature on the distribution systems operation the problem of power delivery recovery in case of the network failure is one of the very important aspects of a proper operation of the distribution systems. An idea of using a classifying system and co-evolutionary algorithm for operation support of electric power distribution systems operators has been presented in the paper. The elaborated method uses the theoretical background of genetic-based machine learning systems. The method shows the ability to collect experience on the base of information on faults, occurred or simulated in the power distribution systems. In the elaborated method the decisive variables, essential from the network operation reliability point of view, described with the use of fuzzy sets theory. A method enabling to formulate scenarios of network configuration changes (at changes in network operation conditions) has been characterised in the paper.*

Keywords: *- Evolutionary Algorithms, classifier system, Distribution Power Networks*

I. INTRODUCTION

The Planning a restoration service for distribution systems is a critical task for dispatchers in a control center. Restoration attempts to supply an ample amount of power to nonfaulty out-of-service areas for as many customers as possible while safely operating the distribution system. Reconfiguration is the process of changing the open/closed status of switches and is done for volt/var support, loss reduction, load balancing and restoration. Reconfiguration for restoration is a combinatorial problem involving searching an enormous space of solutions. The problems with integer variables are NP hard, meaning no known algorithm exists to solve these problems in polynomial time. However, reconfiguration for restoration problem is both NP hard and NP and hence belongs to the class of NP complete problems. For such kind of problems, the solution time increases with an increase in the number of integer variables. However, the solution time generally depends on the formulation.

Many approaches have been proposed to solve the restoration problem from different perspectives. For instance, researchers [1, 2] incorporated dispatcher's experience and operating rules into an expert system to assist the dispatcher. Related investigations formulated the restoration problem as an optimization problem to minimize the number of unserviced customers [3, 4]. This problem has been approached using heuristics [5, 6, 7] mathematical programming [8], meta-heuristics (genetic algorithms, tabu search, simulated annealing) [9, 10] and expert systems [11].

In works [12, 13, 14] are presented methods concerning the use revolution algorithms drawn up to resolve multi-criteria problems in optimising electric power networks. These methods concern the development of specialised means of coding, reproduction methods based on domination and also use of co-evolutionary approaches. Several evolutionary algorithms have been developed to deal with distribution system reconfiguration problems [15, 16, 17, 18]. Although the obtained results have been encouraging, the majority of evolutionary algorithms still demand high running time when applied to large-scale distribution systems. In [14], it was shown that the tree encoding (data structure) used is a critical factor for the performance of evolutionary algorithms applied to such large distribution systems. Other critical aspects of distribution systems are the genetic operators that are implemented. Generally these operators do not generate radial configurations [19]. In order to improve the performance obtained by evolutionary algorithms in distribution system reconfiguration problems, a tree encoding based on graph chains, called graph chains representation, and its corresponding genetic operators were developed in [14]. These operators produce only radial configurations. Although the requirement of a radial configurations is common for distribution system reconfiguration problems, it makes the network modeling more difficult to efficiently reconfigure distribution systems.

The analysed problem of choosing the substitute configuration of the distribution system can be described as a multiobjective programming problem. In the article the author presented the results of his works concerning the method drawn up using the system classifying cooperation with the co-evolutionary algorithm, in order to assist the work of electrical energy distribution systems operators. The elaborated method uses the classifying system to determine, for the assumed conditions, the most profitable distribution network configuration. The important feature of the method is the possibility to form the substitute network configuration with the use of information coming from the simulated network operation states, where the information on reliability parameters of the network or exploitation periods of the network elements can be also exploited.

The article presents, as the application for solution of the analysed problem, the co-evolutionary algorithm cooperating with classifying system as a method typified by the short duration of the calculation process. Reduction of the calculation time (on average by 40 %) results from the fact of use of information written into the population of classifiers, which is the population subject to the evolutionary process. The population of classifiers containing information of various replacement network configurations is formulated with regard to reliability characteristics and operation times of network elements. The principal result presented in this article is an effective method of designating the placement network configurations for cases of breakdown situations for very complex network structures.

II. A METHOD USING THE CLASSIFIER SYSTEM

The classifier system is a system that learns the syntactic simple rules in order to co-ordinate its actions in any environment and includes the three basic components [20, 21]: rule and message system, evaluating system, evolutionary algorithm. In the classifier system the information from the outer environment is processed into the messages of a given format. The messages are further placed on the message list, where they can activate the classifiers. In the elaborated method (based on the classifier system idea) known procedures, performing message processing or classifier evaluation have been used. Certain modifications resulting from the specificity of the considered problem, have been introduced:

- the message about the fault is described in the form: a list with numbers of not supplied nodes, and a list with numbers of fault elements :
  <message>:: =(numbers of not supplied nodes)+ (numbers of fault elements)
- in the classifier notation following syntax has been taken into account in the notation actually used:
  <classifier>::= <condition>:<message>
  <classifier>::=< numbers of not supplied nodes + numbers of fault elements>:<post-fault configuration>

The work [20] contains a detailed description of the procedure implemented by the classifying system connected with the classifiers evaluation and processing. This article below contains a description of the application of the modified co-evolutionary algorithm. In differentiation from the algorithm described in the work [20], for reception of results presented in this work is applied: co-evolutionary article using other genetic operators and modified function sets evaluating solutions contained in particular subpopulations substituted by co-evolutionary algorithm.

With regard for these specific nature of the analysed task the author suggested a two-part description of the announcement (describing the breakdown situation of the network). The first part of the announcement is recorded as a length of zero-ones relating to the number of elements equal to the number of network line sections of the analysed network. Value 1 on the defined position corresponding to the number of the network length, indicates length with power supply, and 0 indicates network node without power supply as a result of breakdown. The second part of the announcement contains information about the damaged elements and also information about the configuration of network elements. For the description of this part of the announcement the author introduced the following marking notation: 0 - means damaged element, 1 - means actually used element, # - means element remaining in reserve. Below is showing an example of the process of creating announcements for the breakdown status of the electric power network system (composed of a small number of elements), the structure of which is reflected in graphic form on drawing 1. For the network graph from drawing 1, the case is examined of a breakdown on line l4.

The announcement describing the considered breakdown status was described as follows:

message 1

111101000110111 | 11#0#####1#11####11##1

The sought for classifiers in the first stage (fig.2):

classifier 1

111101100110111 | 11110###11#1111##11##1

classifier 2

111101111111111 | 11111#01#1#11#1##11##1

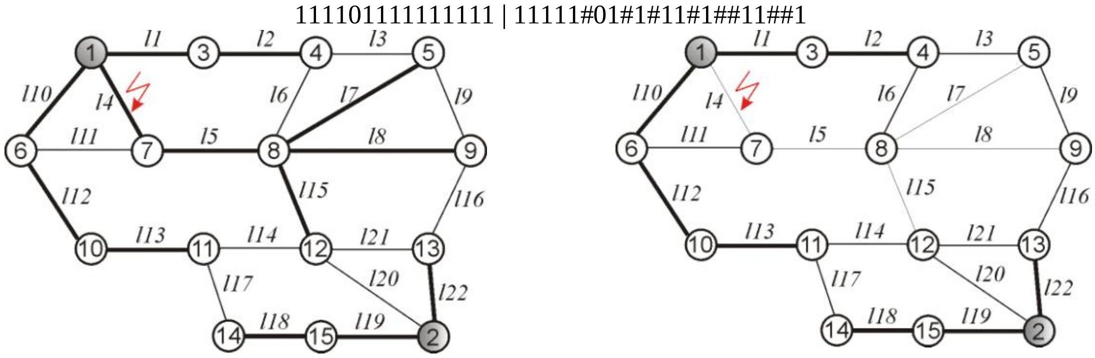

Fig. 1. Graph of the analysed distribution network

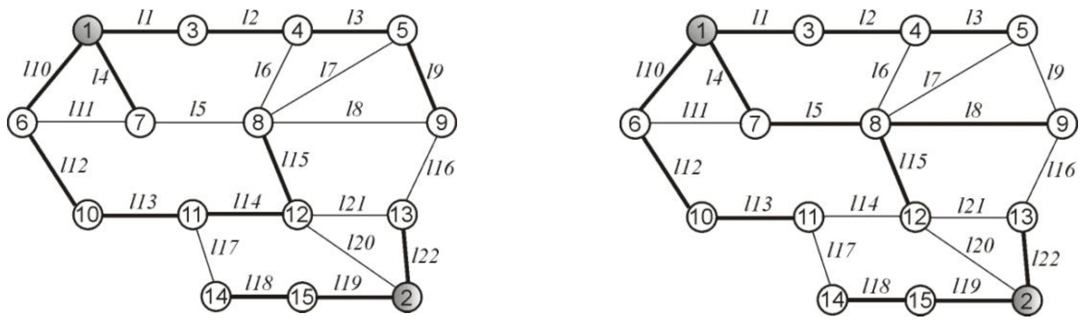

Fig. 2. Graph of the analysed distribution network for classifier 1 and classifier 2

The performance of the process of creation of announcements enables search in the collection of classifiers for information, the use of which assists the process implemented by the co-evolutionary algorithm.

In the initial part of calculations a message on the fault occurring in the network is being read. Procedures verifying the matching between the classifiers and the generated message are performed subsequently and then the classifiers are assessed. The strength S of the classifier, which has shown the best bid in the so-called auction process, is increased by the reward given by the system. Simultaneously its strength is decreased by the value of the bid given by the classifier. The bid of the best classifier increases the strength of other active classifiers proportionally to their bids. Moreover, the strength of all the active classifiers is decreased by a certain, determined value. The effective bid value has been calculated in a following way [20, 21]:

$$S_i(t+1) = S_i(t) - c_{bid} \cdot S_i(t) - c_{tax} \cdot S_i(t) + r(t) \tag{1}$$

$$B_i = c_{bid} \cdot (e_{bid1} + e_{bid2} \cdot Sp_i) \cdot S_i \tag{2}$$

$$EB_i = c_{bid} \cdot (e_{bid1} + e_{bid2} \cdot Sp_i) \cdot S_i + e_{br} \tag{3}$$

where: B_i - bid value of the i-th classifier, EB_i - effective bid value of the i-th classifier, Sp_i - specificity of the i-th classifier, S_i – strength of the i-th classifier, c_{bid} – investment coefficient (c_{bid}=0,1), e_{bid1}, e_{bid2} – coefficients of the classifier linear specificity function (e_{bid1}=0,65, e_{bid2}=0,35), e_{br} – random value generated with the use of a normal distribution generator, c_{tax} - turnover tax coefficient c_{tax}=001, r - coefficient of reward paid for the best classifier r=2.

The rule and message procedures perform the process of classifiers checking and evaluation, in aspect of using the information contained in them for solving the problematic situations. This allows for appointing of the group of classifiers containing the useful information on the searched post-fault network configuration.

To modifications of the evolutionary algorithm enabling solutions of multi-criteria tasks are counted among others the application of the co-evolutionary approach. Application of the co-evolutionary algorithm to the analysed task creates m population; in each of them the adaptation function is defined on the basis of another component quality indicator vector. After successive performance (population supplementation with new elements), and through renewed reproduction, these populations are connected, and then were again divided so that each population elements may attain an unlimited population. The sought-after solution is the Pareto-optimal collection of solutions.

To encode the individuals representing various network configuration variants in a form of a sparse graph, the bequest of chromosomes in the form of a vector of inversion has been assumed. Each component of the vector of inversion, corresponding to the number of the graph node, is equal to the number of the supplying node. A well-known roulette selection method on the remaining fractional part has been used as a selection method. Two specialised reconfiguration operators have been used in the algorithm to create new solutions (crossover probability pk=0,95, mutation probability pm=0,15). In the presented calculation method creating of new variants of the analysed problem solutions has been realised according to the following procedure:

1) selection of two network configuration variants from the current population (recorded in the vectors of inversion),
2) node selection from the list of nodes with no supply,
3) rewriting of the supply routes of the formerly selected node from the vector selected in step 1 to the auxiliary table,
4) roulette selection of the node from the created table,
5) rewriting of the further part of the supply route from the second vector, starting from the node selected in step 4, to the second of the selected vectors.

The aim of using of this kind of operator, creating new variants of distribution network configuration, was to examine the change variants effectiveness in the part of the networks close to the supply points, as well as in parts of the analysed network system affected by failures. The mutation operator enables to introduce the random changes into the network configuration, according to the following procedure:

1) selection of one variant of network configuration from the current population,
2) node selection from the list of nodes with no supply,
3) rewriting of the supply route for the node selected in step 2 from the network configuration selected in step 1 to the auxiliary table,
4) roulette selection of the node from the table created in the last step,
5) the neighbouring nodes, which are supplied, are considered (in relation to the node selected in step 4) and from among them one is roulette selected and its number is recorded in the vector (from step 1) as a number of the supplying node selected in step 4.

In order to obtain proper solutions following limiting constraints resulting from technical requirements for proper operation of the distribution network have been taken into account:

- not exceeding of the maximum transmission currents of the line sections,
- not exceeding of the allowable voltage drops in the network nodes supply routes,

On the base of the source data [18, 19] and own research following values of significant parameters of the calculation system have been assumed in the calculation procedures: number of classifiers n=200, crowding factor for classifier population cs=3.

Following criteria have been assumed substantial for the optimisation problem of post-fault network configuration:

- minimisation of the number of switching activities leading to obtaining a substitute network configuration:

$$\underset{j}{Min}\ u_1(X_j) = n_j - n_0 \quad \text{where } \mathrm{j} = 1, 2, \ldots, \mathrm{m} \tag{6}$$

where: Xj – vector containing information on the j-th variant of the distribution network configuration, m – number of solution variants, nj – number of switching activities, n0 - number of switching activities in the basic configuration.

- minimisation of the undelivered power value:

$$\underset{\mathrm{j}}{Min}\, \mathrm{u}_2(X_j) = \sum_{i=1}^{lw} P_{sr,i} \cdot q_i \cdot T_{p,i} \tag{7}$$

where: $P_{sr,i}$ - average active load of the i-th user node of the network, lw – number of nodes, qi - unreliability factor of the supply circuit of the i-th user node, Tp,i – operation time.

- minimisation of the voltage deviation in the network nodes:

$$\underset{j}{Min}\, u_3(X_j) = \max_i \left(\frac{U_i}{U_N} \cdot 100 \right) \tag{8}$$

where: U_N – distribution network nominal voltage, U_i – voltage value in the i-th user node of the network,

- minimisation of the power load degree coefficient of the found group of the most loaded network elements.

$$\underset{j}{Min}\ u_4(X_j) = \max_k \frac{\sum_{i=1}^{n} P_{\max,i}}{n} \tag{9}$$

where: k - the number of power supply route network nodes of the reception network, n - the number of the most heavily loaded network elements.

- minimisation of the technical losses in the distribution systems:
-

$$\underset{j}{Min}\, u_5(X_j) = \min\{\sum_{i=1}^{g} (\Delta P_i + k_e \cdot \Delta Q_i)\} \tag{5}$$

where: g – number of line section, Pi – loss of active power in i - this line section, Qi – loss of passive power in i- this line section, ke – passive power equivalent,
The assumed membership functions used for the main variables description have been defined as follows:

$$u_{fi}(X) = \begin{cases} 1, & \text{if} \quad f_i(X) \le f_i^{min} \\ \left(\dfrac{f_i^{max} - f_i(X)}{f_i^{max} - f_i^{min}} \right), & \text{if} \quad f_i^{min} < f_i(X) \le f_i^{max} \\ 0, & \text{if} \quad f_i^{max} < f_i(X) \end{cases} \tag{11}$$

III. CASE STUDIES

The pre-analysed calculation problem concerns the designation of the supply network configuration for the breakdown operations statuses of the network, arising from damaged network elements, their loading and also the exceeding of permissible voltage deviations in network line sections. The considered breakdown situation of the Medium Voltage electric power distribution network arising from damage to line number 6_8 coming from main station number 6 supplying distributors station number 8. In the presented graph (fig. 3) the filled nodes symbolise the main supplying points, whereas the bold branches symbolise the elements taking part in the load transfer.

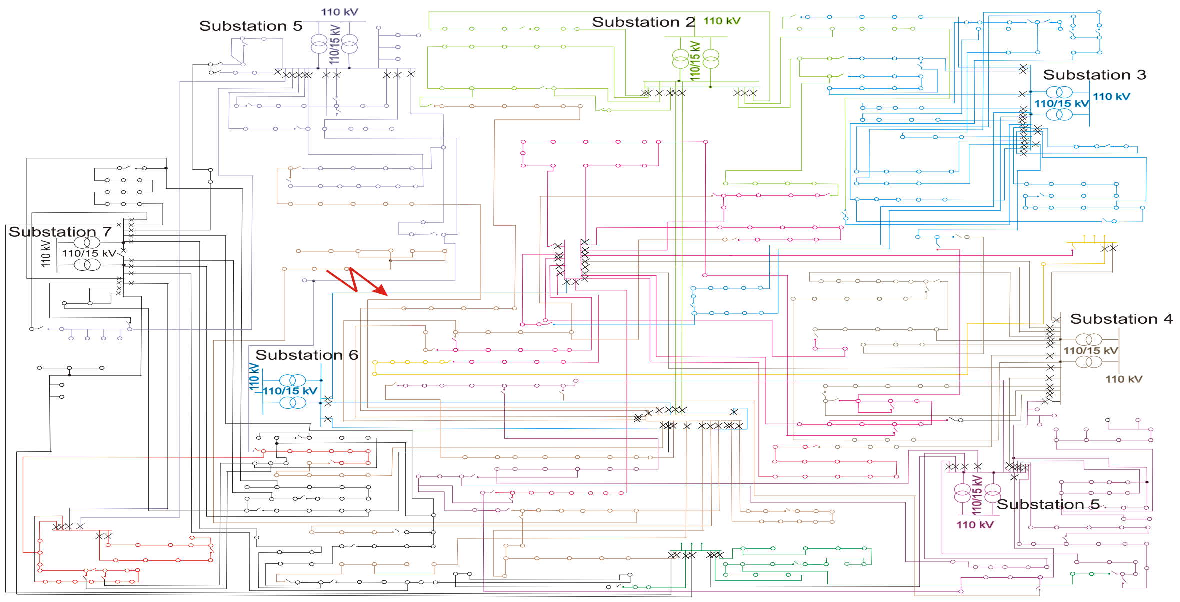

Fig. 3. Diagram of the analysed system of the medium voltage distribution network

For the below considered breakdown situation in the analysed network, which is composed of 556 network nodes the author accepted the abbreviated description of announcements and also classifiers. The abbreviated description however contains instead of the zero-one tract (part of the first announcement) the numbers of line sections deprived of power, whereas as part of the second announcement the numbers of damaged elements are given. In the elaborated calculation model a so-called vector of inversion has been used for the network configuration description. As a result of the accomplishment of the first stage of the process the announcement creation for the searched for classifiers is shown in table 1.

In the column relating to network configurations noted in the inversion vector only the initial and final elements of this vector are noted. According to the idea of classifying systems through the process of announcement creation, then follows the evaluation of the revealed classifiers, which consists of the calculation of the so-called offer of the classifiers being the measure of their suitability to resolve the analysed task. The offer for classifier number 1 (table 1) calculated according to dependencies 2 and 3 amounted appropriately to $B_1 = 0{,}919$ and $EB_1 = 0{,}904$. Whereas the offer for classifier number *2* amounted correspondingly to $B_2 = 0{,}939$ and $E_2 = 0{,}937$ and the offer for classifier number 3: $B_3 = 0{,}827$ and $E_3 = 0{,}840$.

As a result of the performance of the process of the creation and evaluation of announcements executed in the first stage, as the classifier with the best offer is defined as classifier number 1. This classifier served to create the announcement of the following stage of classifiers search. In the analysed case in the process performed in the second stage further classifiers were not sought for.

Table 1. Active classifiers

No	condition: (numbers of non-supplied nodes) and (numbers of fault elements)	answer of system (recorded in the vectors of inversion)	S_i – strength of the *i-th* classifier	Bid
1.	*(178, 179, 180, 181, 182, 177, 178) and (8_22)*	x,x,x,x,x,x,x,6,2,5,7,13,14,15,16,9,29 3,17,18,19,9,,57,9,59,60,450,5, ...	$S_1 = 10$	$B_1 = 0{,}919$ $EB_1 = 0{,}940$
2.	*(29, 73, 72, 71, 70, 69, 68) and (8_29)*	x,x,x,x,x,x,x,6,6,5,1,13,14,15,16,9,18 ,19,20,9,9,8,2,9,59,60,450,5,61,...	$S_2 = 10$	$B_2 = 0{,}939$ $EB_2 = 0{,}937$
3.	*(22, 23, 24, 25, 26) and (8_178)*	x,x,x,x,x,x,x,6,6,5,1,13,14,15,16,9,18 ,19,20,9,9,8,2,9,59,60,450,5,61,...	$S_3 = 10$	$B_2 = 0{,}827$ $EB_2 = 0{,}840$

As a result of the performance of the announcement creation process and the evaluation of active classifiers (table 2), information was obtained, which might be used to create a population (size 100÷120) of solution variants subsequently created by the co-evolutionary algorithm. This algorithm is based simultaneously on 5 subpopulations, from which each evaluation was the basis for another adaptation function (dependencies 6 to 10). The sought-after solution in this case is a collection of solutions in the form of alternative configurations of the analysed network. The choice of the final solution variant depends upon the decision maker decider, who in this instance may be the operator managing the operation of the electric power Medium Voltage distribution network.

The course of the process designating the best solutions in subpopulation no. 3 is shown in drawing 6. Cooperation of the co-evolutionary algorithm with the classification system enables significant reduction of time of obtainment of solutions (reduces the iterative calculation process on average by 40 %), which is significant from the practical point of view in the application of this method in current systems of distribution network operation management.

Figures 4b and 5b show the realisation of the calculation process, which used information for active classifiers. Information on the best solutions in subpopulations no. 3 and no. 4 is shown in graphic form on drawings 6 and 7. As a solution to the task of designating a substitute network configuration in the event of a breakdown of the analysed distribution network, obtained with the use of co-evolution algorithm the best solution variants is accepted from 5 subpopulations.

Table 2. Active classifiers after process evaluating

No	condition: (numbers of non-supplied nodes) and (numbers of fault elements)	answer of system (recorded in the vectors of inversion)	S_i – strength of the *i-th* classifier
1.	*(178, 179, 180, 181, 182, 177, 178) and (8_22)*	x,x,x,x,x,x,x,6,2,5,7,13,14,15,16,9,293,17,18, 19, ,55,56,57,9,59,60,450,5,...	$S_1=10+2$
2.	*(29, 73, 72, 71, 70, 69, 68) and (8_29)*	x,x,x,x,x,x,x,6,6,5,1,13,14,15,16,9,18,19,20,9, 9,856,57,9,59,60,450,5,61,...	$S_2=10+0,47$
3.	*(22, 23, 24, 25, 26) and (8_178)*	x,x,x,x,x,x,x,6,6,5,1,13,14,15,16,9,18,19,20,9, 9,856,57,9,59,60,450,5,61,...	$S_3=10+0,47$
...	...	...	...
4.	*(8,22,28,29,31,73,178,195,291,292,338,339,23,167,32,72,179,196,287,293,337,,,...) and (6_8)*	x,x,x,x,x,x,x,4,6,5,1,13,14,15,16,9,18,19,20,9, 9,856,57,9,59,60,450,5,61, ...	$S_4=10$

a) random generated initial population b) used information for active classifiers

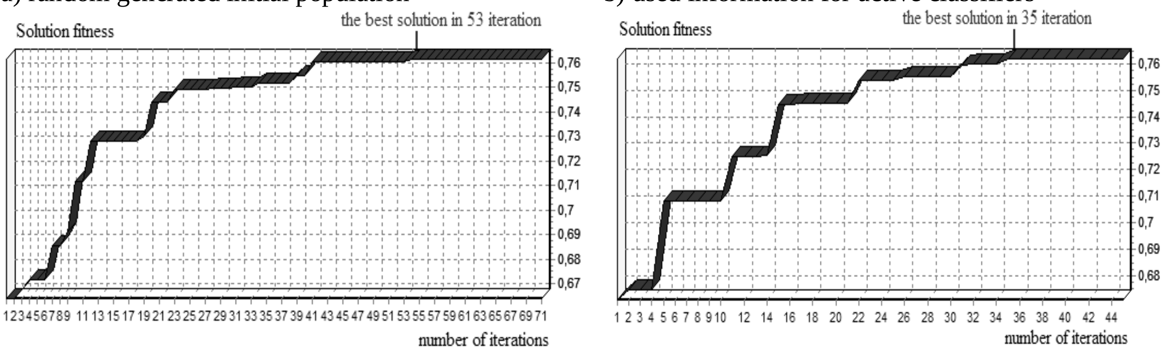

Fig. 4. Example of best solutions fitness waveform in subpopulation number 3

Information concerning the best obtained solutions is shown in table 3. In cooperation of the co-evolution algorithm with the classifying system after performance of the calculation process the best solutions obtained from particular subpopulations the solutions are written into the classifier collection.

a) random generated initial population b) used information for active classifiers

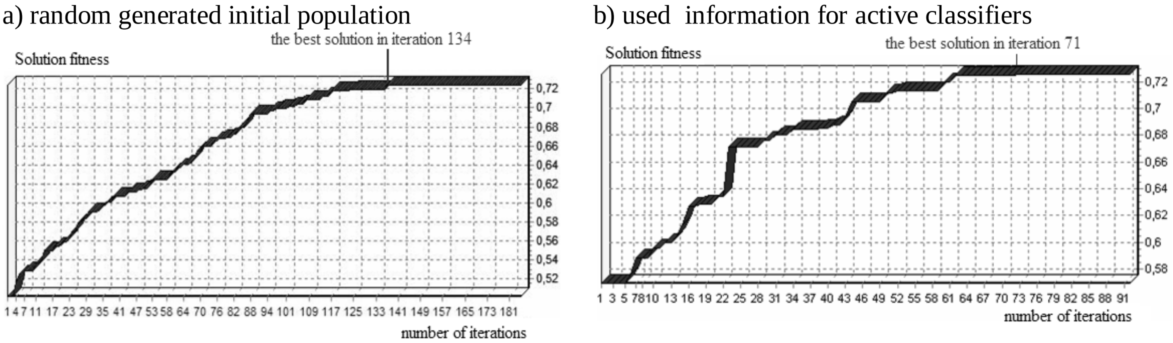

Fig. 5. Example of best solutions fitness waveform in subpopulation number 4

Table 3. Information concerning the best obtained solutions

No.	The value of the affiliation function of the best solution obtained in subpopulation
1	For the best obtained network configurations for criterion 1 the calculated affiliation function value amounted to: $\underline{u_1(x)=0,893}$, additionally: $u_2(x) = 0,896$, $u_3(x) = 0,547$, (maximal voltage deviation 2,23%) $u_4(x)=0,703$ (loading coefficient of the group of most heavily loaded elements in network: 0,669), $u_5(x)=0,535$
2	For the best obtained network configurations for criterion 2: $\underline{u_2(x) = 0,998}$ additionally: $u_1(x)=0,571$, $u_3(x) = 0,752$, $u_4(x)=0,686$, $u_5(x)=0,667$
3	For the best obtained network configurations for criterion 3: $\underline{u_3(x) = 0,765}$ additionally: $u_1(x)=0,607$, $u_2(x) = 0,943$, $u_4(x)=0,698$, $u_5(x)=0,670$
4	For the best obtained network configurations for criterion 4: $\underline{u_4(x)=0,729}$ additionally: $u_1(x)=0,519$, $u_2(x) = 0,985$, $u_3(x) = 0,752$, $u_5(x)=0,682$
5	For the best obtained network configurations for criterion 5: $\underline{u_5(x)=0,740}$ additionally: $u_1(x)=0,521$, $u_2(x) = 0,790$, $u_3(x) = 0,734$, $u_4(x)=0,569$

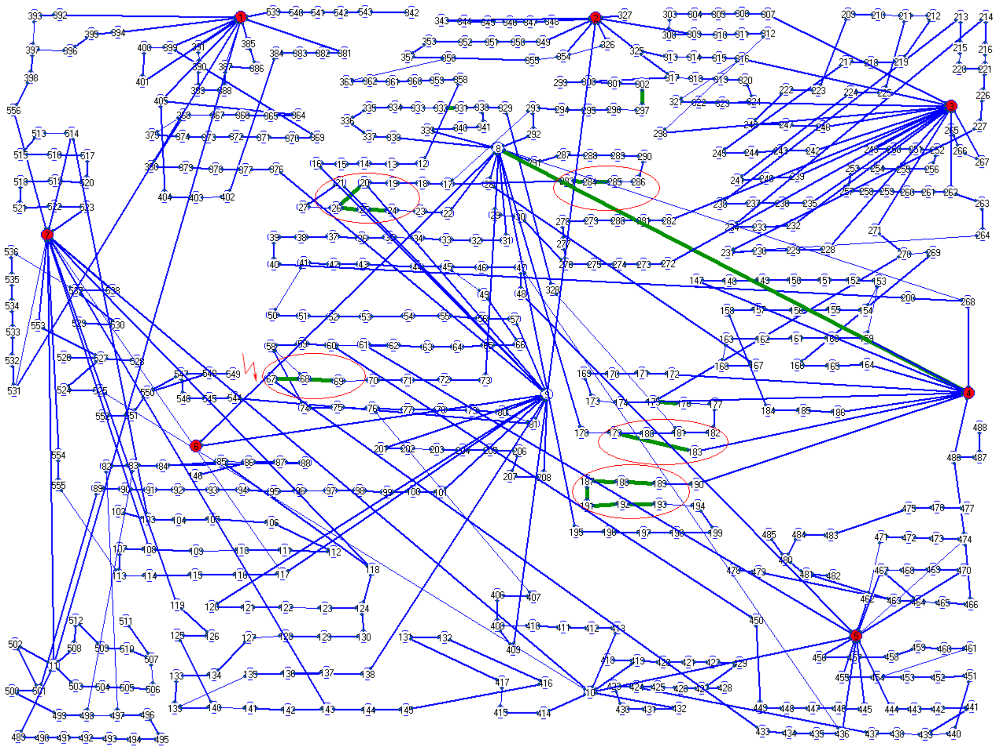

Fig. 6. Graph of the analysed distribution network with network configurations, being the best solution obtained in subpopulation3 (changes highlighted)

IV. CONCLUSION

This article describes the development of this type of calculation methods, simultaneously containing their own innovative solution proposals concerning the application of a classification system working with the co-evolutionary algorithm. The calculations performed for the mapped real system of the medium voltage municipal distribution network of 556 nodes have given satisfactory results, confirming the adequate direction of the research. On the base of the results obtained so far the authors assume that the results can be further used in creation of decisive procedures for complex power electric systems management, taking the fault operation states into special consideration. The method proposed by the author of the work is typified by the short time of designating the most rational post breakdown configurations in complex electric power Medium Voltage distribution network structures. It is the use by the classifying system working with the co-evolution algorithm that enables the effective creation of substitute scenarios for the Medium Voltage electric power distribution network. The method drawn up may be used in current systems managing the work of distribution networks to assist network operators in taking decisions concerning connection actions in supervised electric power systems

REFERENCES

[1] C. C. Liu, S. J. Lee, S. S. Venkata, An expert system operational aid for restoration and loss reduction of distribution system. *IEEE Trans. on Power Delivery*, vol. 3, 1988, pp. 619-629.

[2] Y. Y. Hsu, M. Huang, Distribution system service restoration using a heuristic search approach. *IEEE Trans. on Power Delivery*, vol. 7, 1992, pp. 734-740.

[3] Y. Fukuyama, H. D. Chiang, Parallel genetic algorithm for service restoration in electric power distribution systems. *Electric Power & Energy Systems*. vol. 18, no. 2, 1996, pp. 111-119.

[4] K. N. Miu, H. D. Chiang, B. Yuan, Fast service restoration for large-scale distribution systems with priority customers and constraints. *IEEE Trans. on Power Systems*, vol. 13. no. 3, Aug. 1998, pp. 789-795.

[5] A. L. Morelato, A. J. Monticelli, Heuristic search approach to distribution system restoration. *IEEE Trans. Power Delivery*, vol. 4, Oct. 1989, pp. 2235-2241.

[6] S. Wu. K. L. Tomsovic, C. S. Chen, A heuristic search approach to feeder switching operations for overload, faults, unbalanced flow and maintenance. *IEEE Trans. Power Delivery*. vol. 6. Oct. 1991, pp. 1579-1586.

[7] D. Shirmohammadi, Service restoration in distribution networks via network reconfiguration. *IEEE Trans. Power Delivery*, vol. 7, Apr. 1992, pp. 952-958.

[8] K. L. Butler, N. D. R. Sarma, R. Prasad, Network reconfiguration for service restoration in shipboard power distribution systems. *IEEE Trans. Power Systems*, vol. 16, Nov. 2001, pp. 653-661.

[9] Y. Hsiao, C. Chien, Enhancement of restoration service in distribution systems using a combination fuzzy-GA

method. IEEE Trans. Power Systems, vol. 15, Nov. 2000, pp. 1394-1400.
[10] S. Toune, H. Fudo, T. Genji, Y. Fukuyama, Comparative study of modern heuristic algorithms to service restoration in distribution systems. *IEEE Trans. Power Delivery*, vol. 17, Jan. 2002, pp. 173-181.
[11] C. Chao-Shun, C-H. Lin, T. Hung-Ying, A rule-based expert system with colored petri net models for distribution system service restoration. *IEEE Trans. Power Systems*, vol. 17, Nov. 2002, pp. 1073-1080.
[12] S. Khushalani, J.M. Solanki, N.N. Schulz, Optimized Restoration of Unbalanced Distribution Systems. *IEEE Transactions on Power Systems*, no. 22, Issue 2. 2007, p. 624-630.
[13] Y. Kumar, B. Das, J. Sharma, Multiobjective, Multiconstraint Service Restoration of Electric Power Distribution System With Priority Customers. *IEEE Transactions on Power Delivery*, no. 23, Issue 1, 2008, p. 261-270.
[14] A. C. B. Delbem, A. C. P. L. F. Carvalho, N. G. Bretas, Main chain representation for evolutionary algorithms applied to distribution system reconfiguration. *IEEE Trans. Power Systems*., vol. 20, no. 1, Feb. 2005, pp. 425-436.
[15] K. Nara, A. Shiose, M. Kitagawa, T. Ishihara, Implementation of genetic algorithm for distribution systems loss minimum reconfiguration. *IEEE Trans. Power Systems*, vol. 7, no. 3, Aug. 1992, pp. 1044-1051.
[16] L. Augugliaro, F. R. Sanseverino, Multiobjective service restoration in distribution networks using an evolutionary approach and fuzzy sets. *Elect. Power Energy Syst.*, vol.22, 2000, pp. 103-110.
[17] J. Stępień Z. Madej, Evaluation of structural redundancy efects in medium voltage cable networks. *Rynek Energii* No 4(83), 2009, pp. 55-62
[18] J. Stępień: Changes in demand structure of energy carriers with the use of waste heat and renewable energy. Rynek Energii Issue: 5, OCT 2008, p. 58-62
[19] J. Stępień, Evaluation of structural redundancy effects in medium voltage cable networks. *Przegląd Elektrotechniczny* Volume: 84 Issue: 4 2008, p. 128-131.
[20] S. Filipiak, Application of classifier system and co-evolutionary algorithm in optimisation of medium-voltage distribution networks post-fault configuration. *Electronics and Electrical Engineering*, 9(115), 2011, 9–15.